Master's thesis

NTNU
Norwegian University of Science and Technology
Faculty of Economics and Management
Dept. of Industrial Economics and Technology Management

Viktor Magnus Berg
Aksel Kristiansen Borgmo
Steinar Søvik Opheim

Strategic Planning for Optimal Zero-Emission Passenger Vessel Services

Master's thesis in Industrial Economics and Technology Management
Supervisor: Kjetil Fagerholt
Co-supervisor: Kenneth Løvold Rødseth
June 2023

NTNU
Norwegian University of Science and Technology

Viktor Magnus Berg
Aksel Kristiansen Borgmo
Steinar Søvik Opheim

Strategic Planning for Optimal Zero-Emission Passenger Vessel Services

Master's thesis in Industrial Economics and Technology Management
Supervisor: Kjetil Fagerholt
Co-supervisor: Kenneth Løvold Rødseth
June 2023

Norwegian University of Science and Technology
Faculty of Economics and Management
Dept. of Industrial Economics and Technology Management

NTNU
Norwegian University of
Science and Technology

NTNU
Kunnskap for en bedre verden

Department of Industrial Economics and Technology Management

TIØ4905 - Managerial Economics and Operation Research

Strategic Planning for Optimal Zero-Emission Passenger Vessel Services

Authors:

Viktor Magnus Berg
Aksel Kristiansen Borgmo
Steinar Søvik Opheim

Supervisors:

Kjetil Fagerholt
Kenneth Løvold Rødseth

June, 2023

Preface

This Master's thesis is the final delivery of our Master of Science in Industrial Economics and Technology Management at the Norwegian University of Science and Technology (NTNU), Department of Industrial Economics and Technology Management. In particular, it is our main delivery in the course TIØ4905 - Managerial Economics and Operations Research. The thesis builds upon our specialization project report (Berg et al., 2022) conducted in the fall of 2022. Both the project report and this thesis are part of the (Enabling) Zero Emission (Passenger) Vessel Services (ZEVS) research project, led by the Institute of Transportation Economics (TØI) and supported by 14 partners from both the public and private sectors.

Our two supervisors, Prof. Dr. Kjetil Fagerholt (NTNU) and Dr. Kenneth Løvold Rødseth (TØI), both deserve our deepest gratitude. Their guidance and support have been crucial for the development of this thesis. We would also like to thank the partners of the ZEVS project for their willingness to collaborate and provide us with high-quality data.

Viktor Magnus Berg, Aksel Kristiansen Borgmo & Steinar Søvik Opheim

Trondheim, June 2023

Abstract

Important actors, such as the International Maritime Organisation (IMO) and the Norwegian government, stress the urgency of transitioning the current emission-intensive High-Speed Passenger Vessel (HSV) services to being emission-free in the near future to comply with climate obligations. This thesis contributes with decision support to this transition by investigating whether holistic planning can alleviate some of the related technical and economic challenges. A problem is defined to capture several decisions on strategic, tactical, and operational planning levels. The problem spans a long-term planning horizon of several years and its main objective is to maintain the service level of a set of routes throughout the Zero-Emission (ZE) transition while minimizing passenger and operator costs. The strategic decisions comprise deciding the optimal roadmap for infrastructure, grid, and vessel investments along the planning horizon, while the tactical decisions include allocating the vessel fleet and infrastructures to routes. The operational decisions mainly comprise energy production and consumption management. The emphasis is on the strategic and tactical planning levels. Furthermore, the thesis considers the candidate ZE energy carriers hydrogen and electric batteries, including the novel technology of battery swap.

Since the scope of the problem entails many interdependencies making it highly complex to solve, the proposed solution approach in the thesis is to distribute the problem over two interacting Mixed Integer Linear Programming (MILP) models. These models effectively periodize the long-term planning horizon and decompose the problem into a two-stage stochastic Master Problem, comprising the strategic and tactical decisions, and a Sub-Problem, solving the operational decisions and returning them as input to the Master Problem. To conduct analyses of the problem, the models are solved with data from existing HSV services in Nordland County (Norway). The analyses evaluate how the alternative ZE energy carriers perform in the transition, and in particular, how they compare to the current services. A main observation is that battery-electric services are preferred in the transition but are not feasible for a substantial number of the routes due to range limitations. Hydrogen vessels complement battery-electric vessels well in terms of range limitations. However, the results show that they are significantly more expensive to operate due to (possibly pessimistic) safety regulations. When the sailing speed for each route is optimized, the drawbacks of the ZE energy carriers are somewhat reduced. Generally, however, the abatement costs are far higher than the government's suggested CO_2-tax implies, albeit there are large variations across routes, where some routes are remarkably costly to convert and some are even profitable to convert. Lastly, an analysis of the government's proposed regulation of all new HSV service tenders to be ZE shows a significant increase in total costs compared to a more gradual transition. Hence, the proposal needs to be considered wisely. Emerging technology for ZE HSVs is however promising with regard to the limitations found in this thesis and should be researched further.

Sammendrag

Viktige aktører, som International Maritime Organisation (IMO) og den norske regjeringen, understreker viktigheten av å konvertere de nåværende utslippsintensive hurtigbåt-sambandene til nullutslippsløsninger i nær fremtid for å overholde klimaforpliktelsene. Denne masteroppgaven bidrar med beslutningsstøtte til denne overgangen ved å undersøke om holistisk planlegging kan redusere de relaterte tekniske og økonomiske utfordringene. Et problem er definert for å fange opp beslutninger på strategisk, taktisk og operasjonelt nivå. Problemet strekker seg over en langsiktig planleggingshorisont over flere år, og hovedmålet er å opprettholde servicenivået for et sett med hurtigbåt-samband gjennom overgangen til nullutslipp, samtidig som passasjer- og operatørkostnader minimeres. De strategiske beslutningene omfatter å legge en optimal investeringsplan for infrastruktur, strømnett og fartøy i løpet av planleggingshorisonten, mens de taktiske beslutningene inkluderer å allokere fartøysflåten og infrastrukturer til rutene. De operasjonelle beslutningene omfatter hovedsakelig håndtering av energiproduksjon og -forbruk. Fokuset er i hovedsak på det strategiske og taktiske planleggingsnivået. Videre er det hydrogen og elektriske batterier som er vurdert som alternative nullutslipps-energibærere, inkludert den nye teknologien med batteribytte.

Ettersom omfanget av problemet innebærer mange gjensidige avhengigheter som gjør det svært komplekst å løse, blir det foreslått en løsningsmetode som fordeler problemet på to interagerende *blandet heltalls- og lineær-programmerings*-modeller. Disse modellene distribuerer den langsiktige planleggingshorisonten over en rekke tidssteg og dekomponerer problemet til et to-stegs stokastisk hovedproblem, som omfatter de strategiske og taktiske beslutningene, og et underproblem som løser de operasjonelle beslutningene og returnerer dem som inndata til hovedproblemet. For å gjennomføre analyser av problemet, blir modellene implementert og løst for data fra eksisterende hurtigbåt-samband i Nordland fylkeskommune (Norge). Analysene evaluerer hvordan de alternative nullutslipps-energibærerne presterer i overgangen, og spesielt hvordan de presterer sammenlignet med dagens betjening av sambandene. En hovedobservasjon er at batteri-elektriske hurtigbåter foretrekkes i overgangen, men at rekkeviddebegrensninger gjør at de ikke er anvendbare for et betydelig antall av sambandene. Hydrogenfartøy utfyller rekkeviddebegrensningene ved batteri-elektriske fartøy, men resultatene viser at de er betydelig dyrere å drive på grunn av (muligens pessimistiske) sikkerhetstiltak. Når seilingshastigheten for hver rute optimaliseres, reduseres ulempene ved nullutslipps-energibærerne noe. Generelt sett er imidlertid rensekostnadene langt høyere enn hva den norske regjeringens foreslåtte CO_2-avgift antyder, selv om det er store variasjoner mellom rutene, der noen ruter er svært kostbare å konvertere og noen er lønnsomme å konvertere. Til slutt viser en analyse av regjeringens forslag om at alle nye anbud for hurtigbåtsamband skal ha nullutslippsløsninger, fører til en betydelig økning i totale kostnader sammenlignet med en mer gradvis overgang. Derfor må forslaget vurderes nøye. Kommende teknologi for nullutslipps-hurtigbåter virker imidlertid lovende med tanke på begrensningene som er funnet i denne avhandlingen, og det bør således undersøkes videre hvordan disse påvirker overgangen.

Table of Contents

List of Figures

List of Tables

Abbreviations and Terminology

Abbreviations

CAPEX	Capital Expenditures
DP	Dynamic Programming
HSV	High-Speed Passenger Vessel
IMO	International Maritime Organisation
MGO	Marine Gas Oil
MILP	Mixed Integer Linear Programming
NTNU	Norwegian University of Science and Technology
OPEX	Operational Expenditures
OR	Operations Research
SPPRC	Shortest Path Problem with Resource Constraints
TØI	Institute of Transportation Economics
ZE	Zero-Emission
ZEVIPP	Zero-Emission (Passenger) Vessel & Infrastructure Planning Problem
ZEVS	(Enabling) Zero Emission (Passenger) Vessel Services

Terminology

Bunkering alternatives	The permutations of candidate bunkering ports and the infrastructures types possible to install at these ports
Bunkering port	A port along or nearby a route where it is possible to install bunkering infrastructure

Main port	A resting port where at least one of the vessels serving the route must start and end the operating day
Resting port	A port in a route where vessels may stop between scheduled trips
Route	A connection between ports
Route-serving permutations	The permutations of vessel types and bunkering alternatives for a route
Service frequency	The number of times a sub-route is serviced during an operating period
Sub-route	A connection between a subset of the ports in a route. The sub-routes of a route constitute all the possible ways the ports in a route can be visited
Time step	A point of time in the long-term planning horizon where a short-term planning period occurs

Chapter 1

Introduction

In 2019, the Norwegian Government launched a plan for fossil-free public transport towards 2025 (Norwegian Ministry of Transport & Norwegian Ministry of Climate and Environment, 2019) and an action plan for how to make public maritime transportation green (Norwegian Ministry of Transport et al., 2019). These plans are designed to contribute to Norway's climate obligations towards the Paris Agreement by 2030 and 2050. In particular, the plans highlight a Zero-Emission (ZE) transition for High-Speed Passenger Vessel (HSV) as a focus area in the coming years due to their intensive emission profiles per passenger served. Further, contracts for HSV connections typically span over periods from eight to ten years, and the majority of the current contracts are set to expire in 2025 or 2030 (Statens Vegvesen, 2022). The Norwegian Ministry of Transport recently proposed that all new HSV service tenders shall be emission-free (Tveit et al., 2023). Hence, providing sufficient decision support to the transition as soon as possible is key to reaching the climate obligations.

The preliminary assessment by Aarskog et al. (2020) concludes that $\frac{1}{3}$ of the existing HSV routes in Norway can be served by fully electric powertrains, considering limitations of battery weight and charging availability, while the rest of the routes can be served by compressed hydrogen. The subsequent feasibility study by Sundvor et al. (2021) concludes with somewhat more pessimistic estimates, albeit with the remark that optimization of routes and timetables with respect to the alternative energy carriers likely will increase the potential. This remark has since been supported by Havre, Lien and Ness (2022) and Berg et al. (2022). Nevertheless, the Government seeks to base its climate politics on cost-effective and market-based measures (Norwegian Ministry of Transport & Norwegian Ministry of Climate and Environment, 2019), thus pilot projects such as the fully electric HSV "MS Medstraum" (Skipsrevyen, 2022) and the future hydrogen-fueled connection between Bodø and Lofoten (Danielsen et al., 2022) are integral to assessing the actual competitiveness of the alternative solutions.

This Master's thesis studies a set of given routes operated by HSVs and provides decision support for fleet design and localization, and possibly co-localization and co-utilization, of bunkering infrastructure for the routes. Moreover, it considers a long-term horizon for these decisions and provides a sequential plan for how the transition can be completed optimally. Following the recent international and national ambitions to reduce greenhouse gas emissions from the maritime sector, the thesis only considers ZE energy carriers for new vessels and infrastructures. More specifically, the ZE energy carriers considered are compressed hydrogen and electric (swappable) batteries, while the current fleet may also include Marine Gas Oil (MGO). The compatible infrastructures for hydrogen are large-scale production facilities that distribute hydrogen to filling stations, the mentioned filling stations, and local small-scale production facilities. For electric (swappable) batteries, a battery bank charging station and a battery swap system are considered. The problem at hand is referred to as the Zero-Emission (Passenger) Vessel & Infrastructure Planning Problem (ZEVIPP). The objective of the ZEVIPP is to maintain the service level of the set of routes while minimizing the total system costs, which comprise vessel and infrastructure investment costs, operating costs, and passenger costs, across the long-term planning horizon. In particular, as the ZEVIPP is exposed to uncertain information about the future, the objective is minimized taking

different scenarios into consideration.

Due to its complexity, the ZEVIPP is formulated and modeled as a combination of a two-stage stochastic Mixed Integer Linear Programming (MILP) focusing on the strategic and tactical decisions of the problem, and a MILPs for the operational decisions of the problem. Congruent with the recent hydrogen initiatives in Nordland County, the 20 HSV routes in the county form the basis for the case study conducted in the thesis. Nordland County spans a large area in the north of Norway and has a long coastal line that includes many islands of which a great proportion relies on HSV services to connect with the mainland. Nordland is also the county in Norway with the most HSV connections (Statens Vegvesen, 2022). Moreover, the routes have remarkably different load profiles; the daily distance covered by a route varies between 90 - 570 km, and the daily passenger demand for a route varies between 3 and 225 passengers. Therefore, the solutions derived help reveal how the assessed energy carriers can complement each other to increase the replacement feasibility and contribute to the assessment of whether holistic planning across a set of routes can mitigate the gap in cost-effectiveness to current solutions.

Existing studies on the particular problem are, to our knowledge, restricted to the studies by Havre, Lien, Ness et al. (2022), Havre, Lien and Ness (2022), and Berg et al. (2022), and to some extent the studies by Štádlerová and Schütz (2021), Štádlerová et al. (2022), and Štádlerová et al. (2023). This thesis extends their work by a range of novelties added. The perhaps most important extension is that the problem now is considered for multiple periods comprising a long-term planning horizon, factoring in uncertainty about future markets and time-dependent ZE regulations. This drastically increases the robustness of the proposed results. Among other notable novelties are the inclusion of multiple hydrogen hubs, the possibility for multiple bunkering ports for each route, and the inclusion of electric battery-swapping infrastructures and vessels. Taking the feasibility studies by Aarskog et al. (2020) and Sundvor et al. (2021) and the abovementioned studies into consideration, these extensions contribute to the research by investigating how more holistic planning of the transition to ZE HSV services can limit the feasibility and optimality gap to conventional CO_2 emitting HSV services. Additionally, the proposed solution approach contributes to the range of decomposition literature within public transport problems.

The outline of the thesis is as follows. First, Chapter 2 puts the problem at hand in its context and provides sufficient background knowledge to understand the problem definition. Then Chapter 3 defines and introduces the ZEVIPP by describing its assumptions and main components. In addition, the decisions for the different planning levels of the problem are described. Next, Chapter 4 displays relevant literature for similar problems, explains how certain components have been adopted in the formulation of the ZEVIPP, and discusses how the ZEVIPP separates from other problems. Moreover, it details the contributions of this thesis. Further, the periodization and decomposition of the ZEVIPP into a Master Problem and Sub-Problems is described in Chapter 5. Then the mathematical formulation of the Master Problem and explanations of its notation, objective function, and constraints, is presented in Chapter 6. In Chapter 7, the Sub-Problems are introduced and formulated. Chapter 8 presents the input data and test instances used in the implementation of the model. The results from the solutions for the test instances are then presented and analyzed in Chapter 9 to provide managerial insights. Ultimately, Chapter 10 draws the main conclusions from the thesis, before Chapter 11 proposes how the Master's thesis can be utilized in further research.

Chapter 2

Background

This chapter provides context for the problem at hand by elaborating on the possible climate-neutral technologies that may accommodate the Zero-Emission (ZE) transition for High-Speed Passenger Vessel (HSV), as well as describing possible factors that can impact these technologies. The chapter is an extension of the background provided by Berg et al. (2022).

First, Section 2.1 provides background for the HSV services, both on an international and a national level. In Section 2.2, the initiative to which this thesis belongs, (Enabling) Zero Emission (Passenger) Vessel Services (ZEVS), is further introduced. Next, Section 2.3 highlights the potential energy carriers that can be exploited in the transition, while Section 2.4 describes the respective carriers' compatible infrastructure types. Section 2.5 displays some examples of the current ZE initiatives in the HSV service industry.

2.1 High-Speed Passenger Vessels

During the last decades, HSVs have seen great improvement and have been important for serving commuters and for connecting coastal areas, in particular between islands and the mainland. As Cass (1985) points out, many HSV services have traditionally been subsidized, depending on the purposes of the services. For instance, in Scandinavia and Italy, the federal governments have a policy of providing HSV service to outlying islands and hence subsidize that service. On the contrary, in the Hong Kong area where the vessel services are mainly supplementary to the cross-harbor traffic but also connect smaller islands, the services are only implicitly subsidized by cross-route bundling (Wang & Lo, 2008).

On a national level, Brødrene Aa AS and Fjellstrand AS are among the most prominent shipyards. Brødrene Aa AS has great traditions within the industry and does also have an international presence; recently, it delivered three high-speed catamarans to the Hong Kong-based company Zhongshan-Hong Kong Passenger Shipping Co-op Co., Ltd (ZS) (Brødrene Aa AS, 2017). Fjellstrand AS has established itself as a pioneer within battery-electric vessels by delivering both the *MS Ampere* and *MS Medstraum* (Fjellstrand AS, 2023), which will be introduced in detail in Section 2.5.1. Internationally, the Netherlands-based company Damen and the Australia-based company Austal are among the most notable HSV manufacturers.

According to the latest greenhouse gas (GHG) study conducted by the International Maritime Organization (IMO, 2020), the share of shipping emissions in global anthropogenic emissions has increased from 2.76% in 2012 to 2.89% in 2018. Emissions are projected to increase from about 90% of 2008 emissions in 2018 to 90-130% of 2008 emissions by 2050 for a range of plausible long-term economic and energy scenarios. IMO's ambition related to a 2008 emission baseline is to reduce CO_2 emissions per transport work (carbon intensity) by at least 40% by 2030 and reduce the total annual GHG emissions by at least 50% by 2050. However, the IMO GHG study demonstrates that whilst further improvement of the carbon intensity of shipping can be achieved, it will be

difficult to achieve IMO's 2050 GHG reduction ambition only through energy-saving technologies and speed reduction of ships. Therefore, under all projected scenarios, in 2050, a large share of the total amount of CO_2 reduction will have to come from the use of low-carbon alternative fuels. Taking into consideration that HSVs' energy demand per pax-kilometer is considerably larger than for other transportation modes, e.g., 50% higher than jet aircrafts and 300% higher than passenger cars, the HSVs emerge as candidates with significant potential for reducing emissions (Godø & Kramer, 2019).

In Norway, multiple innovative initiatives have begun in order to facilitate and research the transition towards ZE solutions in the sector. The world's first electrical car ferry, MS Ampère, was launched in the county of Vestland in 2015 (Ship-Technology, 2015), while the first liquid hydrogen-driven ferry MS Hydra was launched in 2020 (FuelCellWorks, 2020). In the spring of 2022, Yara launched the world's first fully electric and autonomous container vessel with ZE, MV Yara Birkeland (Yara International ASA, 2022). Sundvor et al. (2021) have studied the replacement potential of Norwegian HSVs with ZE solutions, based on the existing Norwegian fleet in 2018. The feasibility study concluded that 51 out of 73 HSVs in operation, amounting to 60% of the total energy demand, were most suitable for hydrogen propulsion, with 12 vessels also suitable for battery-electric propulsion. However, it also concludes that optimizing and adapting the vessel services and routes to balance out the limitations of the ZE technology is required to reach Norwegian ZE public transport targets. On a political level, The Norwegian Ministry of Transport recently proposed that all new HSV service contracts shall be emission-free (Tveit et al., 2023). This outlines some of the motivations for carrying out this thesis.

2.2 ZEVS

The interdisciplinary project ZEVS is a prominent research initiative on how to support the Norwegian government's objective to uptake fossil-free HSVs and foster a more sustainable transport system and is thus funded by The Research Council of Norway as part of the ENERGIX program (The Research Council of Norway, 2021). The project, which is managed by the Institute of Transport Economics, spans four years from early 2021 to late 2024 and is distributed over six work packages. These work packages are shown in Figure 2.1. It is implemented in collaboration with the Institute of Energy Technology, the Norwegian University of Science and Technology, and KU Leuven (Belgium). The project comprises 15 user partners from the public sector and the industry: Ministry of Local Government and Modernization; Norwegian Coastal Administration; Norwegian Maritime Authority; Norwegian Environment Agency; Viken, Rogaland, Møre og Romsdal, and Nordland county Governments; Ruter; Skyss/Kringom; Brødrene Aa AS; Statkraft Energi AS; SEAM AS; MHTech; and SES-X.

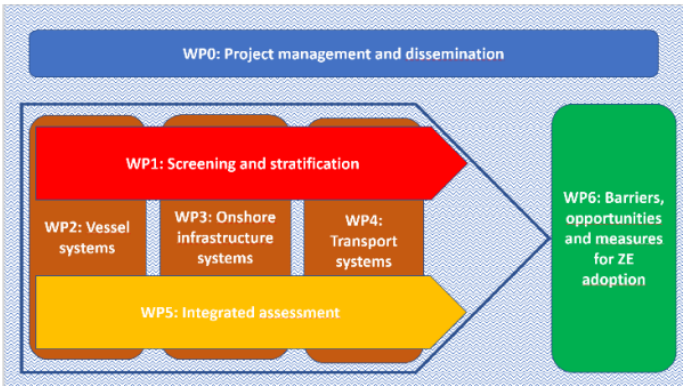

Figure 2.1: The work package structure of the project - illustrating how ZEVS will promote the transition from brown to green energy.

Overall, ZEVS will prepare an overview of technical possibilities and abatement costs, which enables the decision-makers and stakeholders to identify where ZE solutions are manageable and how the costs of ZE requirements are distributed among regions. The overview will be based on tools for

energy and emission calculation, cost optimization of infrastructure and transport services, and visualization that will be developed by the project and published open access. ZEVS will also provide a handbook to help County Governments find cost-effective procurement and business models to limit added costs of ZEs transport.

This thesis aims to contribute to work package 5. This package takes a holistic approach to the ZE transition and aims to make integrated assessments of the prior work packages and make generalized insights based on these. More specifically, the thesis will support the research question "Can integrated transport and energy planning improve feasibility and lower abatement costs?". That is, results from work packages 1-4 will be adapted to optimize and co-localize vessel services based on grouping of technical feasibility and to develop an integrated service that enables co-localization of bunkering stations.

2.3 Energy Carriers

This section describes four candidate energy carriers to consider for HSVs. Among them are three promising candidate ZE energy carriers that may serve as alternatives to conventional fossil fuels and consequently can help accommodate the transition toward ZE HSV services. First, Section 2.3.1 introduces the conventional energy carrier, Marine Gas Oil (MGO). Next, Section 2.3.2 outlines what electric battery technologies that exist, and what developments are being made. In Section 2.3.3, hydrogen alternatives are described and discussed, before Section 2.3.4 elaborates on the use of ammonia.

2.3.1 MGO

MGO, or marine gas oil, is currently one of the most popular energy carriers for HSVs due to its relatively low emissions of sulfur and nitrogen oxide. According to a report by DNV GL (DNV GL AS Maritime, 2019), MGO is a distillate fuel with a sulfur content of 0.1% or less, which makes it a cleaner-burning fuel than heavy fuel oil (HFO), which typically has a sulfur content of 3.5% or more. This lower sulfur content results in significantly lower emissions of sulfur oxide, nitrogen oxide, and particulate matter, which can have significant environmental and health implications. Furthermore, MGO is compliant with the IMO sulfur emissions regulations, which mandate that all vessels must use fuels with a sulfur content of 0.5% or less (IMO, 2016). As a result, MGO has become an increasingly popular fuel choice for HSVs looking to minimize their environmental impact. In Norway, the vast majority of the HSV fleet uses MGO as the energy carrier (DNV GL AS Maritime, 2018).

2.3.2 Electric Batteries

Sundvor et al. (2021) showed that the electric battery technologies available at the moment restrict the number of feasible routes for battery replacements significantly. Specifically, the report found that only 12 out of 73 vessels operating along the Norwegian coast were candidates for replacement. This low replacement potential can be explained by the relatively low energy densities of today's battery technologies compared to the conventional solutions, thus it is required substantial weight increases in order to operate longer routes. However, the report did not consider the optimization of route structures or timetables with respect to the alternative technologies investigated, which possibly could improve the feasibility potential.

In the context of HSVs, there are nevertheless several factors that appear advantageous for electric batteries. Ianssen et al. (2017) point out that battery-electric vessels are preferable for operations with large variations in load, which often is the case for passenger vessels. Additionally, passenger vessels are frequently docked and thus do potentially have many slots in which they can charge if there is installed extensive charging networks. Moreover, they operate "noise-friendly" and are less exposed to maintenance requirements

Power availability does however remain a big problem, as local grid capacities, in particular on islands and in rural areas, are limited compared to the energy demand of the route profiles (DNV GL AS Maritime, 2019). This limitation includes not fully utilizing the potential of fast charging. To compensate for these limitations, both Ianssen et al. (2017) and DNV GL AS Maritime (2019) propose an on-shore battery bank solution where the battery bank recharges at low power, which does not require large expansion of the grid, and serves high-power output. Applications of this technology are detailed in Section 2.4.2.

2.3.3 Hydrogen

Hydrogen has the potential of being an emission-free fuel if it is produced from renewable energy resources, and Sundvor et al. (2021) conclude that around 60% of the conventional vessels in the study were subject to hydrogen replacement given the assumptions in their report. Additionally, the energy profiles of passenger vessel routes appear to fit well with hydrogen production as large proportions of the total energy demand are concentrated around junctions, which might enable large-scale hydrogen production at these locations. This is further described in Section 2.4.3.

The technology to produce hydrogen is relatively mature. Today, nearly all hydrogen is produced by processing natural gas (DNV GL AS Maritime, 2019). However, there are emerging ZE methods such as processing natural gas produced by carbon capture and storage (CSS) or by producing it through electrolysis of water. Currently, the Norwegian company NEL is a major player and researcher in several parts of the hydrogen value chain (NEL Hydrogen, 2022).

On the other hand, the employment of hydrogen in the maritime sector is still very immature. Today, hydrogen is most efficiently utilized in fuel cells with an efficiency typically around 50-60% (DNV GL AS Maritime, 2019), however with the possibility to exploit some of the energy loss for vessel heating (Ianssen et al., 2017). Further, Ianssen et al. (2017) emphasize some lacking assessments of hydrogen operation at sea; for instance, how salts impact the fuel cell processes, what safety measures are required, what infrastructure network needs to be installed, and how the hydrogen should be stored on the vessel. The latter does in particular impose a large limitation. With today's technology, which mainly consists of storing hydrogen as compressed gas or as liquid, hydrogen seems limited to shortsea shipping due to high onboard storage costs (DNV GL AS Maritime, 2019).

2.3.4 Ammonia

Ammonia, which traditionally has been used to produce fertilizers in agriculture, has received significant attention as a potential marine energy carrier in the last decade. DNV GL AS Maritime (2019) concludes the following about ammonia as a possible marine fuel:

> "With an energy transition to renewables, ammonia will have the potential to become a carbon-free energy carrier with higher density than hydrogen, and in principle technically feasible for deep sea. However, the current maturity is low and green ammonia is expensive, limiting the feasibility of use as an alternative fuel. Moreover, the lack of a bunkering infrastructure represents a barrier to using ammonia as an alternative marine fuel and is likely to remain a barrier for a long time while the market matures. Similarly to hydrogen, GHG emissions from ammonia remains high with the current production from fossil energy sources without CCS, until the transition to renewable power production is well underway. However maritime projects opting for ammonia may ensure the use (and contribute to increased production) of ammonia produced from renewables, at the expense of higher costs and likely slower uptake. It should also be noted that costs for required safety systems and mitigating measures(considering the toxicity of ammonia) may represent additional costs."

Nevertheless, Atchinson (2021) foreshadows the potential of utilizing already existing infrastructure to transport ammonia on a large scale without the need for compression, which yields a significant

advantage compared to hydrogen.

2.3.5 Comparison of Energy Carriers

Out of the potential energy carriers described, the ones considered in this thesis are MGO, electric LI-ion batteries, and compressed hydrogen (200 *bar*). These energy carriers are selected based on several factors, including energy density, maturity and availability, and the potential to support the transition toward ZE HSV services.

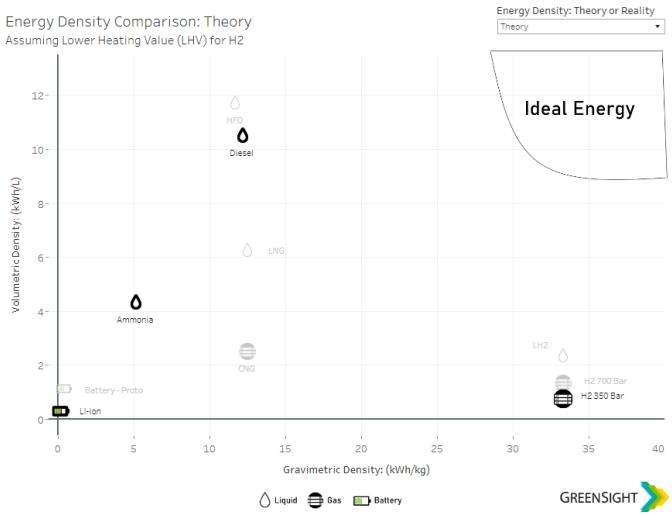

Figure 2.2: Comparison of theoretic energy densities for the energy carriers with respect to volume and weight. The plot is developed by Greensight (2021).

MGO is included as the majority of the current Norwegian HSV fleet consists of conventional vessels using the energy carrier. As MGO is comparable to diesel in terms of density, Figure 2.2 shows that it has a high energy density, especially with regard to volume, which is attractive to HSVs. The MGO supply chain is also well-established, with a very mature infrastructure for production, storage, and transport. The obvious drawback of the energy carrier is that it does indeed pollute. Additionally, the MGO price comes with a supplementary CO_2 tax that is expected to increase in the future in line with the environmental regulations. The MGO price itself is quite uncertain as it is a distillate from crude oil.

The electric LI-ion battery is a highly efficient ZE energy carrier (see Figure 2.3), making it an attractive option for reducing emissions from HSVs. The electric LI-ion battery is also relatively mature and cheap, and has in recent years been put into operation in several passenger- and car vessels. Some examples of these are detailed in Section 2.5. However, as seen in Figure 2.2 the rather large drawback of the electric LI-ion battery is its poor energy density, which leads to a limited range. Traditionally, long charging times have made it not so suitable for HSVs that require fast and frequent travel. The charging time drawback is however on its way to being mitigated, as is elaborated on in Section 2.4.2.

Compressed hydrogen (200 *bar*) is also a promising ZE energy carrier for HSVs, especially for medium-to-long-range applications. In terms of density, it is quite comparable to the electric LI-ion battery. Figure 2.2 shows they are more or less equal with regard to volumetric energy density. Compressed hydrogen does however have far higher gravimetric energy density, allowing for more efficient sailing. Compressed hydrogen is also a mature technology in general, with relatively established production, storage, and transport infrastructure. In the maritime sector, it does however remain quite immature and there are concerns regarding safety measures both onboard and onshore. While the cost of producing and storing compressed hydrogen is currently high, it is expected to decrease as production scales up, making it a more cost-effective option in the future. Both hydrogen and the electric LI-ion battery are dependent on electricity prices, which in general

are uncertain and are expected to fluctuate in the future.

Despite having a relatively high energy density, ammonia was not included due to its expected price and immature position in the maritime sector, both currently and in the foreseeable future.

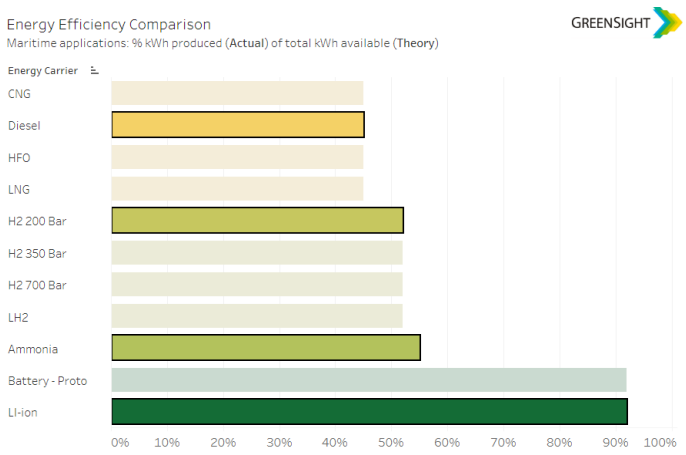

Figure 2.3: Comparison of energy efficiencies of the energy carriers. The plot is developed by Greensight (2021).

2.4 Infrastructures

This section outlines the compatible infrastructure types of the energy carriers considered in the thesis, i.e., MGO, electric (swappable) batteries, and compressed hydrogen. In this thesis, an *infrastructure* is used as a common term denoting a facility at a point that can produce and/or supply energy to vessels. Section 2.4.1, Section 2.4.2, and Section 2.4.3 detail the possible MGO, battery-electric, and hydrogen infrastructures, respectively.

2.4.1 MGO Filling Station

The technology behind MGO filling stations is very similar to that of regular petrol stations and the market is very mature. Typically, there are large terminals located in the major ports, while the remaining part of the coast is covered by delivery points that are supplied with fuel from the terminals. The stations usually have large storage tanks. Bunkering then happens by transferring MGO to the vessel via a hose or pipe that connects the filling station to the vessel's fuel intake system.

In Norway, Bunker Oil is the company with the most delivery points of marine fuel, and in particular MGO, along the Norwegian Coast. With main terminals located in Tromsø, Hammerfest, Båtsfjord, Bergen, Kirkenes, Sløvåg, and Tananger, they also cover the coast with approximately 30 more delivery points (Bunker Oil, 2023).

2.4.2 Electric Infrastructures

Vessels using battery-electric propulsion systems usually recharge their batteries from a battery bank charger, but there also exists a technology for swapping the entire onboard batteries with fully charged batteries from the onshore electric bunkering infrastructure. The second alternative is referred to as a battery swap system and will be explained later in this section.

In 2021 there were 61 battery chargers for maritime transport in Norway (SSB, 2021). The technology is under development and the technical designs vary from port to port since there is little standardization and different requirements among the different vessels (Danebergs et al.,

2023). Typical charging effects required by vessels are in the range between 0.5 and 5.0 MW (Karimi et al., 2020).

A battery charger can either be conductive or inductive, and it has to be connected to the power grid. The conductive charging technology is mature and does arguably work well. On the contrary, inductive charging has some clear benefits regarding convenience and limiting the proneness of mechanical wear and tear. In addition, inductive charging is more compatible with autonomous systems that can reduce docking time and are safer to use as they do not require manual interference. However, inductive charging tends to be less efficient than conductive charging, as factors such as distance and angle can impact the efficiency severely (Karimi et al., 2020).

An emerging technology is onshore battery packs/banks for charging stations. The aim of onshore battery banks is to make it possible to bunker at high power, limiting the total charging time for battery-electric vessels. Karimi et al. (2020) state the following benefits and drawbacks:

> "Utilizing the onshore battery reduces the stress of handling high charging power on the local grid and can allow for reducing the total electricity cost by charging during off-peak hours. On the other hand, drawing the charging power from the onshore battery bank is less energy efficient than using the grid because of the energy loss generated by the additional power electronics converters to interface the onshore battery and the battery itself. In other words, using energy buffers such as onshore battery packs generate additional energy loss in the process of charging and discharging of onshore batteries."

In the later years, battery swap systems have emerged. Battery swap systems utilize the same battery technology as onshore battery bank chargers, but instead of recharging battery-electric vessels from the onshore battery bank, the entire battery is swapped with the onboard discharged battery. An example of how this can be implemented is described in Section 2.5.2. The main benefit of this method is that it can be performed within three minutes, as opposed to other charging systems (Danebergs et al., 2023). Charging of the stationary onshore batteries can be performed outside peak hours without the need for expensive high-power converters for fast charging. However, the process requires large robotic equipment, and multiple battery packs are needed to perform battery swaps frequently (Karimi et al., 2020).

Based on these descriptions and signals from the industry, the infrastructures for electric batteries considered in this thesis are on-shore battery banks with inductive charging and battery swap systems. Note that although the LI-ion electric battery in principle is applicable for both these infrastructure types, there are some practical differences in how the battery must be designed to be used by battery swap systems. Hence, throughout the thesis, the LI-ion electric batteries will be treated as two separate energy carriers; regular electric batteries and electric swappable batteries. Their respective bunkering infrastructures will be referred to as electric charging infrastructures and battery-swapping infrastructures.

2.4.3 Hydrogen Infrastructures

An on-shore design for refueling buses is described in Hancke et al. (2020), where the key components are supply, storage, and dispensing. The supply can either be from on-site water electrolysis or off-site external supply from tube trailers. The storage consists of both high-pressure and low-pressure storage tanks, and compressors to maintain and regulate the pressure levels. Dispensing is what this thesis refers to as bunkering of hydrogen, and it can be performed with what is called slow or fast filling. The type of filling determines the bunkering time, the necessary equipment, and the incurred costs. Fast filling is done using a cascade technique, meaning that hydrogen is filled with low pressure first before bunkering hydrogen at a higher pressure. The cascade technique speeds up the process, but increasing the pressure heats up the hydrogen. Therefore, pre-cooling systems are required to perform the fast filling. In addition, an empty tank has low pressure since hydrogen has to be completely separated from the environment. Therefore, additional pre-cooling

is also required to fill a tank with low levels of hydrogen, because the filling process will increase the pressure and temperature.

The *Next Wave* is a project aiming to make a plan for a roll-out of fuel cell buses in the Nordic Region. This approach is also applicable to the maritime supply of hydrogen. The project states the following about how to supply hydrogen refueling stations:

> "The use of tube trailers may be the first step in building the hydrogen infrastructure. Then, when the demand has increased, they can be partially replaced by pipelines, on-site electrolyzers, or with liquid hydrogen supply options. Tube trailers can also complement the on-site production of hydrogen in hydrogen refueling stations, increasing the security of the hydrogen supply. The hydrogen tube trailers or gas containers are flexible and may first serve one location before being moved to serve another location later on." (Next Wave, 2021)

It is most cost-efficient to centralize production and produce on a larger scale to benefit from economies of scale. However, if the distance between the hydrogen filling station and the central production facility is large enough, and the demand is sufficient, then a smaller local production facility is an alternative (Next Wave, 2021).

Thus, the candidate infrastructure types in the thesis can be summarized into three types. The first is a local production facility that also provides a bunkering possibility for vessels. The second is a hydrogen filling station that is supplied by an external source by truck. The third alternative is a large-scale hydrogen production plant that produces a large amount of hydrogen that is distributed to hydrogen filling stations.

Throughout the thesis, the hydrogen supply chain is assumed emission-free.

2.5 ZE Initiatives

This section provides four examples of initiatives that help accelerate the transition towards ZE solutions for HSVs.

2.5.1 Medstraum

Having already launched the world's first fully battery-electric ferry back in 2015, the Norwegian shipyard Fjellstrand AS delivered the world's first fully battery-electric HSV, MS Medstraum, in July 2022. The vessel is operated by the shipping company Kolumbus and provides passenger service between the city of Stavanger and surrounding communities and islands (Skipsrevyen, 2022).

The vessel, which can take 150 passengers (including crew), has a super-efficient catamaran hull and has a service speed of 23 *knots* (top speed is 27 *knots*), with propulsive efficiency of around 80%. Moreover, the vessel saves GHG emissions by approximately 1500 *tons* per year. Consequently, MS Medstraum presents the future ZE fast ferry concept for safe and efficient passenger transport for the surrounding areas for cities by the sea and was acknowledged with the "Ship of the Year" award by the Norwegian ship magazine, Skipsrevyen (Skipsrevyen, 2022).

Figure 2.4: "Ship of the Year 2022", MS Medstraum, photo courtesy of Marius Knutsen/Maritime Cleantech

2.5.2 Autonomous Battery Swap Project

As motivated in Section 2.3.2 and introduced in Section 2.4.2, measures to compensate for limited on-shore power availability can help increase the potential of battery-electric vessels. For over 2 years, a Norwegian supplier of hybrid and fully electric solutions to ships and the maritime business, SEAM, and a Norwegian shipping company, Norled, have been working on a joint project in the conceptualization and development of a new battery solution for electric express boats (SEAM, 2021). The system is expected to be realized by 2024. According to SEAM (2021):

> "The new system, which Norled has coined as Autonomous Battery Swap (patent pending), will be able to not only maintain the high speed of an express boat but also provide a more even and pragmatic approach to charging batteries at quays. Autonomous Battery Swap is a robotic charging station that swaps out batteries on express boats while at the quay. One part stands permanently on the quay, with its' own battery station. The other is mounted on the boat, with two battery packs on a turntable. The battery station will be able to swap out the empty batteries with fully charged batteries in three minutes."

The system allows for electrifying both new and existing vessels without installing big, heavy battery packs on each boat. Lower weight yields lower fuel consumption, giving greater environmental advantages and lower operating costs. A concept illustration of the system is provided in Figure 2.5.

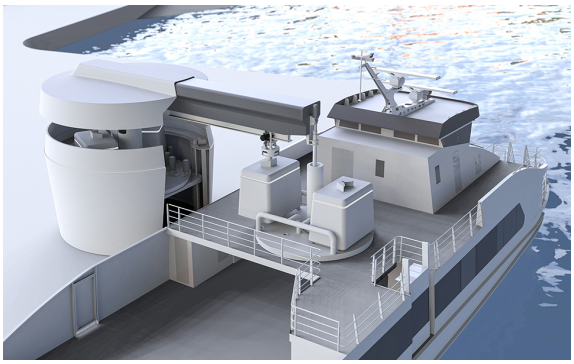

Figure 2.5: Concept illustration of the Autonomous Battery Swap system, illustration courtesy of Norled.

2.5.3 Hydrogen Pioneer Project in Nordland County

Nordland County, which also is the basis for the case study in this thesis, is set to be the area in which the Norwegian hydrogen economy is enabled. In January 2022, Torghatten Nord and Statens Vegvesen signed a deal worth 5 billion NOK to establish 2 hydrogen-driven ferry connections between Bodø and Lofoten within 2025 (Danielsen et al., 2022). The deal will secure approximately 26 500 *tons* of GHG emission savings yearly. With a yearly liquid hydrogen demand of approximately 5-6 *tons*, the deal further represents a domino effect as multiple hydrogen production projects have been initiated in the aftermath. Sintef estimates that around 30-40 hydrogen projects are planned and several actors have already initiated plans for large-scale hydrogen production in Nordland County (Trygstad, 2022).

2.5.4 Fremtidens Hurtigbåt

In November 2021, four Norwegian counties (Trøndelag, Vestland, Nordland, and Troms og Finnmark) signed development contracts with six ship designers with the aim to create designs for next-generation ZE fast ferries with new technology. The project is partly funded by the Norwegian Environment Agency.

The project has ambitiously requested a ZE vessel with a minimum speed of 30 *knots*, 40 *nautical miles* range, and at least a capacity for 150 passengers. The vessel should also have significantly improved (30% better) energy efficiency compared to regular fast ferries. Lastly, the required bunkering time must be no more than 30 *minutes* per stop (Skipsrevyen, 2021).

One of the competitions within the project is to develop a hydrogen-driven HSV. Currently, three consortia are qualified with their designs. One of these designs is the promising Aero 40 H2, developed by Brødrene Aa and industry partners Westcon, Boreal, and Ocean Hyway Cluster, which is already possible to order. The vessel concept design can be seen in Figure 2.6. It is a hydrogen-electric catamaran ferry designed to carry some 300 passengers. The vessel can store up to 600 kg of hydrogen, and its twin engines have a total output of 2.6 MW. This allows the ferry to sail up to 100 *nautical miles* at a speed of 32 *knots* without refueling (The Explorer, 2022).

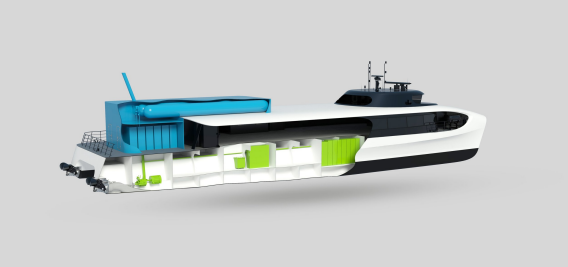

Figure 2.6: Concept illustration of Aero 40 H2, illustration courtesy of Brødrene Aa.

Chapter 3

Problem Definition

This chapter presents and describes the Zero-Emission (Passenger) Vessel & Infrastructure Planning Problem (ZEVIPP). The ZEVIPP is relevant for coastal areas offering High-Speed Passenger Vessel (HSV) services to their inhabitants and where they are planning a transition to Zero-Emission (ZE) services. The problem is typically encountered by governments and counties facing environmental requirements. More specifically, the problem is most relevant for areas with close-proximity routes where co-localization of infrastructure and vessel fleet re-allocation are feasible, which in practice often means routes within a region. Overall, the key decisions in the problem are how to phase in HSVs and associated infrastructures over a long-term planning horizon to cost-efficiently complete the ZE transition of HSV services.

In Section 3.1, the main inputs and the relevant assumptions of the problem are described. Section 3.2 presents the scope of the problem through its objective function, decisions, and constraints. Ultimately, Section 3.3 presents an example solution to the problem. Note that the chapter extends the problem definition presented by Berg et al. (2022).

3.1 Problem Input and Assumptions

In total, the ZEVIPP contains four main categories of input data: ports, routes, vessels, and infrastructures, all of which contain unique properties.

Ports and Routes

A *route* is a connection between ports and is defined by its four main components: a required *main port*, possible *regular port(s)*, possible *resting port(s)*, and *sub-route(s)*. A route has one or more sub-routes that constitute the possible ways the ports in the route can be visited. Each sub-route must start/end in the main port or in a resting port. I.e., main ports and resting ports are ports where vessels may stop for a longer period of time, typically between scheduled trips, with the only difference being that at least one vessel operating the route must start and end the short-term planning period at the main port. The remaining, regular ports are the ports that are just shortly visited during trips for embarking/disembarking, similar to bus stops (approx. 3 *min*). Note that a route does not necessarily have resting ports or regular ports, but requires a main port. All of the abovementioned components are provided as input to the problem. Figure 3.1a illustrates an example route with its main components. The route consists of a main port, one resting port, and two regular ports, all of which can be visited according to the sub-routes defined on the right-hand side. The two left-most sub-routes are trips between the main port and the resting port, while the two right-most sub-routes are round trips starting and ending at the same port.

Service frequency is defined as the number of times a sub-route in a route is serviced during an operating period (within the short-term planning period). Figure 3.1b illustrates the service frequencies during an example operating period of six hours for the four sub-routes comprising the

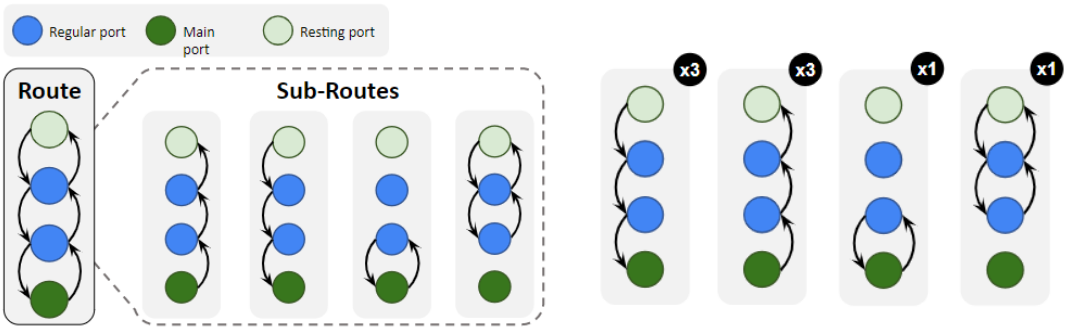

(a) Example route and its main components

(b) Example of frequencies to be served for each sub-route in an operating period of six hours

Figure 3.1: Example route and its service frequencies

example route in Figure 3.1a. The respective frequencies are denoted with a number above the sub-route. Service frequencies are given as input to the problem according to a timetable and it is assumed not possible to deviate from these.

For each sub-route, there is a given passenger demand for the short-term planning period. These demands are assumed to be (perfectly) inelastic and equal the current demands for HSV service specifically. In other words, they are expected to be fully met. As a consequence, it is assumed to be penalty costs associated with unmet demand. To further incentivize a good service level, it is assumed to be a passenger value of time during transit. This value is assumed to be constant per time unit. Thus, there are passenger time costs calculated based on the total time a vessel spends serving a route, the number of passengers on board, and the passenger value of time. On that note, remark that waiting time costs are not considered.

Having defined routes, the *set* of such routes can be introduced. Typically, the routes in the set are located within close geographical proximity and sometimes share ports. Figure 3.2 illustrates how three routes are combined into a set of routes. Recall that each of the routes has its own main components, such as sub-routes. In fact, Route 3 here is similar to the example route from Figure 3.1a. From the figure, one can see that Route 3 has two intersecting ports with Route 1 and Route 2. Route 3 and Route 2 both have their main port in the same port. The shared port between Route 3 and Route 1 is a regular port for Route 1, while it is a resting port for Route 3.

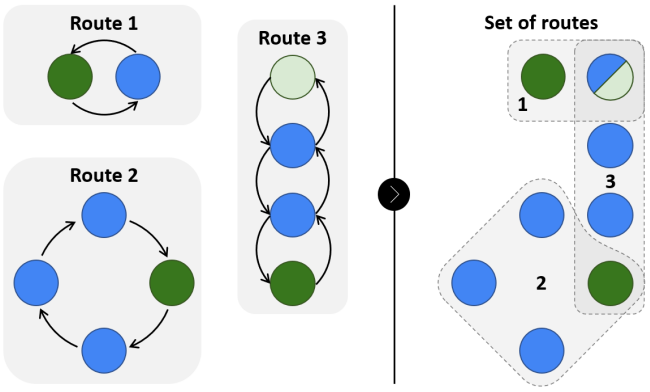

Figure 3.2: Example set of routes

Vessels

The problem also takes a set of candidate *vessels* as input. A candidate vessel has several associated attributes. Based on Chapter 2, a vessel's energy carrier can either be Marine Gas Oil (MGO),

electric batteries, electric swappable batteries, or hydrogen. All vessels have a lower energy level bound to secure enough energy available in case of unforeseen weather conditions, etc., in addition to an upper energy level bound limited by the energy storage capacity of the vessel. Moreover, there are energy carrier-dependent energy level bounds. Vessels with (swappable) electric batteries have energy level bounds to preserve and prolong the life of the batteries. Similarly, hydrogen vessels have energy level bounds to avoid significant increases in bunkering costs due to high or low pressure in the storage tanks. Further, all vessels have energy consumption rates for given speeds. To reduce problem complexity and based on current HSV services, it is assumed that each route can be serviced by only one *vessel type*, i.e., one specific vessel design. Nevertheless, it is possible to serve a route with multiple vessels of similar vessel type. Further, salvage value for vessels is neglected, but it is possible to reallocate vessels across routes. Lastly, vessels are associated with crew shift costs that are dependent on passenger capacity and energy carrier; larger vessels incur more personnel for each shift, while hydrogen vessels also need security measures which are calculated into the cost. Crew shifts last for six hours.

Infrastructures

As described in Section 2.4, there are six *infrastructure archetypes* considered, summarized in Table 3.1. There may be several instances of each infrastructure archetype with minor variations, but the archetype defines the main operational attributes. For MGO-driven CO_2 emitting vessels, there is an associated conventional infrastructure archetype. For battery-electric vessels and electric battery-swapping vessels, the two associated bunkering infrastructure archetypes are battery bank chargers and battery swap systems, respectively. However, in this thesis, these are referred to as electric charging infrastructure and battery-swapping infrastructure. On the hydrogen side, there are three infrastructure archetypes: central large-scale hydrogen production hubs, hydrogen filling stations, and local hydrogen production facilities.

<table>
<tr><th>Infrastructure Archetype</th><th>Main Characteristics</th><th>Bunkering Price Components</th></tr>
<tr><td>MGO Filling Station</td><td rowspan="2">Supports bunkering</td><td>MGO price
CO_2 tax</td></tr>
<tr><td>Hydrogen Filling Station</td><td rowspan="2">Electricity price
Energy conversion efficiency
Distribution cost</td></tr>
<tr><td>Large-Scale Hydrogen Production Hub</td><td>Energy-producing</td></tr>
<tr><td>Local Hydrogen Production Facility</td><td rowspan="3">Energy-producing
Supports bunkering</td><td rowspan="3">Electricity price
Energy conversion efficiency</td></tr>
<tr><td>Electric Charging Infrastructure</td></tr>
<tr><td>Battery-Swapping Infrastructure</td></tr>
</table>

Table 3.1: Summary of infrastructure archetypes

All infrastructure archetypes have associated energy storage capacities, while all bunkering-supporting infrastructures are associated with implicitly derived bunkering prices. The components of these prices are listed in Table 3.1 and elaborated on in Appendix A. "Energy-producing" infrastructures have a maximal rate of production. However, how large proportions of this rate are utilizable depends on the available grid capacity at the location. Since there usually is little, if any, currently available grid capacity at the locations, it is assumed possible to expand the grid capacity at the locations. This comes at a cost per MW the grid capacity is expanded together with an upper limit to the expansion. The currently available grid capacity is assumed cost-free to utilize. Further, it is assumed that hydrogen filling stations are supplied daily, possibly by different hubs. All infrastructures are associated with a set of locations where it is possible to install the infrastructure, typically limited by road connection and/or grid availability. Conversely, each route is associated with a set of candidate *bunkering ports*, i.e., the ports along or nearby a route where it is possible to install a bunkering infrastructure. Figure 3.3 displays an example set of candidate bunkering ports, denoted by white triangles, for Route 3 from Figure 3.2. Lastly, it is assumed that once an infrastructure is installed at a location, it cannot be removed again.

Planning Horizons and Uncertainty

The problem is divided into two planning period levels; *short-term planning periods* and a *long-term planning horizon* of a given number of years. The long-term planning horizon is granulated into a number of time steps - these time steps are represented by a short-term planning period of one operating day. During the long-term planning horizon, upper bounds for the share of non-ZE energy consumption are provided as input for the different time steps. There is also assumed a latency of a given number of years associated with infrastructure and vessel investments, meaning that it takes time to install infrastructure and receive procured vessels. Further on, at a given point of time in the long-term planning horizon, new information about some central components of the problem is revealed. The components that are subject to uncertainty are the CO_2 tax, the MGO price, and the electricity price.

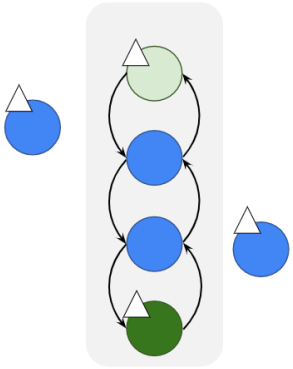

Figure 3.3: Example candidate bunkering ports for Route 3, denoted by white triangles

3.2 Decisions, Objective Function, and Restrictions

3.2.1 Decisions

Given the inputs and assumptions described in Section 3.1, the problem enables decisions on three levels: strategic, tactical, and operational. On the strategic level, the problem includes decisions regarding large investments, i.e., deciding what vessels are procured at what time, when and where to install what infrastructures, and possibly when to expand the grid to support the infrastructure installments. The tactical decisions are how these investments should be allocated; which routes the vessels are assigned to and what bunkering ports are assigned to which routes at what time. Lastly, the operational decisions are related to energy consumption, i.e., deciding when and how much vessels bunker. Consequently, it needs to be decided how much energy is produced to ensure feasible solutions. All of the decisions in the ZEVIPP are summarized in Table 3.2.

Decision Level	Decision
Strategic	Vessel fleet development When and where infrastructures are installed When and how much the grid is expanded
Tactical	Which routes the vessels are assigned to at what time Which bunkering ports the routes are assigned to at what time
Operational	How much energy is produced How much and when vessels bunker

Table 3.2: Summary of decisions in the ZEVIPP.

3.2.2 Objective Function

Following the decisions, the objective of the ZEVIPP is to minimize the total costs of phasing in a ZE HSV service, including the compatible infrastructures throughout the given long-term planning horizon. These costs consist of Operational Expenditures (OPEX) associated with the vessels, Capital Expenditures (CAPEX) associated with the vessels, infrastructures, and grid, and variable energy and passenger costs.

Following how OPEX is defined in shipping, this cost group mainly comprises costs related to crew, maintenance, insurance, dry docking, etc., and can be interpreted as fixed daily costs for

each vessel. These costs are dependent on the total time the vessels are in service. CAPEX includes investment costs for vessels, infrastructures, and the grid. The investment costs for infrastructures and the grid are highly interlinked as it is only relevant to invest in grid expansion for a location if it unlocks more possible infrastructures to install at the location. The energy cost group is divided into two subgroups; bunkering costs for vessels and energy production costs for infrastructures. Since there is no incentive to produce excess energy and it is assumed that the operator handles both energy production and energy consumption, the bunkering costs equal the energy production costs (no markup). Hence, only the bunkering costs are included in the objective. Recall that Table 3.1 demonstrates the energy price components for the different infrastructure archetypes. Therefore, the respective energy consumption at the different infrastructure archetypes multiplied with the corresponding energy price comprises the bunkering costs. Lastly, the passenger cost group consists of the passenger costs described in Section 3.1, i.e., penalty costs for unmet demand and passenger transit time costs.

3.2.3 Restrictions

The restrictions in the ZEVIPP are designed to ensure feasibility in a real-world case. The identified restrictions are mainly related to maintaining service levels, ensuring energy feasibility, and respecting chronology.

Service Level

First and foremost, the service frequency level for each route (and sub-route) needs to be maintained by one or more vessels. However, the route can only be operated by one vessel type. Again, this implies that the only way to impact how large proportions of the demand is met is through the vessel type (and its passenger capacity). It is not strictly necessary to meet the passenger demand entirely, but the consequence of not doing so is incurring passenger alternative costs.

Energy Feasibility

Serving routes creates energy demand, which the system of energy-producing infrastructures must supply. Generally, both the total energy in the system and the energy in each component must be conserved, accounting for energy conversion efficiencies, and energy can only flow according to the compatibilities illustrated in Figure 3.4. Moreover, the infrastructures and vessels cannot have more energy stored than their energy storage capacities and energy level bounds allow. Vessels must also start and end the operating period at the same energy level.

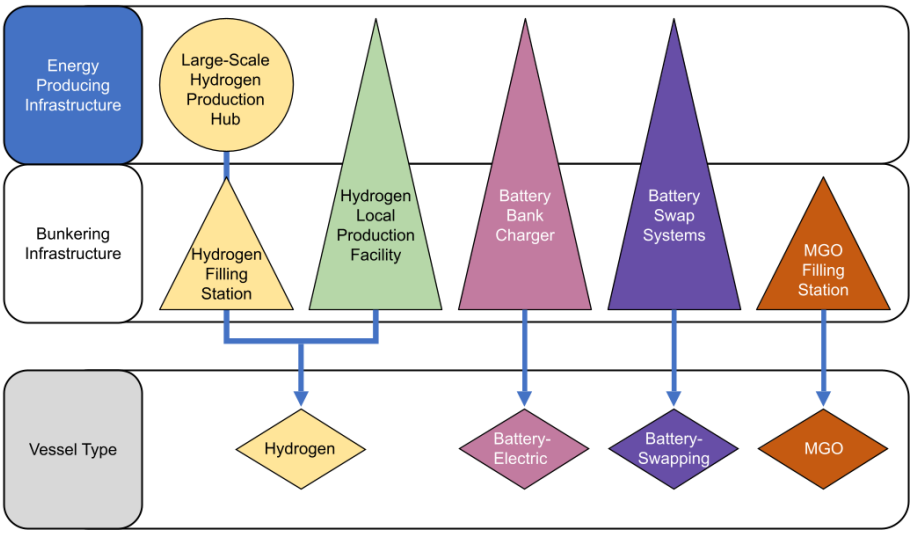

Figure 3.4: Figure displaying the compatibility between infrastructure archetypes and vessel types.

Further, energy production is restricted by the grid capacity at the location and the combination of

the maximum production rate and energy conversion efficiency of the infrastructure. As mentioned, to accommodate sufficient energy production, the power grid might need to be expanded at some locations. Thus, there needs to be an interconnection between the infrastructures installed, the currently available grid capacity, and the expansion needed for the grid.

Each route must be assigned one or more bunkering ports where the vessels operating the route can bunker. The total bunkered energy cannot exceed the total energy available at the infrastructures installed at these bunkering ports. E.g., if there are two routes operated by hydrogen vessels that are assigned to the same bunkering port, the combined energy bunkered by these vessels at this port cannot exceed the amount of hydrogen available at the port.

It is assumed that there can only be one hydrogen-producing infrastructure at a port. Consequently, a port can have a local hydrogen production facility or large-scale producing hub, but not both. Similarly, it is also assumed that there can only be one hydrogen bunkering infrastructure at a port, meaning that a local hydrogen production facility and a hydrogen filling station are mutually exclusive at a port.

Lastly, as introduced in Section 3.1, there are restrictions for the amount of non-ZE energy consumption that must be respected. These restrictions get tighter along the long-term planning horizon.

Chronology

There are also several chronology constraints in the problem. On the strategic level, investments in the vessel fleet and infrastructures must be available at a later stage. That is, vessels procured at one stage in the planning horizon must be available at all later stages, taking into consideration the latency of investments. The same goes for the installment of infrastructures and expansions of grid capacity. Furthermore, the problem is initiated with the current fleet, but it is only possible to invest in ZE vessels and infrastructures as the overall object of the problem is a complete ZE transition.

At the operational level, the problem is concerned with chronology restrictions in terms of energy needing to be produced before it can be bunkered, and bunkered before it can be used for propulsion. Nor can there be produced or consumed more energy between two moments than what is physically possible. The problem is also concerned with the location of vessels, i.e., if a vessel is at a given port at one moment, it cannot be in another port the next moment without having sailed there (and spent the corresponding sailing time and energy). Similarly, it cannot bunker unless it is located at a bunkering port.

3.3 Problem Example Solution

Having introduced the rather detailed ZEVIPP, a toy example solution is provided and explained step-by-step in Appendix B. It can be useful to go through the example to better grasp the strategic and tactical dynamics of the problem. However, most of the example's dynamics will be explained in detail in subsequent chapters.

Chapter 4

Literature Review

This chapter aims to provide insight into literature relevant to the Zero-Emission (Passenger) Vessel & Infrastructure Planning Problem (ZEVIPP). By reviewing relevant literature, the modeling choices in this thesis can be discussed and possibly supported, highlighting key components of the problem. Considering the context of this thesis, the emphasis will be on literature within Operations Research (OR).

In particular, the model proposed in this thesis extends the model presented by Berg et al. (2022). Accordingly, this literature review builds upon their literature review. This means that literature regarding public transport problems, facility location problems, and fleet design problems is highly relevant. However, while most of the main facets of the problem remain the same between the report by Berg et al. (2022) and this thesis, some impactful novelties are added, increasing the problem's complexity. Whereas Berg et al. (2022) only considered a short-term planning horizon of one operational day for the complete Zero-Emission (ZE) transition, this thesis also has a long-term planning horizon including uncertainty (stochasticity), enabling a gradual investment plan towards the complete ZE transition. Additionally, a slightly new solution approach is introduced. Hence, these novelties are highlighted throughout the chapter.

The material discussed in the literature review has been collected either through the academic search engines Scopus (Elsevier, 2023) or Google Scholar (Google, 2023), by following citations in relevant papers, or directly from the (Enabling) Zero Emission (Passenger) Vessel Services (ZEVS) project's literature database. The collection source will be presented for all discussed literature.

The outline of the chapter is as follows. First, Section 4.1 conducts a general review of studies on public transport problems. Next, several facility location problems and fleet design problems are discussed in Section 4.2 and Section 4.3, respectively, with an emphasis on the novelties of this thesis. Lastly, the literature review is synthesized through a summary of the contributions of this thesis in Section 4.4.

4.1 Public Transport Problems

This section presents some relevant literature on public transport problems within OR, summarized in Table 4.1. Typically, these problems relate to key challenges like route optimization, vehicle scheduling, demand forecasting, network design, capacity allocation, reliability analysis, congestion management, and integration with other transportation modes. The aim of the review is to reveal recurring challenges and innovative approaches that are applicable to the ZEVIPP.

Article	Relevance to the ZEVIPP	Source
Durán-Micco and Vansteenwegen (2022)	Survey	Scopus
Iliopoulou and Kepaptsoglou (2019)	Combined objective function	Scopus
Klier and Haase (2015)	Demand modeling	Scopus
Berg et al. (2022)	Resembling problem and decisions	ZEVS
Havre, Lien, Ness et al. (2022)	Resembling problem and decisions	ZEVS
Havre, Lien and Ness (2022)	Resembling problem and decisions	ZEVS

Table 4.1: Results from the literature search within Public Transport Problems

Durán-Micco and Vansteenwegen (2022) present an extensive survey of studies addressing the Transit Network Design Problem (TNDP) and Transit Network Design and Frequency Setting Problem (TNDFSP). The survey elaborates on the different assumptions, constraints, objectives, solution approaches, and testing instances that have been considered in the literature. Firstly, Durán-Micco and Vansteenwegen (2022) find that most studies consider both the passenger's and operator's points of view in the objective function(s), which is also the case in the ZEVIPP. Such an approach is exemplified by Iliopoulou and Kepaptsoglou (2019) which account for both perspectives through a bi-level formulation. According to Durán-Micco and Vansteenwegen (2022) passengers' point of view is typically modeled by the total travel and waiting time of all passengers, and, in some cases, by an additional penalization for unsatisfied demand. Consequently, how the demand is modeled is important. Klier and Haase (2015) present a service level-dependent approach to demand, in contrast to the ZEVIPP where demand is considered inelastic. Further, Durán-Micco and Vansteenwegen (2022) state operator's point of view is mostly modeled by the sum of the length of all the lines, i.e., the distances of routes, or a function directly related to it and the fleet size. Some studies also consider additional cost elements related to infrastructures such as the investment costs.

Havre, Lien, Ness et al. (2022), Havre, Lien and Ness (2022), and Berg et al. (2022), do all present quite similar problems to the ZEVIPP and will consequently be referred to throughout the literature review. On a high level, their objective function design has been very influential for the construction of the objective function in this thesis. All studies divide the objective function into operator costs and passenger costs including investment costs in the vessel fleet and infrastructures, energy costs, crew costs, passenger alternative costs, and sailing time costs, while Havre, Lien, Ness et al. (2022) and Havre, Lien and Ness (2022) also consider passenger waiting time costs. Furthermore, they share the same decision planning levels as this thesis, i.e., strategic decisions regarding investments, tactical decisions regarding the allocation of available assets, and operational decisions of operating the route(s) optimally under these conditions. The concrete decisions within these planning levels do however vary to some extent among all four papers. E.g., Havre, Lien, Ness et al. (2022) and Havre, Lien and Ness (2022) include frequency setting (with endogenous passenger demand), route structure design, and speed optimization, while Berg et al. (2022) and this thesis consider several routes simultaneously and also decide the optimal production of energy at infrastructures.

4.2 Facility Location Problems

The facility location problem is a classical optimization challenge that has garnered significant attention due to its practical implications across various industries. The objective of this problem is usually to determine the optimal locations for facilities to minimize costs, maximize efficiency, and satisfy demand in a given geographic region. The ZEVIPP is a variant of the problem since perhaps its most important decisions are to determine the type and location of bunkering infrastructure. In this section, relevant literature concerning the problem is presented and discussed in the context of the ZEVIPP. The literature reviewed is summarized in Table 4.2.

Article	Relevance to the ZEVIPP	Source
Turkoglu and Genevois (2020)	Survey	Following citations
Farahani et al. (2019)	Survey	Following citations
Patil et al. (2023)	Charging infrastructure location	Following citations
He et al. (2022)	Charging infrastructure location	Following citations
Lee et al. (2021)	Charging infrastructure location	Following citations
Roni et al. (2019)	Charging infrastructure location	Following citations
Londoño and Granada-Echeverri (2019)	Charging infrastructure location	Scopus
Brandt et al. (2021)	Charging infrastructure location	Following citations
Villa et al. (2020)	Charging infrastructure location	Following citations
Havre, Lien, Ness et al. (2022)	Charging infrastructure location	ZEVS
Havre, Lien and Ness (2022)	Charging infrastructure location	ZEVS
Štádlerová and Schütz (2021)	Hydrogen infrastructure location	Following citations
Štádlerová et al. (2022)	Hydrogen infrastructure location	Following citations
Štádlerová et al. (2023)	Hydrogen infrastructure location	Google Scholar
Berg et al. (2022)	Mixed infrastructure location	ZEVS

Table 4.2: Results from the literature search within Facility Location Problems

The facility location problem has been well studied. E.g., the surveys by Turkoglu and Genevois (2020) and Farahani et al. (2019) provide comprehensive comparisons of studies within the field, both concluding there has been a significant shift from manufacturing-oriented facility location problems towards service facility location problems, often in urban areas, in later years.

There are several studies concerning charging infrastructure location. However, contrary to the ZEVIPP, most of these studies focus on charging infrastructures in urban areas and road transportation. E.g., He et al. (2022) and Lee et al. (2021) study the problem for electric buses, Roni et al. (2019) study the problem for shared vehicles, Londoño and Granada-Echeverri (2019) study the problem for electric vehicles for freight transportation, and Brandt et al. (2021) study the problem for private cars. The recent review by Patil et al. (2023) compares the approaches and data sources used to elicit electric vehicle charging behavior and patterns from a demand-side perspective to how supply-side studies on charging infrastructure deployment and management incorporate charging behavior. Albeit not directly comparable, the challenge of connecting both strands of literature is evident in the ZEVIPP also. Contrary to the previously mentioned literature, Villa et al. (2020), Havre, Lien, Ness et al. (2022), and Havre, Lien and Ness (2022) study more directly comparable problems. Villa et al. (2020) consider the location of solar-powered charging infrastructures for electric riverboats sailing fixed routes through rural areas, while Havre, Lien, Ness et al. (2022) and Havre, Lien and Ness (2022) analyze the optimal placement of charging infrastructures to facilitate battery-electric High-Speed Passenger Vessel (HSV) services in rural and coastal areas. However, in contrast to the ZEVIPP, they do not include hydrogen infrastructures as a possibility and they only consider one passenger vessel route at a time and not a set of routes within a region.

On the hydrogen side, the studies by Štádlerová and Schütz (2021), Štádlerová et al. (2022), and Štádlerová et al. (2023) provide very interesting approaches relatable to this study. The different studies more or less concern the same problem, i.e., planning the location and expansion of hydrogen facilities for the maritime transportation sector in Norway over multiple periods while also choosing optimal production quantities and distribution solutions in each period. Štádlerová and Schütz (2021) propose a deterministic solution approach considering two demand scenarios, whereas Štádlerová et al. (2022) and Štádlerová et al. (2023) model the demand stochastically. In contrast to the ZEVIPP, they do not consider a possible mix of hydrogen, electric charging, and battery-swapping infrastructures. Furthermore, in the ZEVIPP, the energy demand relates to passenger vessel operations (that are explicitly modeled), while the mentioned studies consider general demand projections associated with several actors and industries (but without specifically relating the demand to economic activities, which also makes these demand forecasts more uncertain). A similar study that considers a mix of hydrogen and electric charging infrastructures is the already introduced study by Berg et al. (2022). However, this study only considers a single period.

4.3 Fleet Design Problems

Another important decision in the ZEVIPP is to determine an optimal fleet size and mix of vessels to service the different routes. This makes the problem part of the group of fleet design problems, revolving around the strategic decision-making process of designing an optimal fleet to meet operational requirements efficiently. This problem encompasses various aspects, such as determining the fleet size, vehicle types, capacity allocation, and routing strategies, with the overarching objective of minimizing costs and maximizing service quality. This section provides some examples of studies concerning the problem, summarized in Table 4.3, and relates them to the ZEVIPP.

Article	**Relevance to the ZEVIPP**	**Source**
Pantuso et al. (2014)	Survey	Following citations
Hoff et al. (2010)	Survey	Following citations
Slette et al. (2023)	Heterogeneous vessel fleet	Google Scholar
Stålhane et al. (2019)	Deciding fleet mix under uncertainty	Following citations
Havre, Lien, Ness et al. (2022)	Heterogeneous battery-electric fleet	ZEVS
Havre, Lien and Ness (2022)	Heterogeneous battery-electric fleet	ZEVS
Berg et al. (2022)	Heterogeneous fleet w/mix of energy carriers	ZEVS

Table 4.3: Results from the literature search within Fleet Design Problems

This problem has also been studied to some extent. The survey by Pantuso et al. (2014) analyzes the available scientific literature on the problem and its variants and extensions, summarizes the state of the art, and highlights the main contributions of past research before it uncovers the main areas where more research will be needed. Hoff et al. (2010) add to this survey by investigating the combined problem of fleet composition and routing.

There are multiple studies on how to design vessel fleets according to the operation of routes. E.g., Slette et al. (2023) assess the performance of two different fleets serving a set of fish farms, while Stålhane et al. (2019) optimize the vessel fleet size and mix to support maintenance operations at offshore wind farms under the uncertainty of weather conditions and the occurrence of failures. However, according to our knowledge, very few of the previous vessel fleet design problem studies concern passenger vessels. Nevertheless, some exceptions are the already introduced studies by Havre, Lien, Ness et al. (2022), Havre, Lien and Ness (2022), and Berg et al. (2022), which all consider the fleet design of HSVs. As mentioned previously, Havre, Lien, Ness et al. (2022) and Havre, Lien and Ness (2022) do not include the possibility of having a mix of hydrogen and battery-electric vessels. Berg et al. (2022) consider such a mix but unlike this thesis, they do not decide how the vessel fleet evolves over multiple periods.

4.4 Contribution

This thesis adds to the already existing research on decision support for determining optimal ZE infrastructure mix and locations and vessel fleet size and mix for HSV services. The literature search and review revealed that the most notable existing studies on the particular problem, to our knowledge, are Štádlerová and Schütz (2021), Štádlerová et al. (2022), Štádlerová et al. (2023), Havre, Lien, Ness et al. (2022), Havre, Lien and Ness (2022), and Berg et al. (2022). Štádlerová and Schütz (2021), Štádlerová et al. (2022), and Štádlerová et al. (2023) optimize the locations and sizes of hydrogen production facilities over multiple periods, both under deterministic and stochastic demand conditions. Havre, Lien, Ness et al. (2022) and Havre, Lien and Ness (2022) combine the problems of deciding where to install electric charging infrastructures and deciding the battery-electric fleet size for a given route. Berg et al. (2022) extend the work by Havre, Lien, Ness et al. (2022) by including hydrogen infrastructures and vessels in the combined problem and solving it for a set of routes, possibly enabling co-localization and co-utilization of infrastructures across routes.

This thesis extends the work by Berg et al. (2022) by a range of novelties added. The perhaps

most important extension is that the problem now is considered for multiple periods comprising a long-term planning horizon. This means that the decisions from Berg et al. (2022) have been converted to time-dependent decisions in this thesis. This conversion facilitates decisions in line with the Norwegian government's plan for the transition (Tveit et al., 2023). Further, the conversion entails several other novelties as well. Conventional MGO infrastructures and vessels are included in the problem, time-dependent emission regulations are added, and future bunkering prices are considered uncertain. Among other notable novelties are the inclusion of multiple hydrogen hubs, the possibility for multiple bunkering ports for each route, and the inclusion of battery-swapping infrastructures and vessels. The inclusion of these novelties is a consequence of Berg et al. (2022) who found that the large-scale hydrogen production hub served as a very cost-effective infrastructure and that not all routes were feasible to serve with only one bunkering port. Taking the feasibility studies by Aarskog et al. (2020) and Sundvor et al. (2021) and the abovementioned studies into consideration, these extensions contribute to the research by investigating how more effective and realistic planning of the transition to ZE HSV services can limit the feasibility and optimality gap to conventional HSV services.

Chapter 5

Solution Approach: Periodization and Decomposition of the Problem

This chapter combined with Chapter 6 and Chapter 7 present the modeling approach and models of this thesis. This chapter provides a detailed explanation of the most important modeling approaches. In particular, the periodization of the long-term planning horizon and the decomposition of the Zero-Emission (Passenger) Vessel & Infrastructure Planning Problem (ZEVIPP) into a *Master Problem* and *Sub-Problem* are described. The decomposed problems are then presented separately with proposed models in Chapter 6 and Chapter 7, respectively.

Section 5.1 explains how the long-term planning horizon of the problem is broken down into time steps. Then, Section 5.2 explains how the decision levels described in Section 3.2 are decomposed into the Master Problem and independent Sub-Problems. Finally, Section 5.3 discusses some of the implications incurred by the solution approach.

5.1 Periodizing the Long-Term Planning Horizon into Time Steps

Recall from Chapter 3 that a solution of the ZEVIPP is a plan for phasing in Zero-Emission (ZE) vessels and infrastructures throughout a given long-term planning horizon. This long-term planning horizon is modeled by periodizing it into *time steps* which represent points in the long-term planning horizon where investment decisions can be made. The purpose of this modeling approach is to discretize moments where it is possible to make investment decisions, effectively reducing granularity and removing complexity. Further, as mentioned in Chapter 3, there is a lead time associated with investing in vessels and infrastructures, causing a latency between the investment decision and when the asset is available for utilization. This latency is approached by letting the investment decisions made in a time step first be available in a given number of time steps later.

In the example illustrated by Figure 5.1, a long-term planning horizon of 15 years is equally split into a number of five time steps. Each time step is represented by its short-term planning period decisions, i.e., investment decisions and how the routes are served for the duration of the time step. In Time Step 1, it is decided to invest in one battery-electric vessel and one electric charging infrastructure. These are available first in Time Step 2 because of the investments' lead time. As can be seen in Time Step 2, the investments replace the conventional High-Speed Passenger Vessel (HSV) service for the uppermost route. Further on, in Time Step 3 it is invested in hydrogen infrastructure and two hydrogen vessels, which enables the rightmost route to be served with hydrogen in Time Step 4. Lastly, in Time Step 4, it is invested in another hydrogen vessel. In Time Step 5 one can see that this vessel replaces the vessel operating the bottommost route. Additionally, this vessel bunkers at the same port as the hydrogen vessels operating the rightmost

route, and thus, shares infrastructure. It can also be noted by the purple arcs that the vessel detours outside its route to bunker.

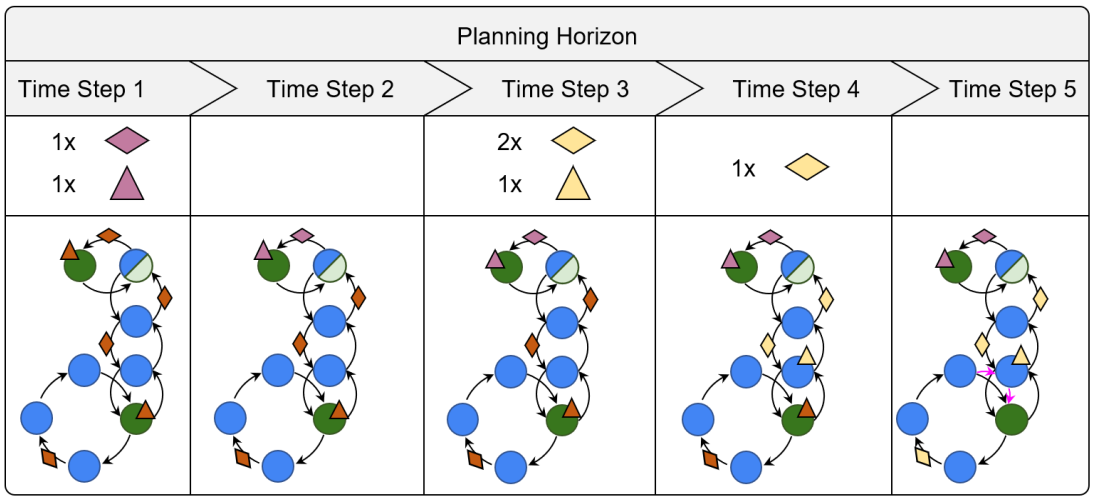

Figure 5.1: The model is solved for several time steps comprising the long-term planning horizon. An optimal investment plan is the main output. The first row shows investments decided in each time step, and the second row shows how the routes are served during each time step.

.

All time steps are solved simultaneously. In that way, the investment plan respects the interdependencies between the time steps; in particular, the continuity of the investments in later time steps. The investment plan is structured around the operational costs of serving the set of routes in each time step. Moreover, it allows different operational configurations within each time step. Thus, cost minimization at the strategic level considers both the total costs of serving the set of routes in each time step and the investment costs. For example, in Figure 5.1, the investments in all time steps are decided simultaneously where the operational configurations in a time step are restricted by the vessels and infrastructures available in the particular time step.

5.2 Decomposition of Decision Levels

As pointed out in Chapter 3, the main objective of the ZEVIPP is to create a cost-effective investment plan that ensures that the set of routes at all times is served while respecting the problem's restrictions. A challenge with this problem formulation is, as Berg et al. (2022) pointed out, that it spans a very large and complex solution space where it in practice is impossible to find the optimal solution within a reasonable time. Consequently, a simplifying approach is needed. Under the assumption that all routes are operated independently of each other, the minimum cost of operating a route can be determined given what vessel type is serving it and at what *bunkering alternatives* are available for the vessels operating it. The term "bunkering alternatives" refers to all permutations of ports along or near the route and the infrastructures possible to install at these ports. Some information is of course lost due to this assumption. This is discussed in Section 5.3. However, with a strategic and tactical approach, the lost information is considered not that decisive. Hence, given this assumption, the ZEVIPP can be reduced to finding the cost of serving each route with every permutation of vessel types and bunkering alternatives and then assigning each route one of these permutations. From now on, these permutations will be referred to as *route serving permutations*. The short-term planning problem of deciding the costs of operating a route is denoted as the *Sub-Problem*. Accordingly, the *Master Problem* creates the long-term investment plan given the route-serving costs generated by the Sub-Problems. Thus, a combined model is proposed, decomposing the problem into a strategic and tactical layer, solved by the Master Problem, and an operational layer, solved by the Sub-Problems.

Figure 5.2 shows how the decomposition into Sub-Problems is done. From the left, the figure

first shows that the problem is solved for a set of routes and possible bunkering alternatives. In the second stage of the illustration, the Sub-Problems are generated for each route. Route 2's feasible route-serving permutations are illustrated in the blue box at the bottom. The illustrated route-serving permutations are hydrogen bunkering at p_1; electric charging infrastructure at p_1; hydrogen bunkering at p_2; and hydrogen bunkering at p_1 or p_2. Next, each generated Sub-Problem is solved, effectively calculating the parameters needed to solve the Master Problem. Lastly, each route is assigned a route-serving permutation for each time step in the Master Problem solution. In the illustrated time step, Route 1 is served with battery-electric vessels bunkering at p_3, while Route 2 and 3 are served with hydrogen vessels bunkering at p_2.

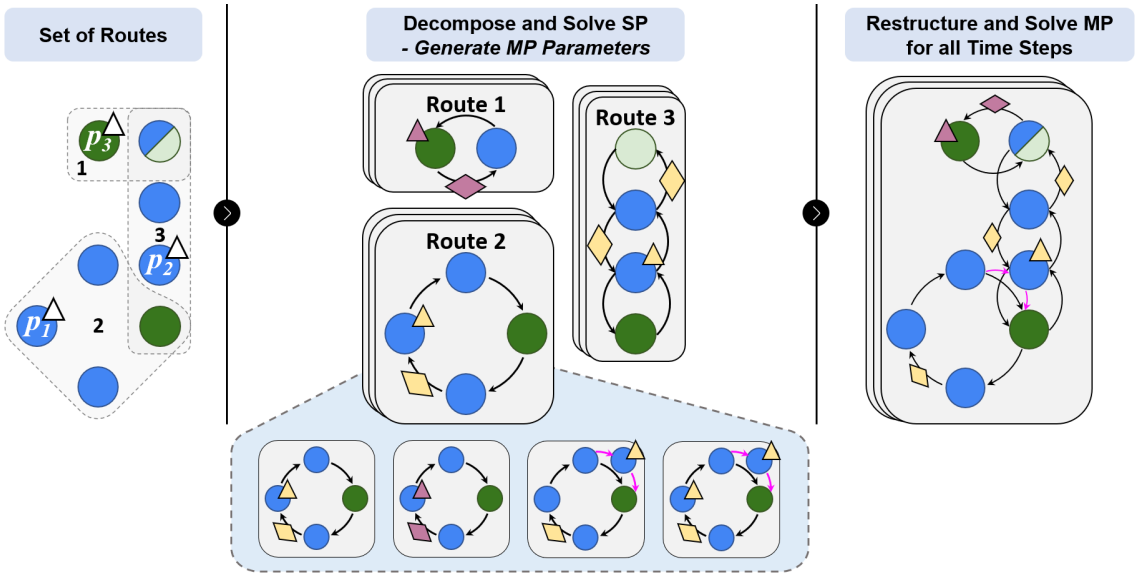

Figure 5.2: The routes-serving permutations are solved independently, then combined to obtain a global solution.

Even though the periodization introduced in Section 5.1 helps to reduce the granularity of the long-term planning horizon, it is still too complex to solve the Sub-Problems for all days within the time steps. Consequently, another applied modeling approach is to solve the Sub-Problems for a short-term planning period of a single operational day. However, the resulting costs are later scaled to the length of the time step. This reduces the complexity of the model, while feasibility is ensured by solving each Sub-Problem for the peak load of the time step. The elevation of passenger time, crew shift, and energy costs due to a peak load solution is later reverted to ensure a better assessed total time step cost of each Sub-Problem. Further on, Figure 5.3 shows that the Sub-Problems are solved for each time step. This is due to the fact that cost coefficients vary across time steps and might induce different Sub-Problem solutions for the same route-serving permutation. The Master Problem restructures all the Sub-Problem solutions in each time step with the corresponding investments needed to facilitate the given route-serving plan.

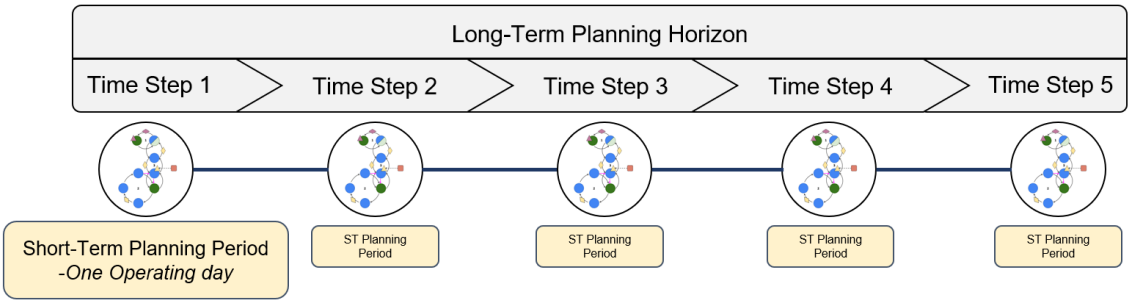

Figure 5.3: The model is solved for all time steps, remembering the investment decisions at each time step that are available in the next time step.

Lastly, a specific example of how the Sub-Problem interacts with the Master Problem is presented. Figure 5.4 illustrates how each time step uses its corresponding Sub-Problem solutions as parameters. The example considers the rightmost Sub-Problem generated for Route 2 in Figure 5.2. The route-serving permutation in Sub-Problem 4 is given by route r_2, bunkering alternative (LP at p_1, LP at p_2), and a hydrogen vessel type ($Hydrogen$). This means that Route 2 is served with hydrogen vessel(s) bunkering at p_1 or p_2. The resulting solution of the Sub-Problem is given by its *total cost*, the *number of vessels* used to serve the route, and the *energy and time* spent bunkering at each bunkering port in the bunkering alternative. In this example, p_2 is considered a better option to bunker at. This might be due to it being close to the main port, and thus, it could be cheap to bunker there between route servings. Finally, the output of the Sub-Problem is propagated as parameters into Time Step 1.

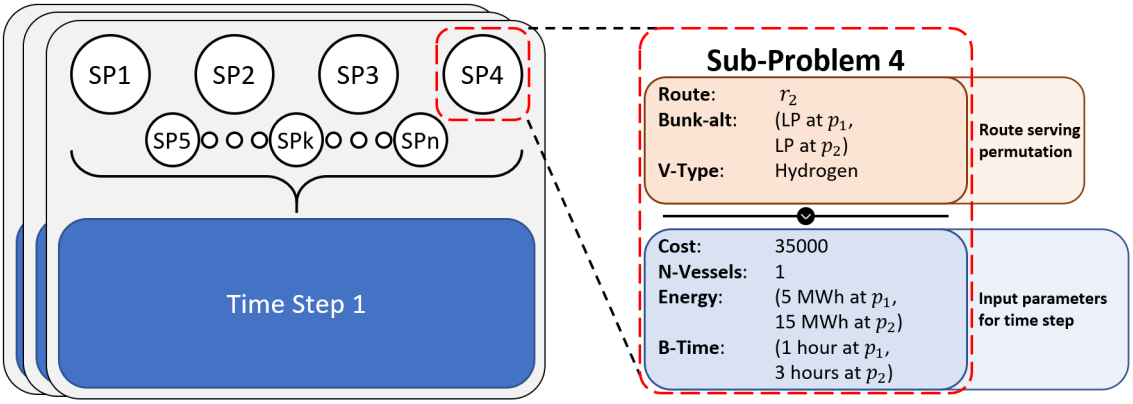

Figure 5.4: The Master Problem assigns the solution of a Sub-Problem to each route. This has implications for the strategic decisions of investing in infrastructures and vessels.

5.3 Implications of the Periodization and Decomposition

This section focuses on some of the implications the solution approach presented incurs. First, Section 5.3.1 elaborates on the generation of route-serving permutations. Next, Section 5.3.2 and Section 5.3.3 describe how global feasibility and optimality are impacted by the solution approach, respectively.

5.3.1 Generation of Route-Serving Permutations

A consequence of the decomposition is that there needs to be generated route-serving permutations for each route in the set. The number of permutations increases as a product of the number of vessel types and bunkering alternatives, which in turn may make the problem too complex for big sets of both. Hence, the permutations must be generated in a smart way. How route-serving permutations are generated is detailed in Appendix C.

5.3.2 Global Feasibility

A consequence of solving the Sub-Problems independently is that it is not possible to schedule bunkering precisely. This means that solutions do not consider that bunkering infrastructures may be used by vessels operating other routes, and are thus prone to congestion at the infrastructures. To cope with this vulnerability, the Master Problem needs some heuristic logic to ensure that the infrastructures are not over-utilized. The implementation of such logic is explained in Section 6.1.

5.3.3 Global Optimality

Operational decisions are determined in the context of the peak load of the time step, which is probably sub-optimal for the actual problem. This is due to the cost ratio of the different cost posts being skewed and a Sub-Problem might prioritize faultily one post over another. However, as mentioned, the peak load costs are scaled back to the average in the Master Problem where the important investment decisions are made, and hence, this problem is considered negligible.

Further, within a Sub-Problem, the distance to the hydrogen hub cannot be decided for a hydrogen filling station. This is due to the installment of large-scale hydrogen-producing hubs being decided in the Master Problem. Thus, a Sub-Problem is solved given that it is provided hydrogen from the closest hub. The actual bunkering price at hydrogen filling stations is obtained in the Master Problem by deciding how much hydrogen is provided by each hub and adding the eventual extra transportation cost. As motivated above, the important investment decisions are made in the Master Problem where the costs are corrected, and hence, this problem is also considered negligible.

Chapter 6

Mathematical Formulation of the Master Problem

This chapter presents the mathematical formulation of the Master Problem, along with the underlying assumptions and modeling approaches relevant to the Master Problem. As described in Chapter 5, the Master Problem is to determine an optimal investment plan for vessels and infrastructures to serve a set of routes by considering investment costs, operational costs, energy costs, and passenger costs. The model presented in the chapter is an extension of the model presented by Berg et al. (2022).

First, Section 6.1 explains the modeling details in the mathematical formulation. Next, Section 6.2 introduces and elaborates on the notation used in the model, before the model itself is presented, including its objective function and constraints, in Section 6.3.

6.1 Modeling Approach

This section summarizes the key modeling approaches for the Master Problem given the assumptions, objective, and restrictions described in Chapter 3 First, the modeling decisions regarding infrastructures and grid capacities are discussed in Section 6.1.1. Then, the approach for modeling uncertainty is presented in Section 6.1.2.

6.1.1 Investments

Since there is assumed no salvage value for vessels and since installed infrastructures cannot be removed, the proposed model does not consider asset salvage directly and the number of Zero-Emission (ZE) vessels and infrastructures can consequently only increase throughout the long-term planning horizon. However, asset salvage is modeled indirectly by the option to not utilize parts of the vessel fleet or installed infrastructures.

As described in Chapter 5, the Master Problem should ensure global feasibility, i.e. mitigate the risk for congestion, when routes share a bunkering infrastructure. Besides restricting the consumed energy to the energy available at the infrastructures, it is assumed sufficient to mitigate the congestion risk by restricting the amount of time an infrastructure can be utilized throughout the operating day, ensuring there is time left in the planning period to circumvent congestion in case it occurs. This approach allows the Master Problem to reduce complexity by neglecting time periods within each operating day.

Although energy-producing infrastructures have associated maximal production rates, producing energy at a lower effect than the maximal input is allowed in the model. This enables ports with low utilization of an energy-producing infrastructure to reduce costs by not expanding the grid

capacity unnecessarily. The only exceptions are electric charging infrastructures, which demand that installed grid capacity is at least as high as its production rate. This is decided because Berg et al. (2022) found that battery-electric vessels empty the onshore battery pack and bunker directly from the grid in most applications.

In Chapter 3, it was assumed that MGO is easily accessible at all ports for a consistent MGO price. In terms of the Master Problem, this means there is no need to invest in infrastructures to supply conventional CO_2 emitting vessels and that there are no energy storage capacity constraints for the MGO filling stations.

6.1.2 Stochasticity and Scenario Tree

As explained in Chapter 2 and Chapter 3, the future CO_2 taxes and the prices of MGO and electricity are generally uncertain, and it is part of the problem doing decisions under these uncertainties.

An important modeling approach in the Master Problem is to integrate the uncertainties by formulating the problem as a two-stage stochastic programming model. The uncertainties are represented by different scenarios with a corresponding probability, where a scenario denotes an instance of the three said values prone to uncertainty. The problem is solved separately for each scenario, but all first-stage decisions, i.e., decisions made before new information is revealed, are restricted to be equal across scenarios. These restrictions are called *non-anticipativity constraints*.

Figure 6.1 illustrates an instance of the problem with time steps along the horizontal axis and different scenarios along the vertical axis. In each node (circle), representing a short-term planning period, it is decided which investments to make, and each route is assigned a route-serving permutation based on the available assets in the time step. From one time step to the next, the less or equal sign ($\leq$) represents that the investments in ZE vessels and infrastructures are binding for the remainder of the long-term planning horizon. The light blue square on the left-hand side highlights the time steps included in the first stage where the CO_2 and the MGO and electricity prices are defined deterministically. The equality signs across the scenarios in the light blue area indicate that the nodes must have the same solution across scenarios (non-anticipativity). Thus, the white nodes in the highlighted blue area are in practice just dummy nodes. Further on, the red-dashed squares above nodes indicate that all Sub-Problems must be solved for these nodes because differing energy prices might induce different Sub-Problem solutions.

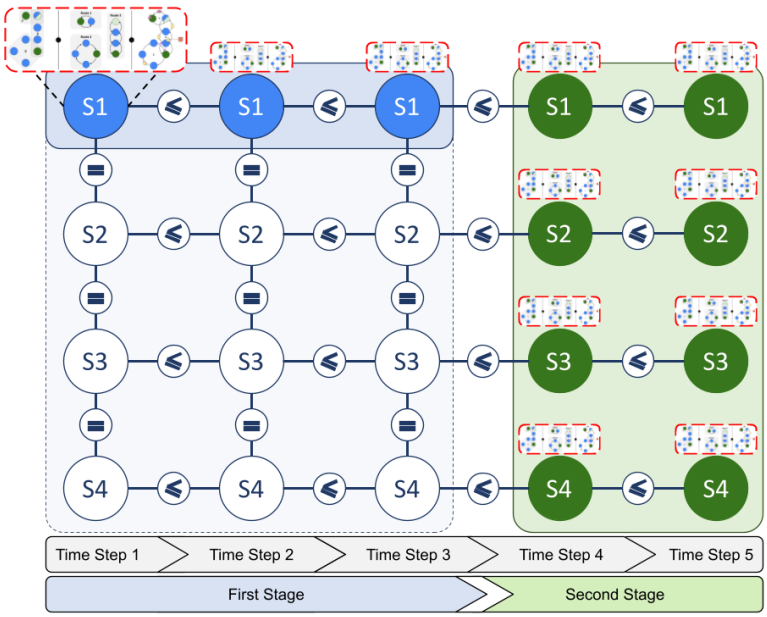

Figure 6.1: The blue shaded area represents the first stage of the problem, while the green shaded area represents the second stage. Decisions are equal across all scenarios for each time step in the first stage but can differ in the second stage.

In this example, the uncertain information is revealed after the third time step. The nodes highlighted by the green square have independent route-serving assignments and investment decisions given the revealed information in the particular scenario. Routes are assigned route-serving permutations independently between the scenarios and the model effectively optimizes the investment plan given that all scenarios are affected by the first-stage decisions.

6.2 Notation

This section introduces and elaborates on the notation used in the mathematical formulation of the Master Problem.

Sets

Let $\mathcal{T}$ and $\mathcal{S}$ denote the time steps and scenarios of the Zero-Emission (Passenger) Vessel & Infrastructure Planning Problem (ZEVIPP), respectively. For each time step and scenario, all routes $r \in \mathcal{R}$ must be served with a bunkering alternative $b \in \mathcal{B}_r$ and one or more vessels of vessel type $v \in \mathcal{V}$.

Recall the definition of a bunkering alternative from Section 5.2. Let $\mathcal{B}_r$ be the set of candidate bunkering alternatives for the route r. Conversely, $\mathcal{R}_b$ denotes the set of routes where bunkering alternative b is included in $\mathcal{B}_r$.

Further on, $\mathcal{P}$ denotes the set of ports and $\mathcal{P}_b$ denotes the set of ports used for bunkering in bunkering alternative b. Further, $\mathcal{B}_{pi}$ is the set of bunkering alternatives where infrastructure i is installed at port p.

The set $\mathcal{I}_p$ denotes all feasible infrastructures at port p, while $\mathcal{I}_p^{ZE}$ only includes all ZE infrastructures feasible at the port. The latter set can be separated into $\mathcal{I}_p^{HUB}$, $\mathcal{I}_p^{F}$, $\mathcal{I}_p^{LP}$, $\mathcal{I}_p^{E}$, and $\mathcal{I}_p^{S}$, all of which are the different archetypes of infrastructures in accordance with Table 6.1. The set of large-scale hydrogen production hubs is denoted by $\mathcal{I}_p^{HUB}$, and these are the only infrastructures where it is not possible to bunker. Thus, the hub is excluded from the set of bunkering infrastructures, $\mathcal{I}_p^{B}$. Let $\mathcal{I}_p^{GC}$ be the set of all infrastructures that consume energy from the grid and may be installed at port p. All ZE infrastructure archetypes are included in this set except filling stations since they are supplied by the hubs. The final set of infrastructures is $\mathcal{I}_p^{SC}$ which denotes the set of self-consuming infrastructures which both produce energy and support bunkering.

Infrastructure Archetype	**Notation**	**Included in Set Superscripts**
MGO Filling Station	*C*	*C, B*
Hydrogen Filling Station	*F*	*ZE*
Large-Scale Hydrogen Production Hub	*HUB*	*ZE, GC*
Local Hydrogen Production Facility	*LP*	*ZE, GC, B SC*
Electric Charging Infrastructure	*E*	*ZE, GC, B SC*
Battery-Swapping Infrastructure	*S*	*ZE, GC, B SC*

Table 6.1: The notation for infrastructure archetypes and what sets they are included in. Every infrastructure is an instance of one of these archetypes.

$\mathcal{V}$ includes all vessel types, while $\mathcal{V}^{ZE}$ and $\mathcal{V}^{C}$ denotes the ZE vessel types and conventional vessel types fueled by MGO, respectively. Further on, $\mathcal{V}_{rb}$ and $\mathcal{V}_{rb}^{ZE}$ denote the vessel types that are

feasible when serving route r with the bunkering alternative b, where the latter only includes ZE vessel types.

The set $\mathcal{T}$ denotes the set of all time steps in the long-term planning horizon. The time steps in $\mathcal{T}^{NS}$ are assumed to have deterministic (non-stochastic) energy costs, and thus, are called first-stage time steps. The decisions made in these time steps are made before the uncertain information is revealed. The uncertain information is given by the scenarios $s \in \mathcal{S}$. Each scenario determines the uncertain information with a given likelihood.

Parameters

P^s gives the likelihood of each scenario for energy prices. At each time step, the conventional energy budget $\overline{E}_t^C$ limits the total amount of consumed energy that can be fossil-based. As the Sub-Problem is solved for a short-term planning period of one day, using the peak load of the time step to ensure feasibility, the parameter R^E is used to scale down operational costs to their average daily level. N^D denotes the number of days in each time step.

One of the key decisions in the Master Problem is to select one Sub-Problem solution for every route r in each scenario s and time step t. Each route-serving permutation, rbv, in a scenario s and time step t has the precalculated parameters $C_{rbvt}^{Os}, N_{rbvt}^{Vs}, T_{rbvpt}^{Us}$, and E_{rbvpt}^{Us}. C_{rbvt}^{Os} represents its operational costs, comprised of vessel-specific operational costs, energy costs, and passenger costs. Further, N_{rbvt}^{Vs} denotes the number of vessels used to solve the Sub-Problem. Finally, the parameters T_{rbvpt}^{Us} and E_{rbvpt}^{Us} denote the time spent bunkering and the energy consumption at each bunkering port p, respectively.

The number of initially available vessels of type v is given by X_v, and the initially available infrastructures at the different ports are given by Y_{pi}^I. The investment costs of vessels of type v and infrastructures of type i are given by parameters C_v^{VI} and C_i^{II}, respectively. Installing a grid-consuming infrastructure at a port requires a sufficient amount of grid capacity which comes at a cost per MW of C_p^{IG}. All investments have latency from when the investment decision is made to the time they are available. The lead time for investments in vessels, infrastructures, and grid expansions is denoted by L_v^V, L_i^I, and L_p^G, respectively, and is measured in a number of time steps.

Each infrastructure has a storage capacity Q_i^S which restricts the production and amount available for bunkering. Further on, R_i^B denotes the bunkering rate at infrastructure i. The maximum production input at an energy-producing infrastructure is given by parameter R_i^P, and when scaled down with the energy conversion efficiency E_i^{CE}, the effective energy production is obtained. The cost of supplying a hydrogen filling station with hydrogen from a large-scale hydrogen production hub is given by C^{HT}, which is the price per kilometer of transportation and kWh of hydrogen. The distance between a filling station at port p and a hub at location $\hat{p}$ is given by parameter $D_{p\hat{p}}^{F2H}$. However, the Sub-Problem assumes that a filling station will be provided by its closest hub. Thus, the extra incurred cost of supplying a filling station in the Master Problem will be calculated with $\Delta D_{p\hat{p}}^{F2H}$, denoting the difference between the distance assumed in the Sub-Problem and the actual distance in the Master Problem.

The currently available grid capacity at a port is given by the parameter Q_p^{GA}, while the upper bound for the expansion of grid capacity is given by $\overline{Q}_p^G$.

The parameter N^H denotes the number of hours in the short-term planning period. At each port, this limits the number of hours the infrastructures are available for bunkering, and how much time is available to produce energy. To address the potential problem of congestion at bunkering infrastructures, the parameter U^F limits the amount of time spent bunkering at the infrastructures.

Variables

The binary variable y^s_{rbvt} takes the value 1 if route r is served with bunkering alternative b and vessel type v in time step t in scenario s, and 0 otherwise.

Further, several control variables are needed to track investment decisions. To represent that lead time may vary among investments, there is one variable for when the investment decision is made and one for the current stock of each investment. More specifically, the variable $\tilde{y}^{Is}_{pit}$ takes the value 1 if there is an investment made in infrastructure i at port p in time step t and scenario s, and 0 otherwise. The variable y^{Is}_{pit} takes the value 1 if infrastructure i is already installed at port p in time step t and scenario s, and 0 otherwise. The lead time determines how many time steps are between the investment decision and when it is available at a port. Similarly, $\tilde{x}^s_{vt}$ denotes how many vessels of type v are invested in at time step t in scenario s, while the integer variables x^s_{vt} denote the stock of each vessel type v in scenario s and in time step t. Finally, to control the expansion of grid capacities, the continuous variables q^{GAs}_{pt} represent the amount of available grid capacity at time step t in scenario s. As expanding the grid capacity also requires investment with lead time, $\tilde{q}^{GAs}_{pt}$ denotes the amount of expanded grid capacity in scenario s in time step t at port p.

The continuous variable e^{Ps}_{pit} is defined for all grid-consuming infrastructures, and it denotes how much energy should be produced during the day at port p and infrastructure i in time step t and scenario s. For all ports where a large-scale hydrogen production hub is an alternative, the continuous variable $e^{Hs}_{pi\hat{p}\hat{i}t}$ is defined. This variable keeps track of the amount of energy produced at the hub location $\hat{p}$ by the hub $\hat{i}$ which is allotted to port p where the filling station i is installed in time step t and scenario s.

Sets

$\mathcal{R}$	Set of routes
$\mathcal{R}_b$	Set of routes with feasible Sub-Problems for bunkering alternative b, $\mathcal{R}_b \subseteq \mathcal{R}$
$\mathcal{P}$	Set of ports
$\mathcal{P}_b$	Set of ports which are considered in bunkering alternative b
$\mathcal{B}_r$	Set of candidate bunkering alternatives for route r.
$\mathcal{B}_{pi}$	Set of bunkering alternatives where infrastructure i is installed at port p
$\mathcal{I}_p$	Set of candidate infrastructures at port p
$\mathcal{I}^{ZE}_p$	Set of candidate ZE infrastructures at port p
$\mathcal{I}^{E}_p$	Set of candidate electric charging infrastructures at port p, $\mathcal{I}^E_p \subseteq \mathcal{I}_p$
$\mathcal{I}^{S}_p$	Set of candidate battery-swapping infrastructures at port p, $\mathcal{I}^S_p \subseteq \mathcal{I}_p$
$\mathcal{I}^{HUB}_p$	Set of candidate large-scale hydrogen production hubs at port p, $\mathcal{I}^{HUB}_p \subseteq \mathcal{I}_p$
$\mathcal{I}^{LP}_p$	Set of local hydrogen production infrastructures at port p, $\mathcal{I}^{LP}_p \subseteq \mathcal{I}_p$
$\mathcal{I}^{F}_p$	Set of hydrogen filling stations at port p, $\mathcal{I}^F_p \subseteq \mathcal{I}_p$
$\mathcal{I}^{B}_p$	Set of candidate bunkering infrastructures at port p, $\mathcal{I}^B_p = \mathcal{I}_p \backslash \mathcal{I}^{HUB}_p$
$\mathcal{I}^{GC}_p$	Set of candidate grid-consuming infrastructures at port p, $\mathcal{I}^{GC}_p = \mathcal{I}_p \backslash \mathcal{I}^F_p$
$\mathcal{I}^{SC}_p$	Set of candidate self-consuming bunkering infrastructures at port p, $\mathcal{I}^{SC}_p = \mathcal{I}^{GC}_p \cap \mathcal{I}^B_p$
$\mathcal{V}$	Set of vessel types

$\mathcal{V}^{ZE}$	Set of ZE vessel types
$\mathcal{V}^{C}$	Set of conventional vessel types
$\mathcal{V}_{rb}$	Set of feasible vessel types for a route r given a bunkering alternative b
$\mathcal{V}_{rb}^{C}$	Set of feasible conventional vessel types for a route r given a bunkering alternative b
$\mathcal{V}_{rb}^{ZE}$	Set of feasible ZE vessel types for a route r given a bunkering alternative b
$\mathcal{T}$	Set of time steps
$\mathcal{T}^{NS}$	Set of first-stage time steps
$\mathcal{S}$	Set of scenarios

Parameters

Parameters precalculated by solving the Sub-Problems

C_{rbvt}^{Os}	Running costs for operating route r with bunkering alternative b and vessel type v. Includes energy costs, passenger costs, and vessel Operational Expenditures (OPEX)
N_{rbvt}^{Vs}	Number of vessels used for serving route r with bunkering alternative b, and vessel type v
E_{rbvpt}^{Us}	Energy consumption at port p when operating route r with bunkering alternative b and vessel type v
T_{rbvpt}^{Us}	Time spent bunkering at port p when operating route r with bunkering alternative b and vessel type v

General

N^{H}	Number of hours in the short-term planning period
P^{s}	Likelihood of scenario s to occur
$\overline{E}_{t}^{C}$	Conventional energy budget in time step t
R^{E}	Ratio between peak weekly load and average daily energy consumption
N^{D}	Number of days in a time step

Vessels

X_{v}	The number of initially available vessels of type v
C_{v}^{VI}	Daily cost of investing in one vessel of type v for the duration of its lifetime
L_{v}^{V}	Investment latency for vessel of type v

Infrastructure

Y_{pi}^{I}	Binary parameter taking the value 1 if infrastructure i is available at port p, and 0 otherwise
Q_{i}^{S}	Energy storage capacity for infrastructure i

C_i^{II}	Daily costs of investing in infrastructure i for the duration of its lifetime
R_i^P	Maximum energy production rate for infrastructure i
E_i^{CE}	Energy conversion efficiency for infrastructure i
C^{HT}	Cost of transporting hydrogen (from hub to filling station) per km and kWh
$\Delta D_{p\hat{p}}^{F2H}$	Extra distance above minimum from port p to port $\hat{p}$
R_i^B	Bunkering rate for infrastructure i
U^F	Upper bound for the utilization of infrastructures
L_i^I	Investment latency for infrastructure i

Grid

Q_p^{GA}	Available grid capacity at port p without expanding the grid
$\overline{Q}_p^G$	The upper bound for grid capacity expansion at a port p
C_p^{IG}	Daily cost per MW for expanding the grid capacity at port p for the duration of its lifetime
L_p^G	Investment latency for grid capacity at port p

Variables

y_{rbvt}^s	Binary variable which takes the value 1 if route r is served by vessel type v using bunkering alternative b in time step t and scenario s, and 0 otherwise
y_{pit}^{Is}	Binary variable which takes the value 1 if the infrastructure i is installed at port p in time step t and scenario s, and 0 otherwise
$\tilde{y}_{pit}^{Is}$	Binary variable which takes the value 1 if it is determined in time step t to invest in infrastructure i at port p in scenario s, and 0 otherwise
q_{pt}^{GAs}	Amount of grid capacity available at port p at time step t and in scenario s. The available grid capacity in the initial time step is equal to Q_p^{GA}
$\tilde{q}_{pt}^{GAs}$	Determined amount of grid capacity invested at port p at time step t in scenario s
x_{vt}^s	Number of vessels of type v available in time step t and scenario s
$\tilde{x}_{vt}^s$	Determined number of ZE vessels of type v invested in time step t and scenario s
e_{pit}^{Ps}	Amount of energy produced at port p with the grid-consuming infrastructure i in time step t and scenario s
$e_{pi\hat{p}\hat{i}t}^{Hs}$	Amount of energy produced at the hub location $\hat{p}$ by the hub $\hat{i}$ which is allotted to port p where hydrogen filling station i is installed in time step t and scenario s

6.3 Mathematical Model of the Master Problem

Having completed the notation, the mathematical formulation of the Master Problem can be presented. Section 6.3.1 elaborates on the objective function and explains the different terms. Next, Section 6.3.2 provides both an overview and detailed descriptions of the constraints.

6.3.1 Objective Function

$$\min \quad z = \sum_{t \in \mathcal{T}} \sum_{s \in \mathcal{S}} P^s N^D z_t^s \tag{6.1}$$

$$\begin{aligned} z_t^s = & \sum_{p \in \mathcal{P}} \sum_{i \in \mathcal{I}_p^{ZE}} C_i^{II} y_{pit}^{Is} + \sum_{p \in \mathcal{P}} C_p^{IG} (q_{pt}^{GAs} - Q_p^{GA}) \\ & + \sum_{v \in \mathcal{V}} C_v^{VI} x_{vt}^s + \sum_{r \in \mathcal{R}} \sum_{b \in \mathcal{B}_r} \sum_{v \in \mathcal{V}_{rb}} C_{rbvt}^{Os} R^E y_{rbvt}^s \\ & + \sum_{p \in \mathcal{P}} \sum_{i \in \mathcal{I}_p^F} \sum_{\hat{p} \in \mathcal{P}} \sum_{\hat{i} \in \mathcal{I}_{\hat{p}}^{HUB}} C^{HT} \Delta D_{p\hat{p}}^{F2H} R^E e_{pi\hat{p}\hat{i}t}^{Hs} \end{aligned} \tag{6.2}$$

$$, t \in \mathcal{T}, s \in \mathcal{S}$$

The objective of the ZEVIPP is to minimize the expected costs described in Section 3.2.2 across the long-term planning horizon, as represented by (6.1). Each scenario has a given probability, and the daily costs of serving all routes in time step t in scenario s is represented by z_t^s which is presented in (6.2). The first three terms express that investing and utilizing infrastructure, grid capacity, and vessels comes at a cost. Note that in the second term the, initially available grid capacity is subtracted since expansion costs are not incurred for the initially available capacity. The fourth term sums over the pre-calculated costs from the assigned route serving permutations. Recall that the Sub-Problems assume that the hydrogen supplied to filling stations is procured from the nearest hub. The fifth term represents the additional accrued cost at filling stations for the amount of hydrogen which is not procured from the nearest hub.

6.3.2 Constraints

Logical investment constraints

Constraints (6.3) state that in each time step and scenario, every route should be assigned exactly one route serving permutation. Next, constraints (6.4) show that at any port, there may only be one hydrogen-producing infrastructure. Furthermore, there can only be one bunkering infrastructure of each energy carrier at a port. This is ensured by constraints (6.5), (6.7), (6.6), and (6.8) which restrict the number of infrastructures for hydrogen, electric batteries, electric swappable batteries, and conventional fuel, respectively. Finally, constraints (6.9) ensure that no vessels are used if they are not available in the given scenario and time step.

$$\sum_{b \in \mathcal{B}_r} \sum_{v \in \mathcal{V}_{rb}} y_{rbvt}^s = 1, \qquad r \in \mathcal{R}, t \in \mathcal{T}, s \in \mathcal{S} \tag{6.3}$$

$$\sum_{i \in \mathcal{I}_p^{LP} \cup I_p^{HUB}} y_{pit}^{Is} \leq 1, \qquad p \in \mathcal{P}, t \in \mathcal{T}, s \in \mathcal{S} \tag{6.4}$$

$$\sum_{i \in \mathcal{I}_p^{LP} \cup \mathcal{I}_p^F} y_{pit}^{Is} \leq 1, \qquad p \in \mathcal{P}, t \in \mathcal{T}, s \in \mathcal{S} \tag{6.5}$$

$$\sum_{i \in \mathcal{I}_p^E} y_{pit}^{Is} \leq 1, \qquad p \in \mathcal{P}, t \in \mathcal{T}, s \in \mathcal{S} \tag{6.6}$$

$$\sum_{i \in \mathcal{I}_p^S} y_{pit}^{Is} \leq 1, \qquad p \in \mathcal{P}, t \in \mathcal{T}, s \in \mathcal{S} \tag{6.7}$$

$$\sum_{i \in \mathcal{I}_p \setminus \mathcal{I}_p^{ZE}} y_{pit}^{Is} \leq 1, \qquad p \in \mathcal{P}, t \in \mathcal{T}, s \in \mathcal{S} \quad (6.8)$$

$$\sum_{r \in \mathcal{R}} \sum_{b \in \mathcal{B}_r} N_{rbvt}^{Vs} y_{rbvt}^{s} \leq x_{vt}^{s}, \qquad v \in \mathcal{V}, t \in \mathcal{T}, s \in \mathcal{S} \quad (6.9)$$

Investment constraints across time steps and between scenarios

All variables for the initial stock of each vessel type, installed infrastructures at ports, and available grid capacities are initiated by constraints (6.10), (6.11) and (6.12), respectively. The lead time for investments in vessels, infrastructures, and grid capacities is handled by constraints (6.13), (6.14), and (6.15), respectively. These constraints state that the stock of any asset cannot increase from one time step to the next, without having invested in the said asset in advance in accordance with the lead time. Since the investment variable is non-negative, the stock of the assets cannot decrease either.

$$x_{vt}^{s} = X_v, \qquad v \in \mathcal{V}^{ZE}, t \in \{1..L_v^V\}, s \in \mathcal{S}, \quad (6.10)$$

$$y_{pit}^{Is} = Y_{pi}^{I}, \qquad p \in \mathcal{P}, i \in \mathcal{I}_p^{ZE}, t \in \{1..L_i^I\}, s \in \mathcal{S}, \quad (6.11)$$

$$q_{pt}^{GAs} = Q_p^{GA}, \qquad p \in \mathcal{P}, t \in \{1..L_p^G\}, s \in \mathcal{S}, \quad (6.12)$$

$$x_{vt}^{s} - x_{v(t-1)}^{s} = \tilde{x}_{v(t-L_v^V)}^{s}, \qquad v \in \mathcal{V}^{ZE}, t \in \mathcal{T} \setminus \{1..L_v^V\}, s \in \mathcal{S}, \quad (6.13)$$

$$y_{pit}^{Is} - y_{pi(t-1)}^{Is} = \tilde{y}_{pi(t-L_i^I)}^{Is}, \qquad p \in \mathcal{P}, i \in \mathcal{I}_p^{ZE}, t \in \mathcal{T} \setminus \{1..L_i^I\}, s \in \mathcal{S}, \quad (6.14)$$

$$q_{pt}^{GAs} - q_{p(t-1)}^{GAs} = \tilde{q}_{p(t-L_p^G)}^{GAs}, \qquad p \in \mathcal{P}, t \in \mathcal{T} \setminus \{1..L_p^G\}, s \in \mathcal{S}, \quad (6.15)$$

Non-anticipativity constraints

As described in Section 6.1.2, investment decisions in each time step need to be equal across scenarios in the first stage. The non-anticipativity constraints (6.16), (6.17), and (6.18) enforce this. This also holds for the operational variables, since they will not vary given the investment decisions.

$$\tilde{x}_{vt}^{s} = \tilde{x}_{vt}^{(s+1)}, \qquad v \in \mathcal{V}^{ZE}, t \in \mathcal{T}^{NS}, s \in \mathcal{S} \setminus \{|\mathcal{S}|\} \quad (6.16)$$

$$\tilde{y}_{pit}^{Is} = \tilde{y}_{pit}^{I(s+1)}, \qquad p \in \mathcal{P}, i \in \mathcal{I}_p^{ZE}, t \in \mathcal{T}^{NS}, s \in \mathcal{S} \setminus \{|\mathcal{S}|\}, \quad (6.17)$$

$$\tilde{q}_{pt}^{GAs} = \tilde{q}_{pt}^{GA(s+1)}, \qquad p \in \mathcal{P}, t \in \mathcal{T}^{NS}, s \in \mathcal{S} \setminus \{|\mathcal{S}|\}, \quad (6.18)$$

Energy Production and Consumption Constraints

The constraints for energy production and consumption ensure that the energy consumed when serving the routes is produced and available at the correct location. First, constraints (6.19) restrict the share of fossil energy at each time step in each scenario. Constraints (6.20) state that all self-consuming infrastructures need to produce enough energy at each port to operate the selected Sub-Problems. Additionally, constraints (6.21) ensure that the hydrogen filling stations procure

sufficient amounts of energy from the hubs. Hydrogen distributed from a hub $\hat{i}$ at port $\hat{p}$ to filling station i at port p needs to be produced at the said hub. This is ensured by constraints (6.22). Also, a filling station cannot be supplied with more hydrogen than the storage capacity at the said filling station as stated by constraints (6.23).

It is only possible to produce hydrogen at an infrastructure at a port if it is invested in, as ensured by constraints (6.24). Moreover, M_i^0 should be an upper bound for how much an energy production facility could possibly produce within the given infrastructures' capacities in a time step. Consequently, $M_i^0 = min\{R_i^P N^H E_i^{CE},\ R_i^B N^H\}$, is a reasonable choice for all bunkering infrastructures. The terms are the maximal theoretic amount of energy possible to produce and dispense at the infrastructure, respectively. Note that for hubs, M_i^0 equals the maximal production capacity since the bunkering rate for hydrogen tube trucks is used, and they are assumed higher than the production rate.

The total time spent bunkering at an infrastructure at a port is restricted by constraints (6.25). The purpose of these constraints is to ensure global feasibility in a case where many Sub-Problems use the same infrastructure, which leads to congestion.

$$\sum_{r\in\mathcal{R}}\sum_{b\in\mathcal{B}_r}\sum_{v\in\mathcal{V}_{rb}^C}\sum_{p\in\mathcal{P}_b} E_{rbvpt}^{Us} y_{rbvt}^s \le \overline{E}_t^C, \qquad t\in\mathcal{T}, s\in\mathcal{S} \quad (6.19)$$

$$\sum_{b\in\mathcal{B}_{pi}}\sum_{r\in\mathcal{R}_b}\sum_{v\in\mathcal{V}_{rb}^{ZE}} E_{rbvpt}^{Us} y_{rbvt}^s \le e_{pit}^{Ps}, \qquad p\in\mathcal{P}, i\in\mathcal{I}_p^{SC}, t\in\mathcal{T}, s\in\mathcal{S} \quad (6.20)$$

$$\sum_{b\in\mathcal{B}_{pi}}\sum_{r\in\mathcal{R}_b}\sum_{v\in\mathcal{V}_{rb}^{ZE}} E_{rbvpt}^{Us} y_{rbvt}^s \le \sum_{\hat{p}\in\mathcal{P}}\sum_{\hat{i}\in\mathcal{I}_{\hat{p}}^{HUB}} e_{pi\hat{p}\hat{i}t}^{Hs}, \qquad p\in\mathcal{P}, i\in\mathcal{I}_p^{F}, t\in\mathcal{T}, s\in\mathcal{S} \quad (6.21)$$

$$\sum_{p\in\mathcal{P}}\sum_{i\in\mathcal{I}_p^F} e_{pi\hat{p}\hat{i}t}^{Hs} \le e_{\hat{p}\hat{i}t}^{Ps}, \qquad \hat{p}\in\mathcal{P}, \hat{i}\in\mathcal{I}_{\hat{p}}^{HUB}, t\in\mathcal{T}, s\in\mathcal{S} \quad (6.22)$$

$$\sum_{\hat{p}\in\mathcal{P}}\sum_{\hat{i}\in\mathcal{I}_{\hat{p}}^{HUB}} e_{pi\hat{p}\hat{i}t}^{Hs} \le Q_i^S y_{pit}^{Is}, \qquad p\in\mathcal{P}, i\in\mathcal{I}_p^{F}, t\in\mathcal{T}, s\in\mathcal{S} \quad (6.23)$$

$$e_{pit}^{Ps} \le M_i^0 y_{pit}^{Is}, \qquad p\in\mathcal{P}, i\in\mathcal{I}_p^{GC}, t\in\mathcal{T}, s\in\mathcal{S} \quad (6.24)$$

$$\sum_{b\in\mathcal{B}_{pi}}\sum_{r\in\mathcal{R}_b}\sum_{v\in\mathcal{V}_{rb}^{ZE}} T_{rbvpt}^{Us} y_{rbvt}^s \le N^H U^F, \qquad p\in\mathcal{P}, i\in\mathcal{I}_p^{B}, t\in\mathcal{T}, s\in\mathcal{S} \quad (6.25)$$

Grid Capacity Constraints

At any time step the total available grid capacity at a port is restricted according to constraints (6.26). As constraints (6.27) state, the total available grid capacity at a port also limits the amount of energy that can be produced each operating day. Finally, the electric charging infrastructures are assumed to require sufficient grid capacity to always operate at maximum. This is represented by constraints (6.28).

$$q_{pt}^{GAs} \le \overline{Q}_p^G + Q_p^{GA}, \qquad p\in\mathcal{P}, t\in\mathcal{T}, s\in\mathcal{S} \quad (6.26)$$

$$\sum_{i\in\mathcal{I}_p^{GC}} \frac{e_{pit}^{Ps}}{E_i^{CE}} \le N^H q_{pt}^{GAs}, \qquad p\in\mathcal{P}, t\in\mathcal{T}, s\in\mathcal{S} \quad (6.27)$$

$$\sum_{i\in\mathcal{I}_p^E} R_i^P y_{pit}^{Is} \le q_{pt}^{GAs}, \qquad p\in\mathcal{P}, t\in\mathcal{T}, s\in\mathcal{S} \quad (6.28)$$

Non-Negativity, Binary and Integer Requirements

In order to reduce the number of variables, they are only defined for the ones which are relevant. That is, the variables y^s_{rbvt} are only defined for the Sub-Problems which are feasible. Further on, y^{Is}_{pit} is only defined for the feasible infrastructures at the port p.

$$y^s_{rbvt} \in \{0,1\}, \qquad r \in \mathcal{R}, b \in \mathcal{B}_r, v \in \mathcal{V}_{rb}, t \in \mathcal{T}, s \in \mathcal{S} \quad (6.29)$$

$$y^{Is}_{pit} \in \{0,1\}, \qquad p \in \mathcal{P}, i \in \mathcal{I}_p, t \in \mathcal{T}, s \in \mathcal{S} \quad (6.30)$$

$$x^s_{vt} \in \mathbb{Z}^+, \qquad v \in \mathcal{V}, t \in \mathcal{T}, s \in \mathcal{S} \quad (6.31)$$

$$q^{GAs}_{pt} \in \mathbb{R}^+, \qquad p \in \mathcal{P}, t \in \mathcal{T}, s \in \mathcal{S} \quad (6.32)$$

$$\tilde{y}^{Is}_{pit} \in \{0,1\}, \qquad p \in \mathcal{P}, i \in \mathcal{I}^{ZE}_p, t \in \{1..|\mathcal{T}| - L^I_i\}, s \in \mathcal{S} \quad (6.33)$$

$$\tilde{x}^s_{vt} \in \mathbb{Z}^+, \qquad v \in \mathcal{V}^{ZE}, t \in \{1..|\mathcal{T}| - L^V_v\}, s \in \mathcal{S} \quad (6.34)$$

$$\tilde{q}^{GAs}_{pt} \in \mathbb{R}^+, \qquad p \in \mathcal{P}, t \in \{1..|\mathcal{T}| - L^G_p\}, s \in \mathcal{S} \quad (6.35)$$

$$e^{Hs}_{pi\hat{p}\hat{i}t} \in \mathbb{R}^+, \qquad p \in \mathcal{P}, i \in \mathcal{I}^F_p, \hat{p} \in \mathcal{P}, \hat{i} \in \mathcal{I}^{HUB}_{\hat{p}}, t \in \mathcal{T}, s \in \mathcal{S} \quad (6.36)$$

$$e^{Ps}_{pit} \in \mathbb{R}^+, \qquad p \in \mathcal{P}, i \in \mathcal{I}^{GC}_p, t \in \mathcal{T}, s \in \mathcal{S} \quad (6.37)$$

Chapter 7

Mathematical Formulation of the Sub-Problem

This section presents the mathematical formulation of the Sub-Problem. Section 5.2 detailed the decomposition into a Master Problem and several independent Sub-Problems. Recall that a route-serving permutation is a combination of a bunkering alternative and a vessel type. The Sub-Problems determine the operational implications of each possible route-serving permutation. As illustrated by Figure 7.1, this means that a Sub-Problem is solved with a route-serving permutation as input and provides the outputs *cost*, *number of vessels*, *energy used at each port*, and *bunkering time at each port*, which are used as parameters in the Master Problem. A Sub-Problem solution has to maintain the current service level and manage the energy level at each vessel. First, Section 7.1 details the modeling approach decided for the Sub-Problem. Second, Section 7.2 declares the notation used in the Sub-Problem's mathematical model, presented in Section 7.3.

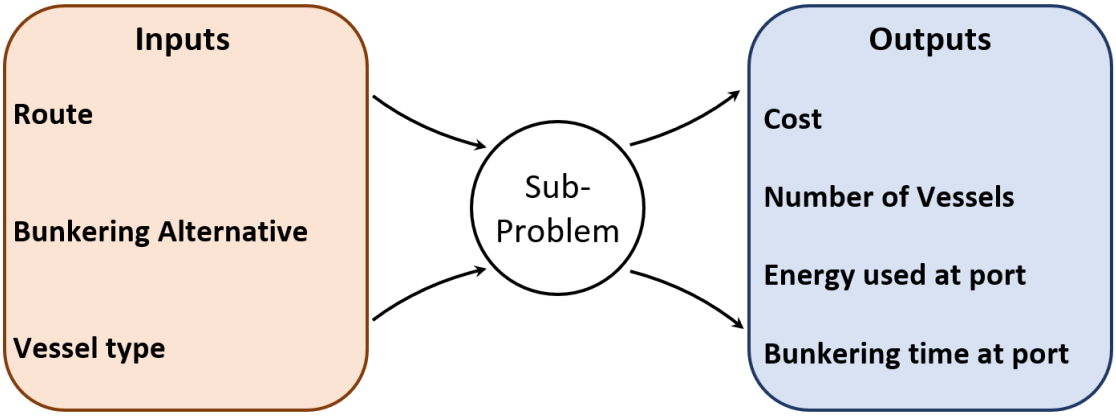

Figure 7.1: Input and output of the Sub-Problem, where the output from the Sub-Problem is used as input to the Master Problem

7.1 Modeling Approach

The main modeling approach for the Sub-Problem is described in Section 7.1.1, while the remaining modeling approaches are included in Appendix D.

7.1.1 Activities and Activity Slots

The main goal of the Sub-Problem is to serve all sub-routes in each time period while minimizing costs. To serve a sub-route, a vessel needs to sail between all ports along the said sub-route. Simultaneously, each vessel has an upper and lower bound for the energy level where it is able to operate. Therefore, the vessels need to bunker to ensure that they have sufficient amounts of energy at any point in time.

The decisions of bunkering and serving sub-routes are abstracted into activities. Conducting an activity is either doing nothing, serving a sub-route, bunkering, or both bunkering and serving a sub-route. For a given activity, it is given if and where the vessel bunkers, how far it sails, if it serves a sub-route, which sub-route it serves, and the starting and ending ports. A set of allowed activities is shown in Figure 7.2. Here, one sub-route is to be served by starting and ending in the same resting port, and the allotted bunkering alternative includes two bunkering ports. A Sub-Problem's allowed activities are generated in the following manner: one *resting* activity for each resting port {**A**}, one *route-serving* activity for each sub-route {**AR**}, one *bunkering* activity for each pair of resting ports and bunkering ports {**B, C**}, and finally, one *bunkering and route-serving* activity for each permutation of bunkering ports for each sub-route {**BR, CR, DR**}.

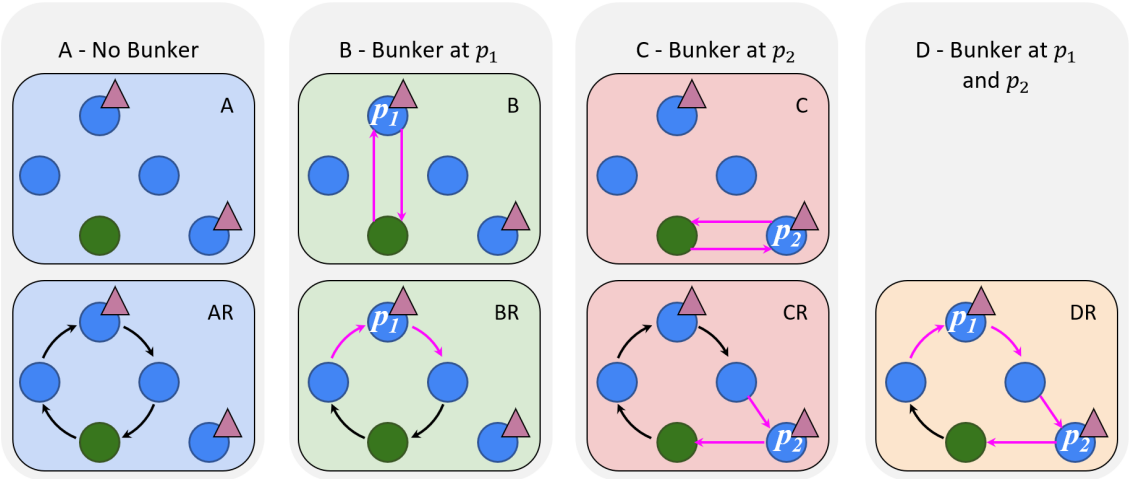

Figure 7.2: Example of which activities a Sub-Problem is allotted. Black arcs represent route-serving, while pink arcs indicate that the vessel bunker at the bunkering port between each pair of pink arrows. All activities in the bottom row serve the sub-route.

Given the allowed activities, a Sub-Problem can be solved by deciding which activities to conduct in which order in each time period. In the model, this is handled by assigning each time period a set of temporally ordered activity slots. Each activity slot is assigned one activity in a Sub-Problem solution. Furthermore, the sub-route's frequency can be maintained by ensuring that the number of route-serving activities assigned to activity slots in a given time period is equal to the demanded frequency.

Figure 7.3 illustrates how a Sub-Problem can be solved by assigning activities to its activity slots. In this example, there are two vessels, the route is comprised of one sub-route, and the required frequencies for the sub-route in the first and second time periods are one and two, respectively. In Time Period 1, Vessel 1 serves the sub-route in Activity Slot 1 and rests for the remainder of the time period. Vessel 2 rests during the entire first time period. Next, in Time Period 2, Vessel 1 starts by bunkering in Activity Slot 4 in order to have enough energy to serve the sub-route in the following activity slot. Finally, Vessel 2 serves the sub-route in Activity Slot 4 and bunkers halfway.

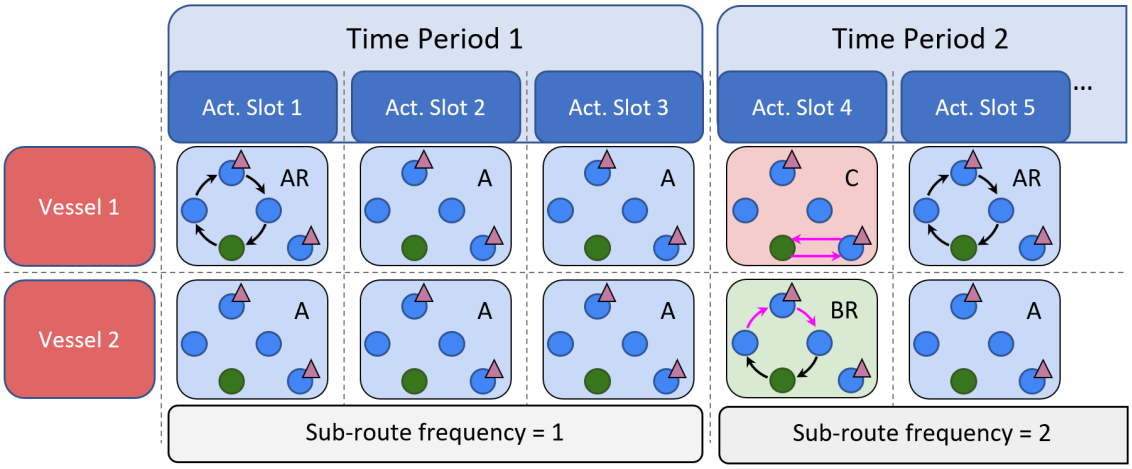

Figure 7.3: Example of how activities might be assigned to activity slots for the first two time periods of a Sub-Problem.

In conclusion, the Sub-Problem essentially remains an assignment problem that decides which activities are conducted by each vessel in each activity slot. An assignment solution, however, has to maintain feasibility in regard to energy, time, and localization. That means that the energy and time level can never breach their respective limits, and an activity can only be served if the vessel is located in the starting port of the activity. These are of course essential parts of the problem. However, this section is sufficient to understand the main modeling approach, so the details of the remaining modeling approaches are attached in Appendix D.

7.2 Notation

In this section, the notations of each set, parameter, and variable are detailed and summarized.

Sets

$\mathcal{V}^{VO}$ represents the set of vessels serving the Sub-Problem. This is typically comprised of one or two vessels, which for all practical purposes are indistinguishable. $\mathcal{T}^{TP}$ denotes the time periods into which the short-term planning period of one day is divided. $\mathcal{R}^{SR}$ is the set of sub-routes which comprises the route r defining the given Sub-Problem.

The two sets $\mathcal{P}^{R}$ and $\mathcal{P}^{B}$ denote resting ports given by the route under consideration, r, and the bunkering ports in the bunkering alternative under consideration, b, respectively. Note that the main port is included in $\mathcal{P}^{R}$, that the two sets may overlap, and that both are indexed by p. Further, $\mathcal{P}^{B}_{ap}$ includes p and the bunkering ports that are visited before bunkering port p during activity a. Essentially, these keep track of the order in which the bunkering ports are visited during activity a. An example of what these sets might include is illustrated in Figure 7.4. Let DR be an activity serving a sub-route visiting two bunkering ports, and p_1 and p_2 denote the first and the second bunkering port the vessel visits during activity DR. In this configuration, the set $\mathcal{P}^{B}_{(DR)p_1}$ contains only p_1 because it has not visited any other bunkering ports before p_1, and $\mathcal{P}^{B}_{(DR)p_2}$ contains both p_1 and p_2 because it has visited p_1 before visiting p_2.

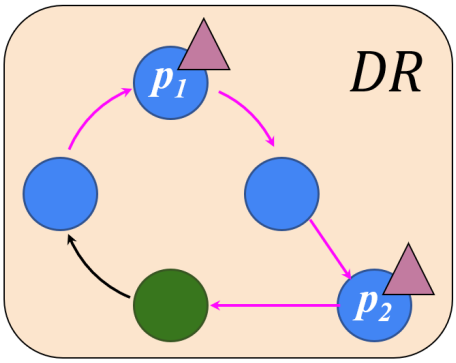

$$\mathcal{P}^{B}_{(DR)p_1} = \{p_1\}$$
$$\mathcal{P}^{B}_{(DR)p_2} = \{p_1, p_2\}$$

Figure 7.4: Set of previously visited bunkering ports for the example activity **DR**

$\mathcal{J}$ is the set of all activity slots. It is comprised of the union of elements in $\mathcal{J}_{\hat{t}}$, which denotes the activity slots available for each time period $\hat{t}$. The number of activity slots in each time period has to be balanced to ensure optimality and reduce the size of the solution space. The number of activity slots available in each time period is determined as presented in Equation 7.1. Here, $F_{\hat{r}\hat{t}}$ denotes the number of times sub-route $\hat{r}$ has to be served during time period $\hat{t}$. The rationale behind this equation is to ensure that both a route-serving activity and a bunkering detour activity can be conducted for each frequency within each time period. The two sets $\mathcal{J}^{\mathcal{S}}$ and $\mathcal{J}^{\overline{\mathcal{S}}}$ include the activity slots that initiate a time period and the ones that do not, respectively.

$$|\mathcal{J}_{\hat{t}}| = max\left\{1, \left\lceil \frac{\sum_{\hat{r}\in\mathcal{R}^{SR}} F_{\hat{r}\hat{t}}}{|\mathcal{V}^{VO}|} \right\rceil\right\} \tag{7.1}$$

Lastly, the sets of activities are presented. $\mathcal{A}$ is the total set of allowed activities. $\mathcal{A}^{R}$and$\mathcal{A}^{R}_{\hat{r}}$ denote the sets of all route-serving activities and activities serving sub-route $\hat{r}$, respectively. Further, $\mathcal{A}^{B}$ and $\mathcal{A}^{B}_{p}$ include all activities that allow bunkering and all activities that allow bunkering at bunkering port p, respectively. $\mathcal{A}^{BR} = \mathcal{A}^{B} \cap \mathcal{A}^{R}$, meaning that it includes all activities that allow bunkering in addition to serving a sub-route. $\mathcal{A}^{REST}$ and $\mathcal{A}^{\overline{REST}}$ denote the activities that are resting at either resting port and the activities which do not rest, respectively. Finally, $\mathcal{A}^{E}_{p}$ and $\mathcal{A}^{S}_{p}$ include the activities ending and starting at port p, respectively.

Parameters

Let D^{P} denote the passenger demand for every route serving. It is assumed that this value is equal for all sub-routes. $F_{\hat{t}\hat{r}}$ denotes the number of times a sub-route $\hat{r}$ has to be served during the time period $\hat{t}$. Further, the time periods have a predetermined ending during the day, encoded as the number of hours after the start of the short-term planning period. This is represented by T^{END}_{j} for each activity slot j.

The cost parameters C^{CREW}, C^{PT}, C^{A} and C^{E}_{p} represent the cost coefficient each term of the objective function is scaled with. Every crew shift incurs a cost of C^{CREW}, while every unmet demand in each route serving is penalized with the alternative cost C^{A}. Further, accrued time with passengers on board is penalized with the passenger time cost C^{PT}. Lastly, C^{E}_{p} is the cost of each energy unit bunkered from bunkering port p.

A Sub-Problem is solved for a given vessel type. This entails uniquely the vessel parameters used in a Sub-Problem. The parameters this applies to are $V^{PAX}, \overline{Q}^{VS}, \underline{Q}^{VS}$ and $\overline{\underline{Q}}^{VS}$. The first determines the number of passengers the vessels can transport at the same time. The last three denote the upper energy bound, lower energy bound, and the vessel type's maximum available energy, respectively.

As discussed in Section D.3, an infrastructure is uniquely defined for each bunkering port. Thus, $Q^{IS}_{p}, R^{B}_{p}, R^{P}_{p}$ and E^{EC}_{p} are indexed by p. The first parameter declares the capacity of the on-shore storage. The two next denote the bunkering and production rate of the infrastructure installed

at bunkering port p, respectively. Finally, the latter gives the fraction between energy used for production and the resulting produced energy, typically known as energy conversion efficiency, of the infrastructure installed at bunkering port p.

Lastly, the activity parameters are presented. A_a^{BT} is the bunkering overhead time, that is, the time activity a uses to initiate and end the bunkering process. A_a^T gives the time needed to sail the total distance sailed during activity a. A_a^{EU} denotes the total energy consumed while sailing the distance given by activity a. A_a^{ER} declares the energy needed to embark on activity a. Finally, A_{ap}^{ELL} is the energy needed to sail the last leg before arriving at bunkering port p during activity a.

Variables

In order to assign an activity a to activity slot j for vessel $\hat{v}$, the variable $y_{\hat{v}ja}^A$ has to be set to 1. This variable restricts the model to assign one and only one activity to each vessel in each activity slot. Further, the crew cost is incurred if and only if a vessel conducts any non-resting activities during a time period. Thus, $y_{v\hat{t}}^T$ is used to either incur a crew shift cost for each time period for each vessel or not. Next, $e_{\hat{v}j}^S$ and $h_{\hat{v}j}$ track the energy storage level and time level of each vessel for each activity slot in order to ensure that the energy level is within the restricted upper and lower energy bound for the duration of the short-term planning period and that the time does not exceed the time periods' limits.

The variable $e_{\hat{v}jp}^B$ monitors the amount of energy bunkered at bunkering port p in activity slot j by vessel $\hat{v}$. In order to keep track of the quantity of energy bunkered by directly filling from the on-shore energy storage and the quantity bunkered after the energy storage is emptied, the variables $e_{\hat{v}jp}^{\underline{B}}$ and $e_{\hat{v}jp}^{\overline{B}}$ are introduced. The energy quantity $e_{\hat{v}jp}^{\underline{B}}$ is bunkered with the bunkering rate, R_p^B, and the energy quantity $e_{\hat{v}jp}^{\overline{B}}$ is bunkered with the effective production rate of the infrastructure at the bunkering port. Finally, the energy is not necessarily bunkered with passengers on board. To account for this, $e_{\hat{v}jp}^{\underline{B}C}$ and $e_{\hat{v}jp}^{\overline{B}C}$ are introduced and denote the energy bunkered while bearing passenger costs.

Sets

$\mathcal{V}^{VO}$	Set of vessel
$\mathcal{T}^{TP}$	Set of time periods
$\mathcal{R}^{SR}$	Set of sub-routes
$\mathcal{P}^R$	Set of resting- and main ports
$\mathcal{P}^B$	Set of bunkering ports
$\mathcal{P}_{ap}^B$	Set of bunkering ports which are bunkered at until bunkering at bunkering port p, including p, during activity a
$\mathcal{J}$	Set of activity slots
$\mathcal{J}_{\hat{t}}$	Set of activity slots in time period $\hat{t}$
$\mathcal{J}^S$	Set of activity slots initiating a time period
$\mathcal{J}^{\overline{S}}$	Set of activity slots not initiating a time period
$\mathcal{A}$	Set of activity types
$\mathcal{A}^R$	Set of activity types serving a sub-route
$\mathcal{A}_{\hat{r}}^R$	Set of activity types serving sub-route $\hat{r}$
$\mathcal{A}^B$	Set of bunkering activity types
$\mathcal{A}_p^B$	Set of activity types bunkering at bunkering port p

$\mathcal{A}^{BR}$	Set of bunkering activities, which also serve a sub-route
$\mathcal{A}^{REST}$	Set of resting activity types
$\mathcal{A}^{\overline{REST}}$	Set of non-resting activity types
$\mathcal{A}_p^E$	Set of activities that *end* in port p
$\mathcal{A}_p^S$	Set of activities that *start* in port p

Parameters

D^P	Passenger demand on all sub-routes
$F_{\hat{t}\hat{r}}$	The frequency demand of sub-route $\hat{r}$ in time period $\hat{t}$
T_j^{END}	The ending time of the time period containing activity slot j
C^{CREW}	Crew shift cost
C^{PT}	Passenger time cost
C^A	Passenger alternative cost
C_p^E	Unit cost of energy at bunkering port p
V^{PAX}	Passenger capacity of the selected vessel type
$\overline{Q}^{VS}$	Upper bound for energy level of the selected vessel type
$\underline{Q}^{VS}$	Lower bound for energy level of the selected vessel type
$\overline{\underline{Q}}^{VS}$	Maximum available energy for the selected vessel type
Q_p^{IS}	The energy storage capacity installed at bunkering port p
R_p^B	Rate of energy bunkering at bunkering port p
R_p^P	Rate of energy production at bunkering port p
E_p^{EC}	Energy conversion efficiency of the infrastructure installed at bunkering port p
A_a^{BT}	Bunkering overhead time associate with conducting activity a
A_a^T	Sailing time for activity a
A_a^{EU}	The total energy consumed when performing activity a
A_a^{ER}	The minimum energy required to initiate activity a
A_{ap}^{ELL}	The energy required to sail the last leg of activity a ending at bunkering port p

Variables

$y_{\hat{v}ja}^A$	1 if vessel $\hat{v}$ performs activity a in activity slot j, 0 otherwise
$y_{v\hat{t}}^T$	1 if vessel $\hat{v}$ is used in time period $\hat{t}$, 0 otherwise
$e_{\hat{v}j}^S$	Energy storage level at vessel $\hat{v}$ at the start of activity slot j
$h_{\hat{v}j}$	Time spent by vessel $\hat{v}$ by the start of activity slot j

$e^{B}_{\hat{v}jp}$ Amount of energy bunkered by vessel $\hat{v}$ in activity slot j at bunkering port p

$e^{\underline{B}}_{\hat{v}jp}$ Amount of energy bunkered from on-shore storage at bunkering port p by vessel $\hat{v}$ in activity slot j

$e^{\overline{B}}_{\hat{v}jp}$ Amount of energy bunkered with *empty* on-shore storage at bunkering port p by vessel $\hat{v}$ in activity slot j

$e^{\underline{B}C}_{\hat{v}jp}$ Amount of energy bunkered from on-shore storage at bunkering port p by vessel $\hat{v}$ in activity slot j while passengers are on board

$e^{\overline{B}C}_{\hat{v}jp}$ Amount of energy bunkered with *empty* on-shore storage at bunkering port p by vessel $\hat{v}$ in activity slot j while passengers are on board

7.3 Mathematical Model of the Sub-Problem

This section presents the mathematical model of the Sub-Problem. Each set of constraints and the objective function are declared and described continuously throughout the section.

Objective

$$\min \quad z = \sum_{\hat{v}\in\mathcal{V}^{VO}} \sum_{\hat{t}\in\mathcal{T}^{TP}} C^{CREW} y^{T}_{v\hat{t}} + \sum_{p\in\mathcal{P}^{B}} \sum_{\hat{v}\in\mathcal{V}^{VO}} \sum_{j\in\mathcal{J}} C^{E}_{p} e^{B}_{\hat{v}jp} + C^{A} M^{UD} \sum_{\hat{t}\in\mathcal{T}^{TP}} \sum_{\hat{r}\in\mathcal{R}^{SR}} F_{\hat{t}\hat{r}} \tag{7.2}$$

$$+ \sum_{\hat{v}\in\mathcal{V}^{VO}} \sum_{j\in\mathcal{J}} M^{PO} C^{PT} \left(\sum_{a\in\mathcal{A}^{R}} A^{T}_{a} y^{A}_{\hat{v}ja} + \sum_{a\in\mathcal{A}^{BR}} A^{BT}_{a} y^{A}_{\hat{v}ja} + \sum_{p\in\mathcal{P}^{B}} \left(\frac{e^{\underline{B}C}_{\hat{v}jp}}{R^{B}_{p}} + \frac{e^{\overline{B}C}_{\hat{v}jp}}{R^{P}_{p} E^{EC}_{p}} \right) \right)$$

The objective is to minimize the total costs of serving a route given a bunkering alternative and a vessel type. The first term is the crew costs. The second term is the energy costs at each port. The third term is the alternative cost of not serving the route passenger demand. The fourth term is comprised of the passenger time costs induced by activities and bunkering conducted with passengers on board. The terms M^{UD} and M^{PO} denote the unmet demand for each route-serving and the number of passengers on board each route-serving activity, respectively. $M^{UD} = max\{0, D^{P} - V^{PAX}\}$ and $M^{PO} = min\{D^{P}, V^{PAX}\}$.

Constraints

Constraints (7.3) assign an activity to all activity slots for each vessel. Further, constraints (7.4) ensure that for every vessel and every time period a crew shift is incurred if the vessel conducts a non-resting activity during the time period.

$$\sum_{a\in\mathcal{A}} y^{A}_{\hat{v}ja} = 1, \qquad j \in \mathcal{J}, \hat{v} \in \mathcal{V}^{VO} \tag{7.3}$$

$$\sum_{j\in\mathcal{J}_{\hat{t}}} \sum_{a\in\mathcal{A}^{\overline{REST}}} y^{A}_{\hat{v}ja} \leq |\mathcal{J}_{\hat{t}}|\, y_{v\hat{t}}, \qquad \hat{v} \in \mathcal{V}^{VO}, \hat{t} \in \mathcal{T}^{TP} \tag{7.4}$$

Energy Constraints

M^{BT}_{p} denotes the bunkering threshold. It is calculated as the storage capacity multiplied by the ratio of the bunkering rate and the emptying rate of the energy storage. The emptying rate is equal to the bunkering rate less the effective production rate. $M^{BT}_{p} = Q^{IS}_{p} \frac{R^{B}_{p}}{R^{B}_{p} - R^{P}_{p} E^{EC}_{p}}$.

Constraints (7.5) constrain the energy bunkered at bunkering port p to 0 when no activity that bunkers at bunkering port p is conducted. Furthermore, they constrain the energy bunkered to the maximum available energy when an activity that bunkers at bunkering port p is selected. Further, constraints (7.6) fix the total bunkering to the sum of the bunkering before and after the bunkering threshold. In order to restrict $e^{\underline{B}}_{\hat{v}jp}$ above by the bunkering threshold, constraints (7.7) are added. Then, constraints (7.8) and (7.9) ensure that energy bunkered with passengers is equal to their corresponding bunkering variables only when a route-serving activity is conducted.

M^0_p denotes the big-M value needed in constraints (7.7) and (7.8). The value of bunkering before the bunkering threshold cannot be larger than either the maximum available energy for propulsion or the bunkering threshold. $M^0_p = min\left\{\overline{Q}^{VS}, M^{BT}_p\right\}$. M^1_p denotes the big-M value needed in constraints (7.9). The amount bunkered after the bunkering threshold can never be higher than the maximum available energy less the maximum amount bunkered before the bunkering threshold. $M^1_p = \overline{Q}^{VS} - M^0_p$. In constraints (7.5), the maximum available energy can be interpreted as its big-M value.

$$e^{B}_{\hat{v}jp} \leq \overline{Q}^{VS} \sum_{a \in \mathcal{A}^B_p} y^A_{\hat{v}ja}, \qquad \hat{v} \in \mathcal{V}^{VO}, j \in \mathcal{J}, p \in \mathcal{P}^B \quad (7.5)$$

$$e^{B}_{\hat{v}jp} = e^{\underline{B}}_{\hat{v}jp} + e^{\overline{B}}_{\hat{v}jp}, \qquad \hat{v} \in \mathcal{V}^{VO}, j \in \mathcal{J}, p \in \mathcal{P}^B \quad (7.6)$$

$$e^{\underline{B}}_{\hat{v}jp} \leq M^0_p, \qquad \hat{v} \in \mathcal{V}^{VO}, j \in \mathcal{J}, p \in \mathcal{P}^B \quad (7.7)$$

$$e^{\underline{B}}_{\hat{v}jp} \leq e^{\underline{B}C}_{\hat{v}jp} + M^0_p \left(1 - \sum_{a \in \mathcal{A}^R} y^A_{\hat{v}ja}\right), \qquad \hat{v} \in \mathcal{V}^{VO}, j \in \mathcal{J}, p \in \mathcal{P}^B \quad (7.8)$$

$$e^{\overline{B}}_{\hat{v}jp} \leq e^{\overline{B}C}_{\hat{v}jp} + M^1_p \left(1 - \sum_{a \in \mathcal{A}^R} y^A_{\hat{v}ja}\right), \qquad \hat{v} \in \mathcal{V}^{VO}, j \in \mathcal{J}, p \in \mathcal{P}^B \quad (7.9)$$

Continuing, constraints (7.10) secure the correct flow of energy from one activity slot to the next. These can be posed as the energy level less the net energy usage of the current activity slot, which should equal the next energy level. Additionally, constraints (7.11) ensure that the short-term planning period is started and ended with the same energy level for each vessel.

$$e^S_{\hat{v}j} + \sum_{p \in \mathcal{P}^B} e^B_{\hat{v}jp} - \sum_{a \in \mathcal{A}^{\overline{REST}}} A^{EU}_a y_{\hat{v}ja} = e^S_{\hat{v}(j+1)}, \qquad \hat{v} \in \mathcal{V}^{VO}, j \in \mathcal{J} \backslash \{|\mathcal{J}|\} \quad (7.10)$$

$$e^S_{\hat{v}j} = e^S_{\hat{v}(j+|\mathcal{J}|-1)} + \sum_{p \in \mathcal{P}^B} e^B_{\hat{v}(j+|\mathcal{J}|-1)p} - \sum_{a \in \mathcal{A}^{\overline{REST}}} A^{EU}_a y_{\hat{v}(j+|\mathcal{J}|-1)a}, \quad \hat{v} \in \mathcal{V}^{VO}, j \in \{1\} \quad (7.11)$$

Finally, constraints (7.12) and (7.13) ensure that the energy level at each vessel is both below the upper bound and above the lower bound at every bunkering port p it visits. For both sets of constraints, each constraint is only restricting if activity a is conducted in activity slot j by vessel $\hat{v}$. This is modeled by the last term in both sets, which relaxes the constraint if $y^A_{\hat{v}ja} = 0$. The upper bound is comprised of the following two components: the starting idle vessel storage, $\overline{Q}^{VS} - e^S_{\hat{v}j}$; and the net energy usage while conducting activity a until arriving at bunkering port p. The latter is equal to the energy spent sailing every leg until reaching p less the energy bunkered at previously visited bunkering ports. The lower bound restrictions are very similar to the upper bounds. It ensures that the available energy at the start of the activity, $e^S_{\hat{v}j} - \underline{Q}^{VS}$, is not exceeded

by the net energy consumed until reaching bunkering port p. Lastly, to account for activities that do not bunker, constraints (7.14) secure that every non-bunkering activity a is only conducted if the available energy at the start of the activity is greater than or equal to the energy required to initiate the activity.

$$e^B_{\hat{v}jp} \leq \overline{Q}^{VS} - e^S_{\hat{v}j} + \sum_{\hat{p} \in \mathcal{P}^B_{ap}} A^{ELL}_{a\hat{p}} - \sum_{\hat{p} \in \mathcal{P}^B_{ap} \setminus \{p\}} e^B_{\hat{v}j\hat{p}} + \underline{\overline{Q}}^{VS} \left(1 - y^A_{\hat{v}ja}\right), \quad \hat{v} \in \mathcal{V}^{VO}, j \in \mathcal{J}, p \in \mathcal{P}^B, a \in \mathcal{A}^B_p \tag{7.12}$$

$$\sum_{\hat{p} \in \mathcal{P}^B_{ap}} A^{ELL}_{a\hat{p}} - \sum_{\hat{p} \in \mathcal{P}^B_{ap} \setminus \{p\}} e^B_{\hat{v}j\hat{p}} \leq e^S_{\hat{v}j} - \underline{Q}^{VS} + \underline{\overline{Q}}^{VS} \left(1 - y^A_{\hat{v}ja}\right), \quad \hat{v} \in \mathcal{V}^{VO}, j \in \mathcal{J}, p \in \mathcal{P}^B, a \in \mathcal{A}^B_p \tag{7.13}$$

$$\sum_{a \in \mathcal{A}^{NR} \setminus \{\mathcal{A}^B\}} A^{ER}_a y^A_{\hat{v}ja} \leq e^S_{\hat{v}j} - \underline{Q}^{VS}, \qquad \hat{v} \in \mathcal{V}^{VO}, j \in \mathcal{J} \tag{7.14}$$

Time Constraints

First, constraints (7.15) state that every vessel starts the first activity slot with a time value of zero. Further, constraints (7.16) ensure that the time value at the first activity slot in each time period is equal to the end time of the previous time period. Finally, constraints (7.17) secure that the time values are at least as high as the last time value plus the time spent on activities during the last activity slot. As stated in Section D.2, the time spent during the last activity equals the sum of the time sailed during the selected activity, the bunkering overhead time incurred by the selected activity, and the time spent bunkering during the activity slot.

$$h_{\hat{v}j} = 0 \qquad \hat{v} \in \mathcal{V}^{VO}, j \in \{1\} \tag{7.15}$$

$$T^{END}_{(j-1)} = h_{\hat{v}j} \qquad \hat{v} \in \mathcal{V}^{VO}, j \in \mathcal{J}^S \setminus \{1\} \tag{7.16}$$

$$h_{\hat{v}j} + \sum_{a \in \mathcal{A}^{\overline{REST}}} A^T_a y^A_{\hat{v}ja} + \sum_{a \in \mathcal{A}^B} A^{BT}_a y^A_{\hat{v}ja} + \sum_{p \in \mathcal{P}^B} \left(\frac{e^{\underline{B}}_{\hat{v}jp}}{R^B_p} + \frac{e^{\overline{B}}_{\hat{v}jp}}{R^P_p E^{EC}_p} \right) \leq h_{\hat{v}(j+1)} \quad \hat{v} \in \mathcal{V}^{VO}, j \in \mathcal{J} \setminus \{|\mathcal{J}|\} \tag{7.17}$$

Frequency Constraints

In order to ensure that all routes are served at the current service level, constraints (7.18) are introduced. The number of route-serving activities selected during each time period for each sub-route has to equal the respective demanded frequency.

$$F_{\hat{t}\hat{r}} = \sum_{v \in \mathcal{V}^{VO}} \sum_{j \in \mathcal{J}_{\hat{t}}} \sum_{a \in \mathcal{A}^R_{\hat{r}}} y^A_{\hat{v}ja}, \qquad \hat{t} \in \mathcal{T}^{TP}, \hat{r} \in \mathcal{R}^{SR} \tag{7.18}$$

Location Constraints

A route-serving activity has a starting port and an ending port. Only vessels positioned in an activity's starting port are allowed to conduct the said activity. In order to make sure that this logic is maintained in the model, the following sets of constraints are included. Constraints (7.19) state that for every resting port, vessel, and activity slot, the sum of selected activities ending in resting port p has to equal the number of selected activities starting in port p in the following

activity slot. Further, constraints (7.20) and (7.21) ensure that at least one vessel starts and ends the short-term planning period in the main port. Lastly, constraints (7.22) ensure that the other vessels are free to start and end the short-term planning period at any resting port as long as they start and end in the same port.

$$\sum_{a \in \mathcal{A}_p^E} y^A_{\hat{v}ja} = \sum_{a \in \mathcal{A}_p^S} y^A_{\hat{v}(j+1)a}, \qquad j \in \mathcal{J} \backslash \{|\mathcal{J}|\}, \hat{v} \in \mathcal{V}^{VO}, p \in \mathcal{P}^R \quad (7.19)$$

$$\sum_{a \in \mathcal{A}_p^S} y^A_{\hat{v}ja} = 1, \qquad j \in \{1\}, \hat{v} \in \{1\}, p \in \{1\} \quad (7.20)$$

$$\sum_{a \in \mathcal{A}_p^E} y^A_{\hat{v}ja} = 1, \qquad j \in \{|\mathcal{J}|\}, \hat{v} \in \{1\}, p \in \{1\} \quad (7.21)$$

$$\sum_{a \in \mathcal{A}_p^E} y^A_{\hat{v}ja} = \sum_{a \in \mathcal{A}_p^S} y^A_{\hat{v}(j+|\mathcal{J}|-1)a}, \qquad j \in \{1\}, \hat{v} \in \mathcal{V}^{VO} \backslash \{1\}, p \in \mathcal{P}^R \quad (7.22)$$

Symmetry Breaking Constraints

The resting activity is used to assign activities to residual activity slots. However, this solution adds symmetry to the solution space of the activity slot assignment. The reason for this is that there is no practical difference between activity schedules that differ only in the order of when to conduct a resting activity. This gives several permutations of equally optimal solutions, which could increase the solution time considerably. This is solved by breaking the said symmetry with the constraints (7.23). These state that for each vessel and each non-initiating activity slot, a resting activity has to be selected if a resting activity was selected in the previous activity slot.

$$\sum_{a \in \mathcal{A}^{REST}} y^A_{\hat{v}(j-1)a} \leq \sum_{a \in \mathcal{A}^{REST}} y^A_{\hat{v}ja}, \qquad j \in \mathcal{J}^{\overline{S}}, \hat{v} \in \mathcal{V}^{VO} \quad (7.23)$$

Non-Negativity and Binary Requirements

Finally, the variables introduced in Section 7.2 are declared. Variables $y^A_{\hat{v}ja}$ and $y^T_{v\hat{t}}$ are binary because an activity is either selected or not, and a crew shift is either incurred or not. Further, the rest of the variables are continuous as they represent either energy- or time-related values.

$$y^A_{\hat{v}ja} \in \{0,1\}, \qquad v \in \mathcal{V}^{VO}, j \in \mathcal{J}, a \in \mathcal{A} \quad (7.24)$$

$$y^T_{v\hat{t}} \in \{0,1\}, \qquad v \in \mathcal{V}^{VO}, \hat{t} \in \mathcal{T}^{TP} \quad (7.25)$$

$$e^B_{\hat{v}jp} \in \mathbb{R}^+, \qquad v \in \mathcal{V}^{VO}, j \in \mathcal{J}, p \in \mathcal{P}^B \quad (7.26)$$

$$e^{\underline{B}}_{\hat{v}jp} \in \mathbb{R}^+, \qquad v \in \mathcal{V}^{VO}, j \in \mathcal{J}, p \in \mathcal{P}^B \quad (7.27)$$

$$e^{\overline{B}}_{\hat{v}jp} \in \mathbb{R}^+, \qquad v \in \mathcal{V}^{VO}, j \in \mathcal{J}, p \in \mathcal{P}^B \quad (7.28)$$

$$e^{\underline{B}C}_{\hat{v}jp} \in \mathbb{R}^+, \qquad v \in \mathcal{V}^{VO}, j \in \mathcal{J}, p \in \mathcal{P}^B \quad (7.29)$$

$$e^{\overline{B}C}_{\hat{v}jp} \in \mathbb{R}^+, \qquad v \in \mathcal{V}^{VO}, j \in \mathcal{J}, p \in \mathcal{P}^B \quad (7.30)$$

$$e^S_{\hat{v}j} \in \mathbb{R}^+, \qquad v \in \mathcal{V}^{VO}, j \in \mathcal{J} \quad (7.31)$$

$$h_{\hat{v}j} \in \mathbb{R}^+, \qquad v \in \mathcal{V}^{VO}, j \in \mathcal{J} \quad (7.32)$$

Chapter 8

Input Data and Test Instances

This chapter provides a thorough description of the input parameters and test instances used in later analyses. First, Section 8.1 elaborates on how the input data was obtained. The parameters are grouped by category and whether it is input to the Master Problem or Sub-Problem. Next, Section 8.2 describes the test instances used to obtain insights into the costs and strategy of transitioning to ZE High-Speed Passenger Vessels (HSVs). This chapter is an extension of Berg et al. (2022) since most of the data input is similar, and the test instances are based on the current HSV routes in Nordland County in Norway.

8.1 Input Data

This section elaborates on the input data required by the model and how the data were acquired. This is summarized by Table 8.1 which lists the data used in the Master Problem and Sub-Problem. The relevant parameters are separated into the categories *scenarios and time steps, routes, ports, infrastructures, vessels, other constraints*, and *Sub-Problem solutions*, denoted with their respective sources. Further, the relevant parameters of each category are listed in their associated problem. Next, in the following sub-sections, each parameter is described in detail.

The main sources for input data are *Nordland County*, the *Norwegian Coastal Administration* (NCA), the *Institute for Energy Technology* (IFE), the *Norwegian Water Resources and Energy Directorate* (NVE), *Paradis Nautica*, and *SEAM* most of which are partners of the (Enabling) Zero Emission (Passenger) Vessel Services (ZEVS) project described in Section 2.2. In addition, some manual data gathering has been required to find missing data.

NCA, a transport agency under the Norwegian Ministry of Trade, Industry, and Fisheries has provided AIS data that has been used to find the shortest sailing distances between ports. The data is also compatible with visualization tools such as *Geopandas*, making displaying the sailing legs on a map easy.

Nordland County, introduced in Chapter 1, provided passenger demands and distances of most legs sailed during the routes.

IFE, a front-runner in international energy research, has provided insights into how the various infrastructures work, and the costs of the components. They are up to date on most of the contemporary research within the field of hydrogen production. Thus, IFE has been an essential partner in obtaining data on infrastructures and finding relevant papers on the topic.

NVE, a directorate under the Norwegian Ministry of Petroleum and Energy, has performed an analysis regarding the current status of grid availability and grid expansion potential at different locations. This data has been used to determine which ports are feasible for installing grid-consuming infrastructures.

Paradis Nautica, a Norwegian shipyard, has provided estimated data on both battery-electric and hydrogen-fueled vessel types.

SEAM, a leading supplier of ZE solutions to the maritime industry, has provided data for the battery-swapping infrastructures and vessel types.

Parameter Type (Data Source)	**Master Problem**		**Sub-Problem**	
Scenarios and time steps	Conventional energy budget	$\overline{E}_t^C$	MGO-price	
	Probability of scenario	P^s	Electricity price	
Routes (Nordland County and Kystverket)	Bunkering alternatives	$\mathcal{B}_r$	Bunkering alternative	
	Initial infrastructures	Y_{pi}^I	Sub-routes	
	Initial fleet of vessels	X_v	Frequency of sub-route	$F_{\hat{t}\hat{r}}$
			Resting ports	
			Main port	
			Distances between ports	
			Passenger demand	D^P
Ports (NVE)	Compatible infrastructures	$\mathcal{I}_p$		
	Available grid capacity	Q_p^{GA}		
	Maximum grid expansion	$\overline{Q}_p^G$		
	Grid expansion costs	C_p^{IG}		
	Investment latency	L_p^G		
	Cost of hydrogen transport	C^{HT}	Cost of hydrogen transport	C^{HT}
	Delta distance to hub	$\Delta D_{p\hat{p}}^{F2H}$	Distance to closest hub	$D_{p\hat{p}}^{F2H}$
Infrastructures (IFE, SEAM)	Archetype		Infrastructure	i
	Max energy production rate	R_i^P	Max energy production rate	R_p^P
	Energy conversion efficiency	E_i^{CE}	Energy conversion efficiency	E_p^{CE}
	Bunkering rate	R_i^B	Bunkering rate	R_p^B
	Energy storage capacity	Q_i^S	Energy storage capacity	Q_p^S
	Investment costs	C_i^{II}	Energy costs at port	C_p^E
	Investment latency	L_i^I		
Vessels (Paradis Nautica, SEAM)	Investment costs	C_v^{VI}	Bunkering overhead time	V^{BT}
	Investment latency	L_v^V	Passenger capacity	Q^P
			Lower energy bound	V^{EL}
			Upper energy bound	V^{EU}
			Crew shift costs	C^C
			Energy consumption	
Other Constants	Number of hours in STPP	N^H	Number of hours in STPP	N^H
	Number of days in LTPH	N^D	Passenger alternative costs	C^A
	Energy consumption		Passenger time costs	C^{PT}
	rate on the busiest day	R^E	Sailing velocity	
	Utilization at infrastructures	U^F		
Sub-Problem solutions	Operating costs	C_{rbvt}^{Os}		
	Energy usage	E_{rbvt}^{Us}		
	Time usage	T_{rbvt}^{Us}		
	Number of vessels used	N_{rbvt}^{Vs}		

Table 8.1: This table is an overview the input given to the Master Problem and the Sub-Problem.
STPP - Short-Term Planning Period
LTPH - Long Term Planning Horizon

8.1.1 Scenarios and Time Steps

The model is solved for a long-term planning horizon of 15 years, ending in 2038. The length between time steps is set to three years, which is suitable considering the investment lead times described in the later sub-sections. The *conventional energy budget* $\overline{E}_t^C$ is 50% in 2030 and 0% in 2050 of the conventional CO_2 emitting energy used in 2005 (Regjeringen, 2023). The amount of energy used in 2005 is not readily available, and thus, the basis used in this thesis is the total energy used by the considered routes in 2023, 173 MW. Further on, due to the ambitious plans of decarbonizing the HSV-industry in Norway, it is assumed that the carbon budget for the final time step in 2038 is zero.

Recall from Section 6.1.2 that the price of MGO and electricity are the uncertain variables that together make up the scenarios. Until 2030, the price of MGO is assumed to be constant at 9.4 NOK/liter until 2030 (Jafarzadeh et al., 2021). Each of these three outcomes is assigned a probability of $\frac{1}{3}$. Further on, the value-added tax of 25% and the CO_2 tax is added to the MGO price. The CO_2 tax may also vary in the future, but these are assumed to be deterministic in accordance with the prices given by Regjeringen (2022). The uncertainty of the CO_2 tax is assumed to be captured by the uncertainty of the MGO price. The prices of MGO are displayed in Figure 8.1. Note that they are in kWh, but they can be converted to NOK/liter by multiplying with 10.08 $\frac{NOK\ kWh}{liter}$ which is the factor for conversion used by Miljødirektoratet (2020).

The future prices of electricity are given by a report from Statnett (2023) which has mapped out three scenarios for the development in prices in all of Europe, including the electricity price area named *NO4* which contains Nordland County. These prices are also displayed in Figure 8.1. Note that before 2030, Statnett assumes the electricity prices decrease linearly from today's high energy price levels towards the initial base price in 2030. The scenarios used in the report are dependent on various factors such as technology development and investment, where the main prediction is their most confident prediction. Hence, the probabilities used for the electricity prices are 25%, 50%, and 25 % for the low prices, expected prices, and high prices, respectively. There is also some positive correlation between the two variables (Statnett, 2023). Accounting for this gives an approximate *probability* P^s of each scenario as shown in Table 8.2.

MGO	Low			Base			High		
Electricity	Low	Base	High	Low	Base	High	Low	Base	High
P^s (%)	11.11	16.67	5.56	8.33	16.67	8.33	5.56	16.67	11.11

Table 8.2: The probabilities of each scenario. Given a scenario, the development of the electricity prices and prices of MGO is predetermined.

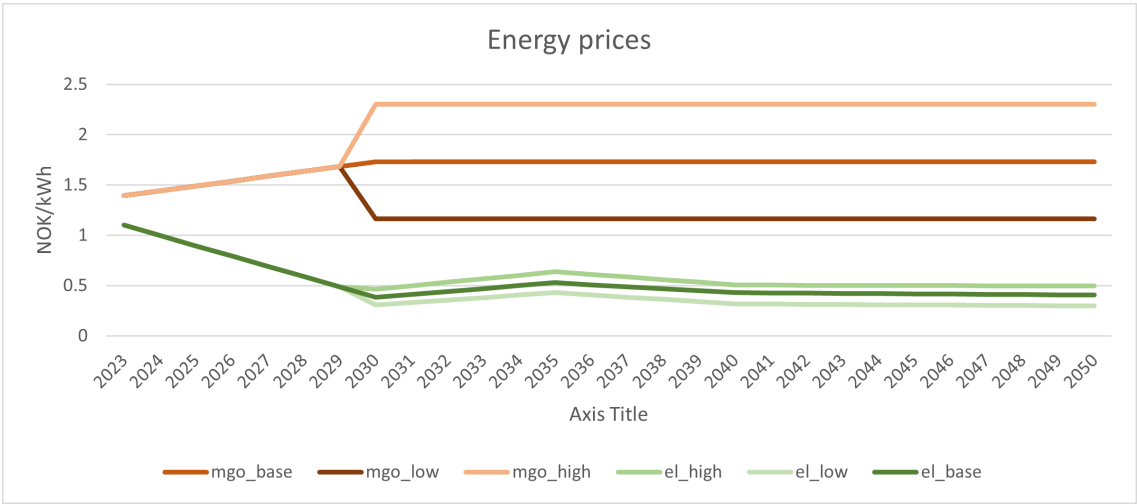

Figure 8.1: The plot of energy prices per kWh

8.1.2 Route Data

The route data was primarily obtained through time schedules from the website of Reis Nordland (2022). The schedule for the busiest weekday (Fridays) in the summer is used since this is when the routes have the tightest schedules, and solving the model for the peak load ensures that a solution will be feasible for the set of routes throughout the whole year. Other supplementary data was provided by Nordland County.

All routes in Nordland County are used as input to the model. They are further detailed in Table 8.1 and Figure 8.2. Table 8.3 provides a summary of all routes, where the first column contains a route number and cell color, indicating the route number and the respective cell colors in Figure 8.2. Note that the first eighteen routes, 111 to 866, are sorted numerically and geographically from south to north. The two final routes 731 and 755, are express routes travelling along the coast in Nordland. Further on, Figure 8.2a shows the routes with distinguishable colors and associated route numbers. The labels for the route numbers are located at the routes' respective main port. Figure 8.2b is supplementary to Figure 8.2a and shows the name of each of the main ports.

Master Problem

For each route, the Master Problem requires the candidate bunkering alternatives $\mathcal{B}_r$ as input since the operating details are abstracted. Recall from Section 5.2 and Figure C.1 that a bunkering alternative denotes a predefined set of bunkering ports with specific infrastructures used to serve the route. If a port should be included in $\mathcal{B}_r$ is decided based on three criteria. First, the port needs to be close to the route. This is determined by the shortest distance between the port and any port visited by the route. If the distance is less than the predetermined threshold of 40 km, the port is considered to be included in $\mathcal{B}_r$. This threshold is assumed based on the longest range of the vessels, 180 km for *H-50*, where spending more than 80km each bunkering is not considered eligible for any vessel type. Second, it must exists a bunkering infrastructure feasible to install at the port. Third, at least one of the Sub-Problems needs to be feasible for a route serving permutation where the port is included.

By this day in 2023, there are no Zero-Emission (ZE) infrastructures installed in Nordland County. Therefore, the parameters for initially available ZE infrastructures Y^I_{pi} and vessels X_v are all set to zero.

Sub-Problem

By web scraping the time schedules from Nordland County's website, each route's *sub-routes, sub-route frequencies, resting ports* and *main port* were obtained. Each sub-route is determined by a unique sequence of visited ports. The frequencies determine how many times each sub-route is served each day. The set of starting and ending ports of the sub-routes comprise the resting ports. Lastly, the main port is the port where the first sub-route starts, that is, where the vessels rest during the night.

The *distances between ports* is necessary to determine the time spent and energy consumption. Data on the sailing legs included in the routes were provided by Nordland County. However, data regarding legs outside of the scheduled routes needed to determine the effect of detouring were mainly unavailable. To decide these distances, geospatial locations of all ports from Google Maps were used. Euclidean distances between ports were used to calculate distances for the legs absent from the data provided by NCA and Nordland County. This is a rather good approximation in most cases, and should not affect the strategic decisions to a high degree.

Passenger demand data, D^P, was provided by Nordland County. The data contained statistics on the total number of passengers served by each route throughout a year. To compensate for potential varying demand among sub-routes, the demand is doubled. Also, the demand is further scaled with the constant for the energy consumption rate on the busiest weekday R^E to account for higher demand on Fridays. This was further processed into passengers served at each frequency

Route	Main Port	Daily Distance km	Freq. All Sub-routes	Number of Sub-routes #	Yearly Pass. $\frac{Pass.}{year}$	Pass. per Serving $\frac{Pass.}{serving}$
111	Bindalseidet	310	[4, 3, 2, 0]	5	6 090	2
151	Rørøy	334	[6, 3, 2, 1]	2	22 962	5
159	Brønnøysund	151	[1, 1, 0, 0]	2	9 213	13
167	Bønå	303	[1, 2, 1, 0]	4	6 643	5
172	Kirkøy	253	[1, 1, 1, 0]	3	14 391	13
182	Sandnessjøen	92	[3, 0, 0, 0]	1	8 282	8
191	Træna	570	[1, 2, 2, 0]	3	53 426	29
193	Sandnessjøen	348	[3, 1, 3, 0]	6	8 639	3
195	Selvær	239	[3, 5, 4, 0]	3	6 263	1
411	Myken	298	[2, 1, 1, 0]	4	15 159	10
413	Storselsøy	144	[2, 1, 0, 0]	3	1 263	1
433	Ørnes	319	[2, 4, 1, 1]	8	7 115	2
445	Bodø	519	[3, 1, 1, 1]	6	18 962	9
539	Helligvær	343	[2, 2, 1, 0]	3	28 289	16
585	Kjøpsvik	216	[3, 1, 2, 0]	5	6 326	3
773	Reine	111	[1, 1, 2, 0]	1	16 768	11
837	Stokmarknes	218	[2, 2, 2, 0]	2	7 702	4
866	Myre	253	[4, 3, 1, 0]	4	15 115	5
731	Sandnessjøen	1 052	[4, 2, 2, 0]	8	82 104	28
755	Svolvær	538	[1, 2, 1, 0]	4	66 644	46

Table 8.3: Summary of the route data. They include all 20 routes in Nordland County.

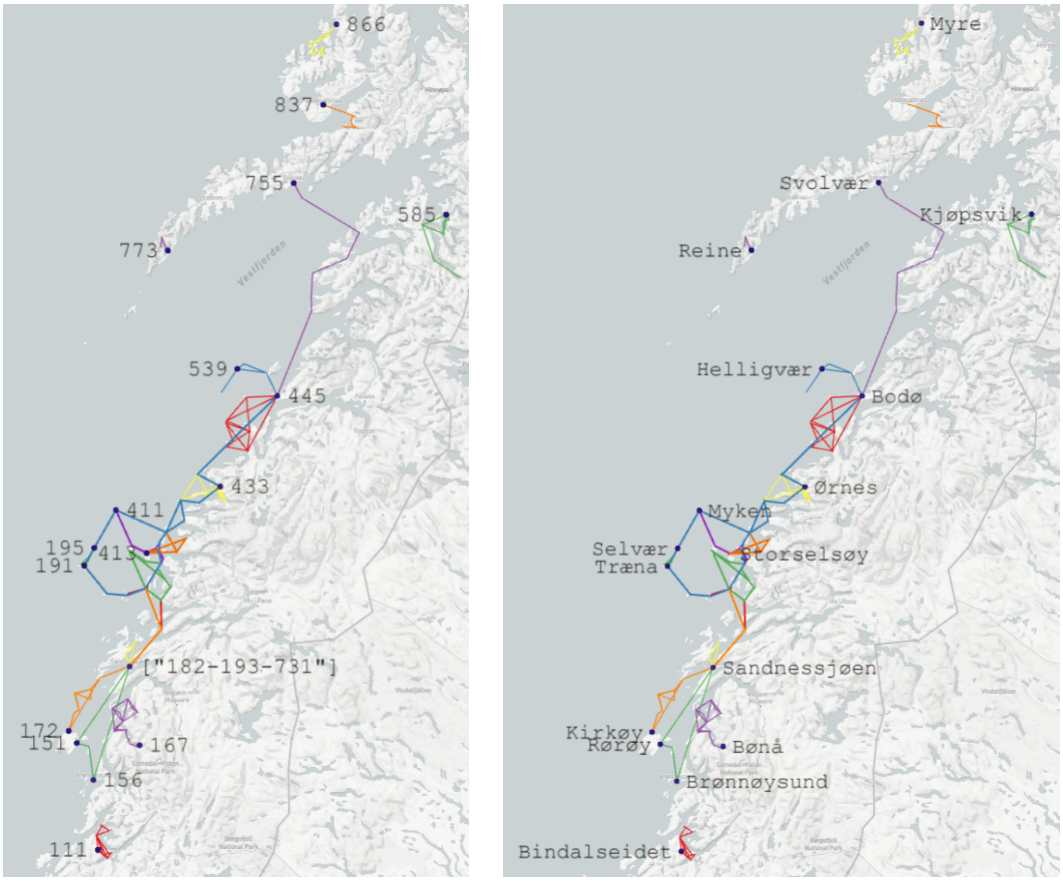

(a) Route numbers

(b) Main ports of each route

Figure 8.2: The main ports and the route numbers

for each sub-route by assuming equal demand each day on each serving.

8.1.3 Port Data

The problem takes the sets *compatible infrastructures* $\mathcal{I}_p$ as input. Recall from Table 6.1 that the infrastructure archetypes include large-scale hydrogen production hubs (HUB), hydrogen filling stations (F), local hydrogen production facilities (LP), electric charging infrastructures (E), battery-swapping infrastructures (S), and MGO filling stations (C). The sets $\mathcal{I}_p$ are generated based on the feasible infrastructures at each port, and each infrastructure has different criteria to be feasible at a port. What these criteria are is defined based on the infrastructure's archetype. If none of these criteria are met for any infrastructures at a port, the port is not a candidate bunkering port.

First of all, there are several candidate hub locations in Nordland County that may be used to install large-scale hydrogen production hubs (HUB). Based on data from Statkraft, these locations include *Bodø, Mo i Rana, Ørnes, Rørvik* and *Narvik*. They are selected since there are ongoing projects for hydrogen production, and there is potential for sufficient grid capacities.

Secondly, all energy-producing infrastructures (HUB, LP, E, S) require a grid connection to be included $\mathcal{I}_p$. This was decided based on a data set on grid potentials provided by NVE, which included 17 different ports in Nordland County. For each port, the data consists of the current *available grid capacity* Q_p^{GA} and different grid-expanding alternatives. Each grid-expanding alternative includes the size of the grid expansion in MW and the total costs of the expansion. Through conversations with NVE, selecting the largest grid-expanding alternative for each bunkering port as the *maximum grid expansion* $\overline{Q}_p^G$ and assuming a fixed *grid expansion costs* C_p^{IG} per MW at each port was considered a viable solution. Furthermore, the *investment latency* C_p^{IG} of grid capacity is assumed to be three years based on data from NVE.

Third, as described in Section 2.4, hydrogen filling stations (F) must be supplied with hydrogen by tube trailers from a large scale hydrogen production hub. Therefore all filling stations need to have a road connection to be included in $\mathcal{I}_p$. The *distance to hub* $D_{p\hat{p}}^{F2H}$ is calculated as the road distance between port p and $\hat{p}$. These road distances have been obtained through Google Maps' API service; returning a distance matrix between each potential hub and each candidate filling station. To obtain the transportation costs in $\frac{NOK}{MWh}$ for hydrogen, these distances are multiplied with the *cost of hydrogen transport* C^{HT}. This unit cost is set to be 1.423 $\frac{NOK}{MWh\ km}$ based on numbers in Danebergs et al. (2021). In the Sub-Problems, the closest hub is assumed to supply a filling station, while the Master Problem corrects the energy costs of a filling station being facilitated by a distant hub using the difference in distance to the closest hub, $\Delta D_{p\hat{p}}^{F2H}$.

Finally, since conventional fuel is assumed to be easily accessible, all main ports have MGO refueling stations (C) as included in $\mathcal{I}_p$.

8.1.4 Infrastructure Data

The infrastructure data are obtained through dialogue with IFE and reviewing relevant literature. Based on the data, a varied selection of infrastructures is given as input to the model. This subsection starts by presenting the instances included in the set of candidate infrastructures and their associated attributes, before the calculation of the costs of the instances are described in Table 8.5.

The Infrastructures

An infrastructure belongs to one of the distinct archetypes, which has implications on its operational attributes. This is highlighted in Table 3.1. All instances are summarized in Table 8.4, where the name is comprised of the archetype and an index for differentiating instances of the same archetype.

Name	Maximum Production Rate	Energy Conversion Efficiency	Bunkering Rate	Storage Capacity	Yearly Investment Costs
	MW	%	MW	MWh	$\frac{MNOK}{year}$
Hub	20.0	75%		100	10.137
LP-1	3.0	68%	8.58	12	3.765
F-1			8.58	6	0.155
F-2			8.58	12	0.193
F-3			8.58	24	0.270
F-4			8.58	48	0.421
E-1	1.0	81%	4.00	1	1.655
E-2	1.0	81%	4.00	2	2.055
E-3	2.0	81%	4.00	1	1.830
E-4	2.0	81%	4.00	2	2.230
S-1	0.5	90%	28.00	2	2.138
S-2	0.5	90%	28.00	4	2.938
S-3	1.0	90%	28.00	8	4.625
C-1			10000.00	100.00	0.000

Table 8.4: The set of candidate infrastructures.

The *max energy production rate*, R_i^B, denotes the maximum MW of input to the infrastructure from the grid. The input energy to the infrastructure is scaled by the *energy conversion efficiency*, E_i^{CE}, to account for the loss during production. Thus, the effective energy production rate is always less than the maximum production rate. For hydrogen infrastructures, the max energy production rate is given by the installed electrolysis tube. The energy conversion efficiency is 68% for a general hydrogen production facility (Danebergs et al., 2021). However, for the hub, the energy conversion efficiency is set to 75% to account for the economies of scale at a HUB.

Recharging the onshore battery pack at electric charging infrastructures and battery-swapping infrastructures is assumed to behave similarly to producing and storing hydrogen with respect to production rate and energy conversion efficiency. The production rate at these infrastructures is synonymous with the charging power of the onshore battery pack. The charging powers used in the thesis are based on Karimi et al. (2020), which present battery charging powers in the range between 0.5 and 5.0 MW. The costs of charging power are high and are assumed to increase linearly with MW installed. Furthermore, the onshore battery packs for both electric charging infrastructures and battery-swapping infrastructures are intended to reduce the load on the local grid. Conservative charging powers of onshore batteries, or maximum production rates, are therefore used as input to the problem. Thus, electric charging infrastructures are assumed to have 1.0 or 2.0 MW, and battery-swapping infrastructures are assumed to have 0.5 and 1 MW. The energy conversion efficiency when charging batteries is 90% (Zhang et al., 2021), which applies to both electric charging infrastructures and battery-swapping infrastructures. However, since batteries are charged in two rounds for the electric charging infrastructure (which has onshore and onboard batteries), the energy conversion efficiency is set to 0.81%.

Data provided by IFE describes a filling concept where 65 kg is filled into a tank with a capacity of 80 kg within a time period of 10 *minutes*. Four of these procedures can be performed in one *hour*, giving a *bunkering rate* R_i^B of 8.58 MW. For electric charging infrastructures, this thesis assumes a bunkering rate of 4 MW which is at the high end of the aforementioned charging powers from Karimi et al. (2020). Further on, the battery-swapping infrastructures systems always swap two entire batteries of 1 MWh in 3 *minutes*, which is equivalent to a bunkering rate of 40 MW.

At hydrogen-producing infrastructures, the *storage capacity* Q_i^S limits the amount of hydrogen that can be bunkered at the given bunkering rate. Therefore, they are given enough storage capacity to not limit the bunkering of vessels. Hydrogen filling stations are assumed to be supplied daily as mentioned in Section 6.1.1, and therefore, they need sufficient amounts of energy to serve the routes during an operating day. Consequently, filling stations are generated with a range of storage capacities, having 48 MWh as the maximum. The model is also provided with electric charging infrastructures with battery-electric storing capacities of one and two MWh. The battery-swapping

infrastructures may either have two, four, or eight MW of onshore battery capacity. MGO fueling stations are assumed to have an unlimited supply.

Infrastructure Costs

To obtain the *daily investment costs* C_i^{II}, the investment costs are depreciated linearly based on the lifetime of each cost group. Daily investment costs are used in order to compare the investment costs with operational and passenger costs. However, the yearly costs are displayed in Table 8.4 and Table 8.5 for readability purposes.

The parameters of the HUB and the LP are defined based on Danebergs et al. (2021) who present two hydrogen-producing alternatives. Each alternative has costs of electrolysis tubes and associated control systems. The electrolysis tubes have a maximum production rate of 20 MW and 3 MW, respectively, and the corresponding costs per MW production capacity electrolysis tubes are 7.5 $\frac{MNOK}{MW}$ and 18.8 $\frac{MNOK}{MW}$. The lifetime of hydrogen electrolysis tubes is estimated to be 30 $years$. This estimation is motivated by IFE, as the expected lifetime is about 100 000 $hours$, which covers at least eight hours of production every day for the next 30 $years$. In addition, there follow yearly operational costs at 3% of the original capital expenditure (Danebergs et al., 2021). The onshore battery bank at the electric charging infrastructures and battery-swapping infrastructures needs recharging, which comes at a cost of 3.5 $MNOK$ per MW of charging power.

The costs of installing hydrogen storage capacity are 6.3 $\frac{MNOK}{tonne}$, which is further converted to 0.191 $\frac{MNOK}{MWh}$ (Danebergs et al., 2021). Battery-electric storage capacity cost is 4.0 $\frac{MNOK}{MWh}$, and has an expected lifetime of 10 $years$ (Cole et al., 2021).

Every bunkering infrastructures need to install a hydrogen dispensing system, electric charging power or a robotic arm to swap the batteries. The cost of the dispensing system of a hydrogen bunkering infrastructure is 1.17 $MNOK$, and the lifetime is estimated to be 10 $years$ (Ulleberg & Hancke, 2020). Data from IFE states that installing charging power at an electric charging infrastructure comes at a cost of 5.4 $\frac{MNOK}{MW}$, i.e., the costs depend on the installed charging power. SEAM, the developer of the battery swap system, could not reveal the exact costs of the battery-swapping infrastructures due to confidentiality, but 25 $MNOK$ with a lifetime of 20 $years$ is assumed to be a reasonable estimate.

Cost Group	**Unit**	**Hub**	**LP**	**F**	**E**	**S**	**C**
Maximal production rate	$(\frac{MNOK}{MW})$	7.5	18.8		3.5	3.5	
Lifetime	$(years)$	30	30		20	20	
Yearly operational costs	$(\frac{MNOK}{MW})$	0.23	0.56				
Lifetime	$(years)$	1	1				
Storage	$(\frac{MNOK}{MWh})$	0.19	0.19	0.19	4.0	4.0	
Lifetime	$(years)$	30	30	30	10	10	
Dispensing system	$(MNOK)$		1.2	1.2			
Lifetime	$(years)$		10	10			
Charging power	$(\frac{MNOK}{MW})$				5.4		
Lifetime	$(years)$				20		
Robotic arm ++	$(MNOK)$					25.0	
Lifetime	$(years)$					20	

Table 8.5: Unit costs for attributes of the infrastructure archetypes.

Energy Costs at the Infrastructures

Recall that the installed infrastructure at a port is predetermined in each Sub-Problem. Therefore, the *energy costs at port* C_p^E is dependent on the installed infrastructure and the global energy prices described in Section 8.1.1. In the case of conventional refueling infrastructures, the energy price is solely determined by the global MGO price and its fees. For hydrogen bunkering infrastructures, there are additional costs of 5.6 $\frac{NOK}{kg}$ for compressing hydrogen after production and a dispensing

cost of 2.8 $\frac{NOK}{kg}$, giving a total of 8.4 $\frac{NOK}{kg}$ (Danebergs & Aarskog, 2020). However, due to a great increase in electricity prices since 2020, the additional costs for bunkering hydrogen are assumed to be 13 $\frac{NOK}{kg}$. Otherwise, the energy price depends on the electricity price, energy conversion efficiency at the infrastructure, and also, the transportation costs of the hydrogen in the case of a hydrogen filling station.

8.1.5 Vessel Data

The input data on vessel types are based on a data set provided by Paradis Nautica, who roughly estimated these parameters based on typical models for conventional vessel types. A summary of the data is presented in Table 8.6. The first column contains the name of each vessel type with first a letter for the energy carrier type, a number for the number of passengers, and for some vessel types, a letter indicating if the vessels of each type have a hull length of 40 *meters* which is denoted by an "L". The most common length is 30 *meters*, but a 40-*meter* hull allows for a larger energy storage capacity on board.

The data set contains a variety of parameters, where the relevant input data are displayed in Table 8.6. The Master Problem only considers the *investment costs* C_v^{VI} which are assumed to have a lifetime of 20 *years* and *investment latency* L_v^V. The investment latency is assumed to be 3 *years* which is equivalent to the length of a time step. The reason for the long delivery time is that the new vessels are based on new technologies.

The remaining parameters in Table 8.6 are input to the Sub-Problem. The *passenger capacity* Q^P and *energy consumption* did not need any preprocessing as they were provided in the data set. Further on, the *lower energy bounds* V^{EL} and *upper energy bounds* V^{EU} were calculated based on the *storage capacity* and the feasible percentage interval for energy storage. For hydrogen vessels, the interval is from 40% to 100%. IFE states that high pre-cooling costs are incurred when filling hydrogen on tanks with low pressure, meaning that it is costly to fill a fuel cell with a low energy level. For battery-electric and battery-swapping vessels, the energy window is in the interval from 20% to 90% of total storage capacity to prevent degradation of the battery (Zhang et al., 2021). The same goes for battery-swapping vessels, but conventional vessels do not have these limits since it is assumed that fuel is not a limiting factor.

Further, the Sub-Problems also need to calculate the total time spent bunkering. Consequently, they require both the bunkering rate and the *bunkering overhead time* V^{BT}. Recall that the bunkering rate is determined by the infrastructure as described in the previous section. Bunkering overhead time is the time spent initializing and terminating the bunkering procedure. For hydrogen vessels, the bunkering overhead time is assumed to be 30 *minutes* since the passengers disembark due to safety regulations. The bunkering overhead time of battery-electric vessels is assumed to be six *minutes*, while battery-swapping vessels and conventional vessels are assumed to have zero bunkering overhead time. The reasoning behind this is that the bunkering rate incorporates the overhead time of swap vessels, and the conventional vessels can bunker without affecting the serving of the route.

Crew shift costs C^C is calculated based on an hourly rate for crew costs from Tveter et al. (2020) which are multiplied by six since a shift is assumed to be six *hours*. The hourly rate is set to 341 $\frac{NOK}{h}$ for each junior crew member and 512 $\frac{NOK}{h}$ for each senior crew member. From the same report, the number of crew members needed for each vessel type is listed for each current vessel in the Norwegian HSV fleet. This indicates that the number of crew members is given by the passenger capacity, and motivates the crew setups listed in Table 8.7, which entails the hourly crew time costs for each vessel type listed in Table 8.6. Also, hydrogen vessels are assumed to require three or four safety staff depending on the boat size, increasing the overall crew shift costs for this carrier type.

Vessel Type	Pass. Cap.	Storage Capacity	Energy Consumption at 20, 25, and 30 *knots*			Invest. Costs	Bunkering Overhead Time	Crew Shift Costs
	#	MWh		$\frac{MWh}{km}$		$MNOK$	$hours$	$\frac{NOK}{shift}$
H- 50	50	9.16	0.018	0.028	0.041	132.7	0.5	14334
H-100	100	9.16	0.019	0.030	0.043	133.7	0.5	16380
H-150	150	9.16	0.021	0.031	0.045	135.8	0.5	18426
E- 50	50	1.50	0.016	0.024	0.036	96.4	0.1	5118
E-100	100	1.50	0.018	0.026	0.040	97.4	0.1	7164
E-150	150	1.50	0.021	0.029	0.044	98.4	0.1	9210
E- 50-L	50	3.00	0.018	0.026	0.040	106.7	0.1	5118
E-100-L	100	3.00	0.020	0.029	0.043	107.7	0.1	7164
E-150-L	150	3.00	0.023	0.032	0.047	108.7	0.1	9210
S- 50	50	2.00	0.018	0.027	0.040	99.8	0	5118
S-100	100	2.00	0.020	0.030	0.044	100.8	0	7164
S-150	150	2.00	0.023	0.033	0.048	101.8	0	9210
S- 50-L	50	4.00	0.024	0.036	0.056	131.6	0	5118
S-100-L	100	4.00	0.026	0.038	0.059	132.6	0	7164
S-150-L	150	4.00	0.028	0.041	0.062	133.6	0	9210
C- 50	50	15.00	0.018	0.027	0.040	99.8	0	5118
C-100	100	15.00	0.020	0.030	0.044	100.8	0	7164
C-150	150	15.00	0.023	0.033	0.048	101.8	0	9210

Table 8.6: The different vessel types. Type names consist of two parts. First, a letter defining energy carrier, *H - hydrogen, E - electric batteries, S - electric swappable batteries, C - conventional.* Second, the passenger capacity.

	Passenger Cap.		
	50	**100**	**150**
Junior Members	1	2	3
Senior Members	1	1	1
Senior safety staff for Hydrogen Vessels	3	3	3

Table 8.7: Number of crew members needed given the passenger capacity of the vessel type

8.1.6 Other Constants

The *number of hours in the short-term planning period* N^H is set to 24 hours, starting from the time of the first route serving at 06:00. This ensures that the operational plan is repeatable and thus feasible for consecutive days. The *number of days in the long-term planning horizon* N^D is set to three years as this provides a solution that is granular enough for the analyses presented in Chapter 9.

To facilitate operational feasibility in each short-term planning period, the *utilization at infrastructures* U^F restricts the total bunkering time for each infrastructure at each port. This parameter is assumed to be 80% which should provide some slack in a time schedule where multiple vessels use the same bunkering infrastructure at a port. The *peak energy consumption ratio* R^E is roughly $19\% \cdot 7 = 1.33$, which is how much more energy is consumed by high-speed vessels during the busiest day of the week (Friday) compared to the average (Sundvor et al., 2021). Further, the *passenger time costs* C^{PT} is estimated at 112 $\frac{NOK}{h}$, as stated in (Flügel et al., 2020). Sailing velocity is homogeneously set at 25 *knots*, or 46.3 $\frac{km}{h}$, in accordance with the AIS data in Aarskog et al. (2020).

8.1.7 Sub-Problem Solutions

Finally, the Master Problem takes solutions from each Sub-Problem as input. Each Sub-Problem is solved to optimality based on a fixed route r, bunkering alternative b, and vessel type v in each time step t and scenario s. From each solution there follows an *operating costs* C^{Os}_{rbvt}, *energy usage* E^{Us}_{rbvpt}, *time usage* T^{Us}_{rbvpt}, and the *number of vessels* used N^{Vs}_{rbvt}.

8.2 Test Instances

This section describes the instances used to test the model and gain valuable insights into the strategic decisions of the Zero-Emission (Passenger) Vessel & Infrastructure Planning Problem (ZEVIPP). The model is solved for two sizes; small and large, which indicate the number of routes included in the respective instances. The main outlines of the test instances are presented in Section 8.2.1 and Section 8.2.2, respectively.

8.2.1 Small Sized Instance

The small test instance includes five routes listed in Table 8.8, which is a subset of the routes in Table 8.3. Figure 8.3a displays the routes and the associated candidate bunkering ports. Every route is visualized with a unique color as a set of straight lines representing the route legs that comprise the route. Note that actual sailing distances are used even though the legs are visualized as straight lines. The candidate bunkering ports are represented by green and blue points. A large green point indicates that it is possible to install a grid capacity, and thus feasible to install grid-consuming infrastructure (HUB, LP, E, S). The small blue dots indicate that the port has a road connection and consequently is a candidate location to install a hydrogen filling station (F). The candidate HUB locations, represented by the purple dots, that are relevant for this instance are Mo i Rana, Ørnes, and Bodø. Conventional infrastructures are available without incurring any costs at the main ports of each route, displayed in Table 8.8.

The small test case is intended to give a comprehensive solution that can provide a better understanding of the elements in a solution of the model. Additionally, some insights can be drawn from comparing how the small instance is solved compared to the solution of the same routes in the large-sized instance. If the solutions are similar, it could imply that a locally optimal solution may also be globally optimal. Lastly, for practical reasons, the small instance is useful for testing the model and comparing the running time for instances of increasing size.

8.2.2 Large Sized Instance

The large test instance contains all 20 routes in Nordland, listed in Table 8.3. As observed in Figure 8.3b, they are spread along the whole coast of Nordland with around 400 km in Euclidean distance between the southernmost and northernmost route. Hence, in contrast to the small instance, the large instance defines several groups of route systems that might be subject to co-utilize infrastructures, including the group of routes in the small test instance. All candidate hub locations are relevant in this instance and are highlighted by the purple circles in the figure.

Route	Main Port	Daily Distance *km*	Freq. All Sub-routes	Number of Sub-routes #	Yearly Pass. #	Pass. per Serving #
191	Træna	570	[1, 2, 2, 0]	3	53 426	29
193	Sandnessjøen	348	[3, 1, 3, 0]	6	8 639	3
411	Myken	298	[2, 1, 1, 0]	4	15 159	10
413	Storselsøy	144	[2, 1, 0, 0]	3	1 263	1
731	Sandnessjøen	1 052	[4, 2, 2, 0]	8	82 104	28

Table 8.8: Summary of the routes included in the small test instance

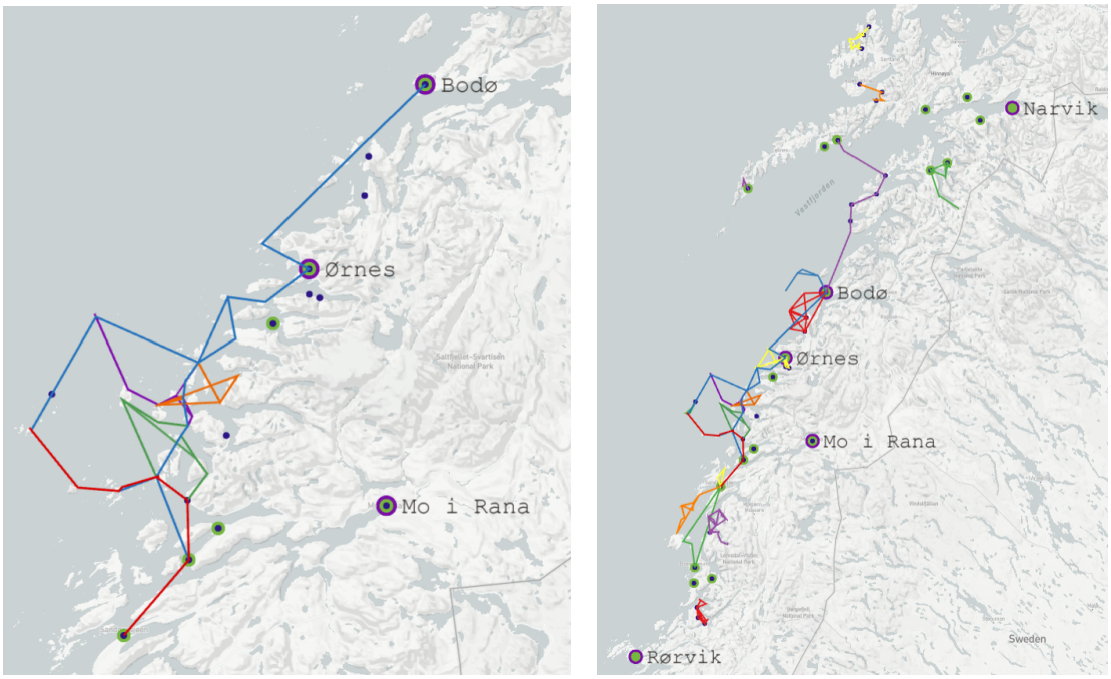

(a) The small test instance

(b) The large test instance

Figure 8.3: Routes and available infrastructures for both small and large test instances. The routes have colors that are mapped to Table 8.8 and Table 8.3, respectively. The points show the candidate bunkering ports, and the colors blue, green, and purple indicate that it is feasible to install hydrogen filling stations, grid-consuming infrastructures, and hubs, respectively.

Chapter 9

Computational Study

In this chapter, the proposed Mixed Integer Linear Programming (MILP) models from Chapter 6 and Chapter 7 are implemented in *Gurobi*, the commercial solver utilized in the study, to conduct analyses on and draw insights from the dataset instances detailed in Chapter 8. First, Section 9.1 discusses the complexities of the implemented models and their implication on running times and scalability. Next, Section 9.2 presents the strategic and tactical decisions made by solving the Zero-Emission (Passenger) Vessel & Infrastructure Planning Problem (ZEVIPP) for the large test instance, while using the small test instance solution as a reference. These decisions are then discussed in light of the cost decomposition and abatement cost of the solution. In particular, an analysis is conducted to find the respective abatement cost of each route. Ultimately, Section 9.3 presents additional analyses to further enhance the decision support. These analyses include optimizing the sailing speed for each route, forcing all new tenders to be ZE (based on the Norwegian government's proposal (Tveit et al., 2023)), and then evaluating the impact these configurations have on the strategic and tactical decisions.

The model executions were performed on local computers provided by the Department of Industrial Economics and Technology Management at Norwegian University of Science and Technology (NTNU). The model executions were conducted on identical computers with the same software and processing power. The applied software and hardware are described in further detail in Table 9.1.

Computer	Dell OprPlex 7780 AIO
Processor	Intel Core i7-10700 @ 2.90GHz
RAM	16 GB
Operating System	Windows 10 Education
Gurobi Licence Type	Academic
Gurobi Version	10.0.1
Python Version	3.8.8
Geopandas Version	0.12.1

Table 9.1: Hardware and software specifications

9.1 Solution Times

The computational study is initiated by analyzing the complexity of the Master Problem and the Sub-Problems in several configurations. Model complexity is mainly discussed in light of the running time and the size of the decision space. The Master Problem is analyzed for all configurations used throughout this chapter, while the Sub-Problems are analyzed with average solution times.

In Table 9.2, the running times and problem sizes are listed for all instances. Recall from Chapter 8 that the instances are named as follows. S and L determine if the instance is based on the small

or large data set, respectively. The suffix *VS* (varying speed) declares that a mixed set of speeds is used (20, 25, and 30 *knots*). The suffix *D* denotes that the instance is solved with a deterministic planning horizon, i.e., a single average scenario is considered. The suffix *wo/NA* means that the model is solved without the non-anticipativity constraints. Further, *#Bin Vars* states the number of binary variables used in each instance's Master Problem, while *#SP* states the number of Sub-Problems being solved for each instance. Finally, *MP Sol Time* and *SP Sol Time* present the respective solutions time for the Master Problem and the Sub-Problems in aggregate.

	ZE Solution			
Instance	**#Bin Vars**	**MP Sol Time**(sec)	**#SP**	**SP Sol Time**(sec)
S	16 092	10.2	1 204	361.5
S-VS	33 318	30.2	3 612	900.8
S-D	1 422	0.5	992	235.7
L	57 888	1 010.7	4 569	1 315.3
L-VS	121 338	381.9	13 707	4 141.1
L-D	5 490	1.9	3 488	841.7
L-wo/NA	57 888	57.3		

Table 9.2: Complexity and solution times for instances

9.1.1 Master Problem

In this sub-section, the ground for complexity in the Master Problem is discussed, particularly in relation to the running time and the number of binary variables present in the model. The termination criterion for Gurobi is set by default to an optimality gap of 0.01 %. This setting has been used for all instances.

A general finding is that a solution time correlates positively with the number of binary variables in the Master Problem. This is typically due to the size of the decision space increasing. However, *L-VS* and *L-wo/NA* deviate from this tendency. Thus, it does not suffice to solely consider the size of the decision space of the problem for understanding the running times. In this case, the running times are affected more by the complexity, rather than the decision space itself.

The first driver of complexity in this problem is making investment decisions in chronological order and finding an optimal investment plan. Further, the complexity can be an intrinsic attribute of the data set, e.g., big and dense route clusters can generate complexity, while dominant route assignments can remove complexity. L-VS having three times the number of binary variables, and still running three times faster than L suggests that some route assignments are dominant in optimum. Moreover, the decision space is increased when adding scenarios, but complexity is added first when the scenarios are solved as a system, bounded by the first-stage decisions. This distinction can be shown as L-wo/NA is solved for an identical data set as L, but ignoring the non-anticipativity constraints. When the binding between the scenarios is removed, the complexity is reduced as well, effectively reducing the running time 20 times. L-wo/NA solves each scenario deterministically, similar to L-D, but for nine scenarios in the same model. The number of binary variables is increased nine times, and the solution time increased 30 times. This illustrates how the solution time increases linearly with the number of binary variables if the complexity remains the same.

Instance L with 20 routes included is solved 100 times slower than S, which includes five of the routes. This suggests that the model does not apply to very large problems. In particular, this holds for very granular time steps and very large sets of routes. Having said that, the case studied in this thesis, Nordland County, is the county with the most High-Speed Passenger Vessel (HSV) connections in Norway (Statens Vegvesen, 2022), so one will rarely face a larger set of routes. Moreover, the planning problem is not time critical and has only been solved on a single computer in this study. Hence, it should be able to solve the problem for most practical purposes.

9.1.2 Sub-Problem

This sub-section completes the discussion regarding the solution times of the models used to solve the ZEVIPP. It starts by assessing the aggregated solution time for each instance. Finally, the average Sub-Problem solution times are assessed per route.

The aggregated solution time should increase roughly linearly with the number of Sub-Problems being solved for an instance since they are solved sequentially. This is also what the results show in Table 9.2. The average Sub-Problem solution time varies from 0.24 to 0.3 *seconds* across the instances. This suggests that the running time of the Sub-Problems should not be problematic as the number of routes increases for larger data sets. However, the number of Sub-Problems solved for each route still grows as a product of the number of bunkering alternatives, number of scenarios, and number of time steps, which could become very high if not considered when determining the scope of the data set.

Figure 9.1 depicts the average solution time for the Sub-Problems solved for each route. This shows that there are vast differences in the running time. This is presumably due to differences in demanded frequencies, the number of different sub-routes that are served in the given route, and the number of vessels that are needed to solve each Sub-Problem. In Berg et al. (2022) a solution method for the (more or less similar) Sub-Problem is presented as a Dynamic Programming (DP) algorithm, which reduces the problem to a Shortest Path Problem with Resource Constraints (SPPRC). The average running times of the DP algorithm are represented by the red bars, while the average running times of the MILP implementation presented in this thesis are represented by grey bars. For the more time-consuming Sub-Problems, it is evident that the MILP is the preferred option. When the MILP was designed and tested initially it was a better counterpart to the SPPRC, that is, when each route was only allowed bunkering at a single bunkering port. Then the model was twice as fast as the current implementation of the MILP, possibly due to the restrictions being tighter. Nevertheless, the difference would be even greater if the SPPRC was compared to its MILP counterpart.

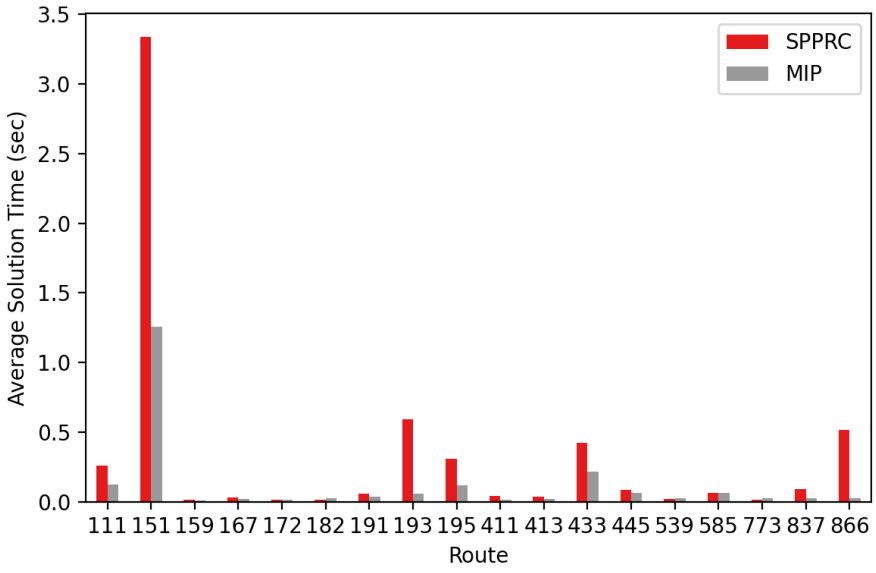

Figure 9.1: Average solution time of Sub-Problems for each route solved as both an SPPRC and a MILP. The red bars represent the solution times of the SPPRC, while the grey bars represent the solution times of the MILP

To further analyze the solution time of each Sub-Problem, the six figures in Figure 9.2 are presented where a larger dot means that the solution time takes a longer time. These scatter plots show the average running time of Sub-Problems for each combination of *#Sub-Routes* and *Total # Frequencies*. The assumption is that these factors are the main contributors to the complexity of

the Sub-Problem. The main insight to draw from these plots is that, in general, the solution time increases faster with increasing complexity for the SPPRC than that of the MILP. This can be seen by inspection when comparing Figure 9.2a to Figure 9.2c, and when comparing Figure 9.2b to Figure 9.2d. However, to more readily perceive this tendency, Figure 9.2e and Figure 9.2f are presented. They illustrate whether the MILP is fastest (grey dot) or if the SPPRC is fastest (red dot) in each route configuration. The dots are typically red for Sub-Problems solved with fewer frequencies and fewer sub-routes, while they are typically grey in the opposite case. This tendency is the main reason for solving the Sub-Problem with the MILP in the ZEVIPP. Including the option to bunker at several bunkering ports increases the complexity of the Sub-Problem considerably. Thus, these findings suggest that the MILP solve Sub-Problems with several bunkering ports much faster. Additionally, solving the Sub-Problem as MILP removes some feasibility and optimality issues that the SPPRC is prone to, as discussed in Appendix D.

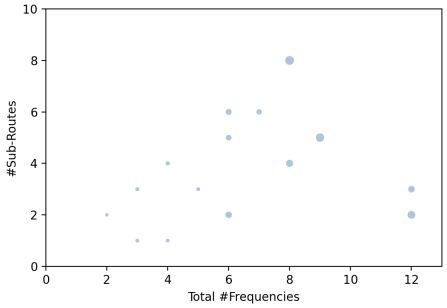

(a) MIP - One vessel

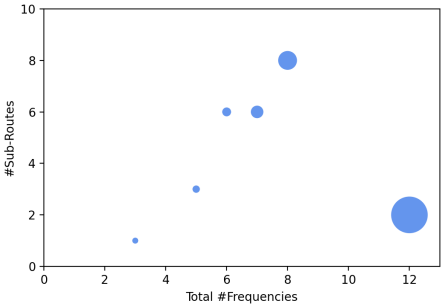

(b) MIP - Two vessels

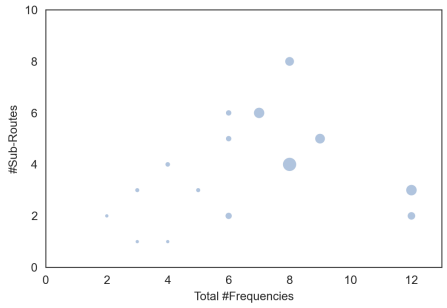

(c) SPPRC - One vessel

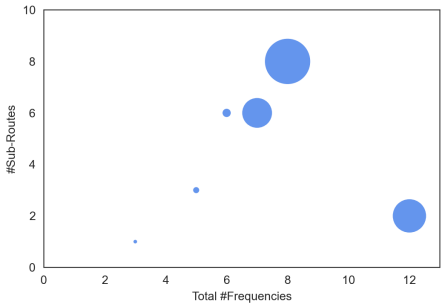

(d) SPPRC - Two vessels

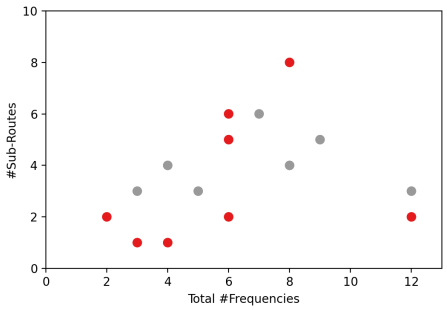

(e) One vessel - Grey dot: MILP is faster than SPPRC

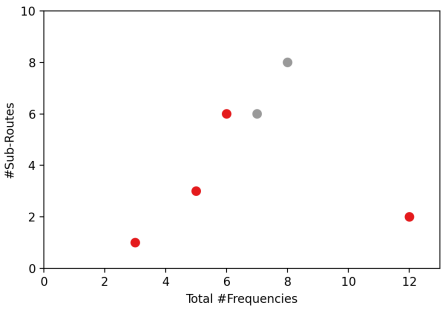

(f) Two vessels - Grey dot: MILP is faster than SPPRC

Figure 9.2: The average solution time for Sub-Problems solved for routes with a given total number of frequencies and a number of sub-routes. In the left column (9.2a, 9.2c, 9.2e), the Sub-Problems are solved with one vessel, and in the right column (9.2b, 9.2d, 9.2f), they are solved with two vessels. The first row (9.2a, 9.2b) is solved as MILP, the second row (9.2c, 9.2d) is solved as SPPRC, and the last row (9.2e, 9.2f) shows which modeling approach is fastest of MILP and SPPRC

9.2 Solutions to Main Instances

This section presents and discusses the main results and findings in this paper. First, the strategic decisions selected for the main test instances, Large (L) and Small (S), are presented in Section 9.2.1. It discusses the investment plan for both and relates them to each other. Second, Section 9.2.2 elaborates on the cost compositions in light of the strategic decisions. Third, the CO_2-tax sensitivity of each route in the Large instance is evaluated in Section 9.2.3. Finally, the stochastic solution approach is evaluated in Section 9.2.4.

9.2.1 Strategic and Tactical Decisions

In this sub-section, the strategic decisions of the ZEVIPP are presented. The analysis focuses mainly on the large (L) test instance, however, the small (S) test instance is used for comparison.

Large Test Instance

Figure 9.3 illustrates the states of installed Zero-Emission (ZE) infrastructures throughout the long-term planning horizon and which bunkering ports the routes are assigned to. The color mapping of the infrastructures and routes is shown in the legend topmost in the figure. Dots indicate installed infrastructure and the size increases with the energy consumption/production at each infrastructure. Note that the local hydrogen production infrastructure archetype is never installed and is therefore excluded from the figure. Further, note that the 2029, 2032, and 2038 time steps are the only ones included in the figure. This is due to no additional infrastructures (compared to previous time steps) being installed in 2023, 2026, or 2035. Lastly, recall from Section 8.1.1 that the allowed amount of conventional CO_2 emitting energy consumption is set to 0% in 2038. Thus, all routes are serviced with ZE solutions in the last time step. To capture all solutions, the 2038 time step is therefore split into the two figures 9.3c and 9.3d. Next, a few insights from this investment plan are presented.

First, note that only one investment plan is included in the figure, despite there being nine separate scenarios all of which could have resulted in different solutions. However, all scenarios, given the first stage decisions being equal, generated the same investment plan. These results might indicate that the value of the stochastic solution is insignificant or non-existing. This is however discussed more extensively in Section 9.2.4. Further, the results indicate that the optimal solution to this problem is robust to changes in the energy market. I.e., the conventional solutions remain dominant for a wide range of energy prices and CO_2-taxes.

Second, there is only one route being converted to ZE in a time step before a CO_2 threshold is added, i.e., before 2032 (when an upper bound of 50% is introduced). This should mean that its abatement cost was negative in this time step and onward, but not earlier. Section 9.2.3 elaborates on this matter. Further, Figure 9.3b shows that only 12 out of 20 routes (route names are listed in brackets beside infrastructures) have transitioned to ZE. This is approximately equal to the CO_2 restrictions introduced in 2032 of maximum 50% emission-generating energy consumption and further supports the indication of the conventional solution being dominant for almost all routes in current and near-future economic environments.

Third, it is evident from comparing the 2032 and 2038 solutions that the electric batteries and electric swappable batteries are preferred over hydrogen, as these are installed earlier. The proportion of electric charging infrastructures and battery-swapping infrastructures installed in 2032 is considerably larger than that of the proportion in 2038, despite that the hydrogen hub is installed already in 2032 and thus could be considered sunk costs for the filling station options. It appears that the reason why the proportion is not maintained is simply that the remaining routes that are not yet transitioned in 2032 are not feasible for battery-electric and battery-swapping vessels.

Fourth, by inspecting the two figures Figure 9.3c and Figure 9.3d, representing the optimal state in 2038, one can observe that filling stations are highly utilized bunkering alternatives in this

Archetype colors		Route colors									
HUB	E	111	151	159	167	172	182	191	193	195	411
F	S	413	433	445	539	585	773	837	866	731	755

(a) 2029

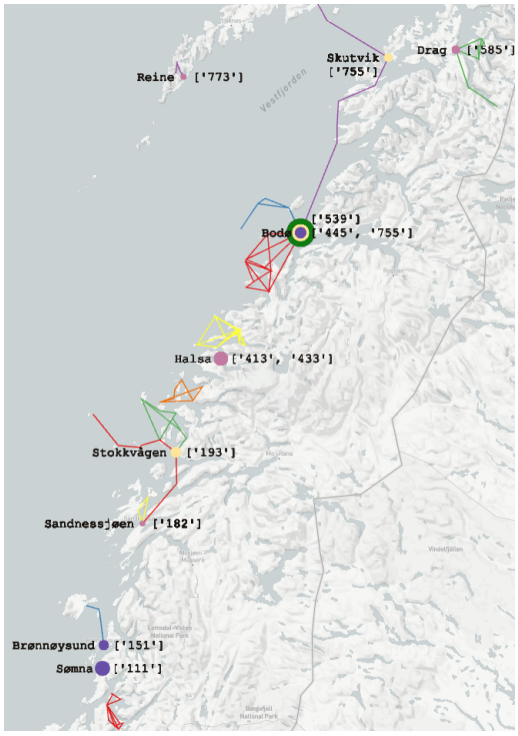

(b) 2032

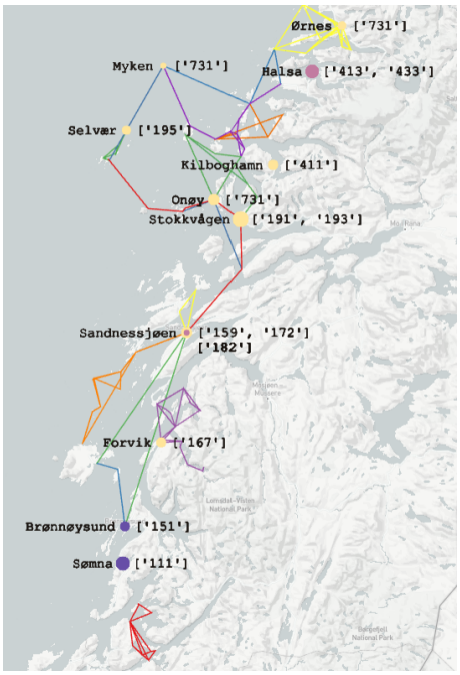

(c) 2038 - South

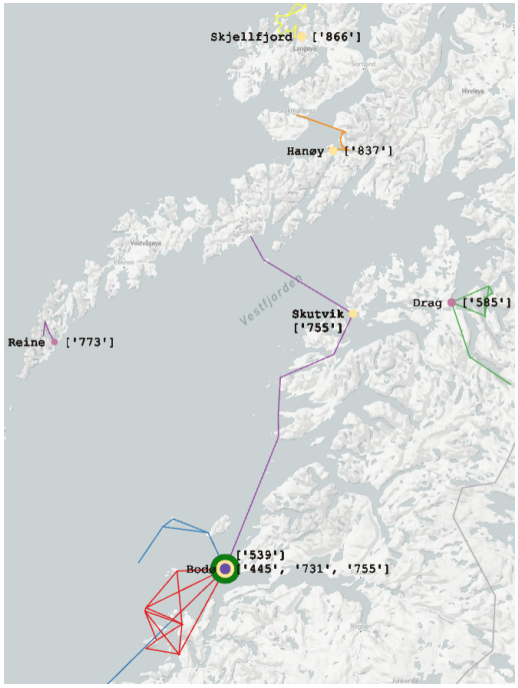

(d) 2038 - North

Figure 9.3: Development of strategic and tactical decisions. The lines represent routes in accordance with the color mapping in the table above. The colors of the dots represent the archetypes of the installed infrastructures, while the label indicates the location of the infrastructure and the routes using it. The size of the dots increases with total energy bunkered or produced at the port.

solution. They are all supplied with hydrogen by the central hydrogen production hub in *Bodø* (which explains the difference between the green and yellow dots in Bodø). Thus, a single hub is able to provide sufficient hydrogen to secure Nordland's demand. An insight that can be drawn from these results is that it is highly expensive to invest in hydrogen production facilities, compared to the additional tube truck transportation costs. This becomes particularly evident for *Skjellfjord*, which is 622 *km* away from the Bodø. There are some strong drivers supporting the dominant choice of filling stations. Installing a hub is inevitable since some routes are localized such that a filling station is the only viable bunkering alternative, i.e., without a grid connection. This enables other routes to disregard the cost of the hydrogen hub as sunk when comparing the costs of using a filling station to other bunkering alternatives. Moreover, many ports only enable filling stations as a bunkering alternative because of low grid capacity. Finally, hydrogen vessels have a considerably greater sailing range than both battery-electric and battery-swapping vessels, which enables them to operate longer routes.

Fifth, the only installed hydrogen hub is localized in Bodø, contrary to the choice of Mo i Rana in the study by Berg et al. (2022). It is shown in Section 9.3.1 that the optimal placement of the hub is in Mo i Rana if only considering a fully ZE solution. However, the time steps 2032 and 2035 with 50% ZE energy consumption are cheaper if the hub is in Bodø. Having the hub in Bodø ensures that hydrogen can be produced cheaply and that there are low transportation costs.

This result shows that extending the model formulated by Berg et al. (2022) with the availability of multiple hubs is important to find an optimal hub localization. Further, the placement of a hub in Bodø is a good option and in alignment with Nordland's plans for hydrogen infrastructure development, as presented in Chapter 2.

Finally, the results show that routes co-utilize infrastructures to a high degree. Routes 159 and 172 share the filling station in Sandnessjøen, routes 191 and 193 share the filling station in Stokkvågen, Routes 413 and 433 share the electric infrastructure in Halsa, and routes 445, 731, and 755 all share the filling station in Bodø. These decisions make sense for several reasons. Sandnessjøen is a resting port for both routes 159 and 172. Routes 191 and 193 visit Stokkvågen during several of their sub-routes. Routes 413 and 433 must detour in order to bunker at Halsa. Finally, Bodø is Route 445's main port, and it is a resting port for both routes 731 and 755.

Figure 9.4a illustrates the total energy consumption for each time step distributed over the energy carriers. As routes are transitioned to ZE, the total energy consumption for the system increases, especially in the leap from 2029 to 2032. This can be reasoned as vessels need to detour further and more frequently to bunker because the ZE vessels have a shorter range than conventional vessels and because ZE bunkering locations are not as ubiquitous as conventional filling stations. Furthermore, the bunkering prices for ZE vessels are cheaper than for conventional vessels, which possibly enables doing more energy-demanding operations to avoid incurring other costs, e.g., avoid bunkering with passengers onboard to save passenger costs. Both of these mechanisms apply the most to battery-electric and battery-swapping vessels, and thus, the highest increase in energy consumption is in 2032 when many routes transition to electric (swappable) batteries. Finally, the increase in total energy consumption further substantiates the importance of using green energy. It also implies, in case of energy deficits, that other use cases for the energy could utilize the same energy to reduce the total CO_2 emission even more than transitioning HSV's to ZE.

The vessel fleet development throughout the long-term planning horizon is depicted in Figure 9.4b. Generally, the development of the vessel fleet reflects the development of infrastructure installment in Figure 9.3. That is, the fleet starts out and remains fully conventional until 2029 when a battery-swapping vessel is acquired. In 2032, when at most 50% of the energy consumption can be conventional, many of the conventional vessels are replaced by battery-electric and battery-swapping vessels, but also some hydrogen vessels. The fleet then remains unchanged until the last requirements in 2038, when the remaining conventional vessels are replaced by hydrogen vessels.

By comparing the vessel fleet size in 2023 and 2038, one can see that number of vessels required to serve each route is almost equal. The exception is route 191. This route is served with one vessel in the conventional solution in 2023 but requires two hydrogen vessels when it transitions to ZE to maintain the service level. This indicates that the transition to ZE is costly for this route, and as expected, it is postponed to the last time step. These results stand in contrast to Havre, Lien and

Ness (2022) who experienced that most routes saw an increase in the number of ZE vessels needed to maintain the service level. This emphasizes the possible importance of including multiple energy carriers and technologies and planning for multiple routes simultaneously.

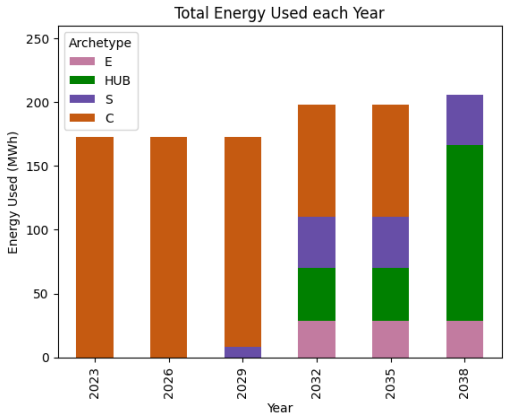

(a) The daily energy distribution in all time steps

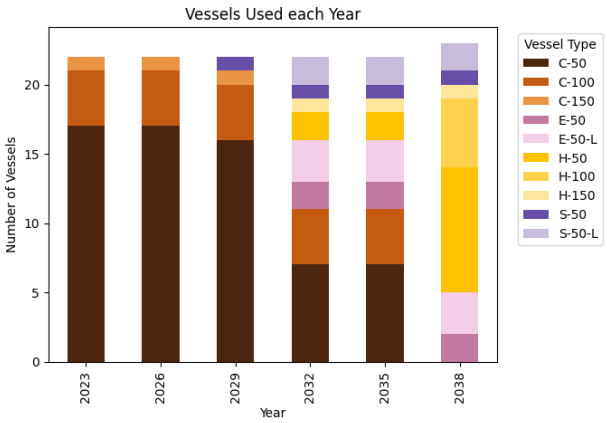

(b) The distribution of vessel types

Figure 9.4: The distribution of energy for energy carriers across time steps and the development of the vessel fleet.

Small Test Instance

The small test instance was solved in order to check both how the running time of the model scales with increasing problem sizes and to investigate if strategic decisions could be determined locally and still be robust to interference with peripheral route interactions. Figure 9.5 shows that the final results for the small instance only differ from the large instance's solution by installing battery-swapping infrastructure in Halsa and placing the hydrogen hub in *Mo i Rana*. The replacement of the hub is an obvious choice as Mo i Rana is much closer to the center of the routes in the small instance than Bodø. It is possible to install a battery-swapping infrastructure in Halsa because Route 413 does not have to co-utilize its infrastructure with Route 433. The co-utilization requires too much energy for the battery-swapping infrastructure to produce during an operating day and is thus not viable for the large instance. This result indicates that battery-swapping is preferred over battery-electric, but its energy production capability is often too restricted in these test instances. It also indicates that disregarding the placement of the hydrogen hub, the local decisions are rather good. Thus, with an intelligent way of handling the hub placement(s) globally, the model could be suitable for even larger networks of routes where the routes are optimized locally in order to ensure a low running time. Chapter 11 elaborates on how this possibly can be implemented with a matheuristic.

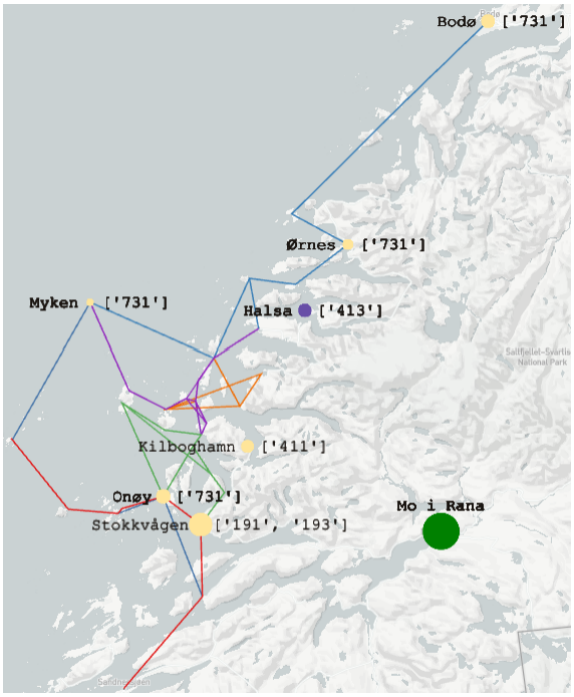

Figure 9.5: The solution of the small instance in 2038

9.2.2 Cost Decomposition

This sub-section provides a detailed description of the costs of the solution obtained when solving the large instance (L). The costs are separated into six components, similar to the ones found in the objective functions of the Sub-Problem and Master Problem. The considered components are *crew costs, energy costs, passenger alternative costs, passenger time costs, vessel investment costs*, and *on-shore investment costs*. The first four components follow from the assigned route serving permutation, which is determined in the Sub-Problem. The last two components are investment costs decided in the Master Problem.

Since the Master Problem is summed over all time steps and scenarios, these costs can be distributed among the time steps as displayed in Figure 9.6. Note that only the base scenario for MGO and electricity prices is displayed. This decision is made for interpretability purposes and since the solutions were identical in all branches of the scenario tree.

Figure 9.6 depicts the daily costs incurred in each time step. The main observation is that the total costs increases by 160 000 NOK in 2032, and further increases by 350 000 NOK in 2038. A big portion of these increases is generated by the increase in crew costs. Hydrogen vessels are associated with significant crew costs related to safety measures and personnel, which explains the rather large increase in the cost group. Passenger costs and investment costs also increase noticeably during the long-term planning horizon. Note that there are no passenger alternative costs, which means that all passenger demand is met. Contrary to the other cost components, the energy costs decrease when transitioning to ZE and comprise a very small part of the total cost in 2038.

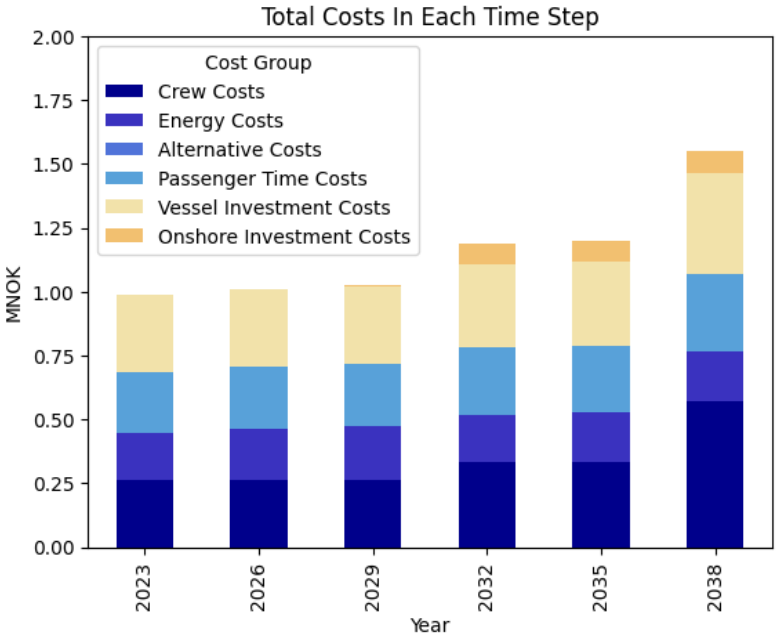

Figure 9.6: The daily cost distribution in all time steps

Now, the pillars for 2023 and 2038 in Figure 9.6 are distributed among the routes in Figure 9.7. This is straightforward for the crew costs, energy costs, passenger alternative costs, passenger time costs, and vessel investment costs, which are incurred for each route separately. Onshore investment costs are, however, distributed among the routes based on the respective route's energy consumption at the infrastructures. Similarly, the costs of the large-scale hydrogen production hub and its associated grid expansion costs are also split among the routes bunkering at filling stations based on energy consumption.

First, Figure 9.7a and Figure 9.7b compare the magnitude of the costs of each route in the conventional solution in 2023 before any investments are made and the fully ZE solution in 2038,

respectively. Since the y-axes are identical, routes can be compared across the two figures, and the color indicates which energy carrier is being used.

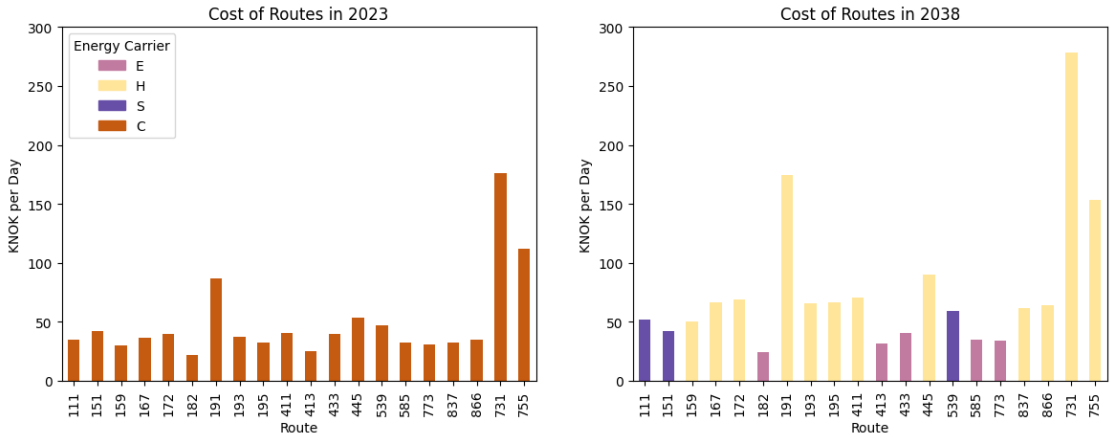

(a) Daily costs in 2023

(b) Daily costs in 2038

Figure 9.7: The cost composition of each route in 2038. The x-axis shows all the route numbers.

Table 9.3 provides an overview of how the cost components of the routes change from the initial solution using conventional vessels, to the fully transitioned ZE solution. This is based on the same data plotted in Figure 9.7 and is meant to give an in-depth understanding of how the cost component change, mapped to the different traits of each route. The first three columns contain the route name, total distance sailed during a day, and the passenger demand data per route serving. The same information is shown in Table 8.3 which is also accompanied by a map showing where the routes are located. The cell color of the first column indicates what energy carrier is used in 2038 when all routes are fully transitioned to ZE. Next, the following six columns describe the percentwise change from the solution with conventional vessels in 2023.

In general, most changes in the energy used are positive which makes sense since the ZE is less available compared to MGO refueling stations. Therefore, some routes need to perform detours to bunker energy. This is evident by viewing Route 111 and Route 413 on the map, which bunker far away from any port they visit during their routes. This is due to the sparsity of grid capacity resulting in unfortunate placements of their bunkering infrastructures, and it results in their routes increasing the energy used by more than 100%. Further on, six routes operated by a hydrogen vessel with a capacity of 50 passengers, all have an increased energy usage of exactly 10%. This is due to the hydrogen vessels spending more energy per kilometer sailed. It also indicates that these vessels sail the exact same distance, and thus, do not detour in order to bunker during their operational day. In addition to some routes having the exact same increase in energy usage, there are some routes that have reduced their energy usage when transitioning to ZE. This is, however, not the case in practice. Due to the use of Euclidean distances for missing data, some routes have used detouring in order to sail the shorter Euclidean distance, effectively taking a shortcut to reduce the length of a leg in their route. This causes at least a 13% difference in energy usage for some routes, and thus, it is an important finding. Any further development on this model should endeavor to use actual sailing distances, even for detouring. Finally, this column is mostly green on the face of the table. This is natural as energy usage grows together with crew, passenger, and energy costs, which makes it important to keep it at a minimum.

From the column containing the change in crew costs it is evident that there are rather large changes for routes using hydrogen as an energy carrier. This is due to the safety regulations, demanding safety personnel on board.

The column containing changes in energy costs shows that battery-electric and battery-swapping vessels are considered cheap compared to hydrogen due to the difference in the value chain. There is a greater energy loss when producing hydrogen than charging batteries, and filling stations also need to pay transportation costs for the hydrogen. This is seen by viewing routes 195, 837,

Route	Daily Dist km	Pass. per serving	Energy Used	Cost groups				All Costs
				Crew	Energy	Pass.	Inv.	
111	310	2	157 %	0 %	-5 %	29 %	125 %	**49 %**
151	334	5	0 %	0 %	-63 %	0 %	43 %	**1 %**
159	151	13	10 %	180 %	29 %	15 %	41 %	**68 %**
167	303	5	10 %	180 %	41 %	30 %	50 %	**82 %**
172	253	13	10 %	180 %	29 %	18 %	46 %	**72 %**
182	92	8	-3 %	0 %	-61 %	15 %	30 %	**13 %**
191	570	29	8 %	281 %	17 %	40 %	197 %	**100 %**
193	348	3	12 %	180 %	22 %	29 %	51 %	**76 %**
195	239	1	10 %	180 %	130 %	19 %	47 %	**105 %**
411	298	10	25 %	180 %	42 %	16 %	51 %	**74 %**
413	144	1	105 %	50 %	-16 %	43 %	22 %	**25 %**
433	319	2	33 %	0 %	-46 %	74 %	29 %	**4 %**
445	519	9	21 %	180 %	-13 %	18 %	61 %	**67 %**
539	343	16	33 %	0 %	-51 %	0 %	126 %	**26 %**
585	216	3	7 %	0 %	-56 %	9 %	41 %	**8 %**
773	111	11	-3 %	0 %	-61 %	17 %	33 %	**10 %**
837	218	4	10 %	180 %	51 %	21 %	46 %	**87 %**
866	253	5	10 %	180 %	56 %	18 %	48 %	**84 %**
731	1 052	28	4 %	167 %	36 %	26 %	54 %	**58 %**
755	538	46	-1 %	100 %	-16 %	26 %	64 %	**37 %**

Table 9.3: Percentwise change from 2023 to 2038 of the energy usage and cost components for each route. The first column uses the same color mapping as Figure 9.7 to show the resulting energy carrier of each route. The next two columns display two key characteristics of the routes, the daily distance to cover and the number of passengers to serve for each route service. The next columns show the percentwise change of energy usage and cost components. Finally, the total percentwise cost changes of each route in 2023 are displayed in the last column

and 866 which are the furthest away from the hub in Bodø. Further on, the energy costs from electric charging and battery-swapping infrastructures are also cheaper than the initial solution using conventional fuel despite using more energy for most routes. This makes sense based on the development of the prices per kWh presented in Chapter 8.

Passenger time increases in 18 out of 20 routes. The two factors determining the passenger costs are the time spent with passengers on board, and the number of passengers. Consequently, the increased passenger time is explained by that bunkering infrastructure is not always easily accessible for the ZE energy carriers. This results in cases where vessels need to bunker with passengers on board or even detour during a route serving.

The increase in investment costs is partly explained by conventional infrastructures already being available, while the ZE infrastructures have associated costs. Routes 111 and 539 both require the battery-swapping infrastructure S-3 installed, which is more expensive than S-1, used by route 151. Also, route 191 has a large increase in investment costs since it requires an additional vessel to maintain the current service level. The two routes with the smallest increase in on-shore investment costs are routes 413 and 433, which also share an electric charging infrastructure, as seen in Figure 9.3c. Furthermore, the number of passengers on the said routes is relatively low. In these cases, the penalty for bunkering at unfortunate bunkering locations is low.

The final column shows the change in total costs. Here, it is evident that the routes being served by battery-electric and battery-swapping vessels are significantly less costly than those served by hydrogen vessels. The table shows that the main cost drivers for this difference are the crew costs and the difference in energy costs. Comparing the cost components shown in Figure 9.6 shows that the crew time costs are the most significant one of the two.

9.2.3 CO_2-Tax Sensitivity

The abatement cost of each route is hard to assess as the service of each route to some extent is interlinked with the service of all other routes. For instance, the second route to utilize an infrastructure could consider the infrastructure investment costs as sunk, which reduces its abatement costs. On the contrary, a route could be prevented from using its ideal bunkering alternative because another route occupies it, which increases its abatement costs. In this sub-section, a sensitivity analysis of introducing an *additional* CO_2-tax is presented. This analysis determines for each route the CO_2-tax threshold at which it is cheaper to transition to ZE than to continue operating conventionally in each time step. Since the results in Section 9.2.1 show that the strategic decisions are robust to fluctuations in energy prices, the analysis here is conducted only for the base case scenario, which is considered the most likely out of the scenarios.

Abatement cost is the general term used to describe the cost of reducing carbon emissions by one *tonne* of CO_2-equivalents. For the case of fully transitioning HSVs to ZE solutions, this could be determined by dividing the cost difference between the ZE solution and its conventional counterpart. This has been discussed thoroughly in Section 9.2.2 and is important to see the consequences of having hard emission thresholds. However, it does not give the idea of how an increased CO_2-tax would affect the profitability of the HSV operation. Figure 9.8 illustrates the lowest CO_2-tax at which each route has a non-positive abatement cost. This is presented for each time step in the long-term planning horizon. These values were calculated by adding soft constraints requiring all routes to operate with ZE energy carriers. The constraints allow for conventional energy usage if an additional CO_2-tax is paid. Accordingly, by increasing the additional CO_2-tax incrementally, the threshold is found at which each route transitions to ZE without an abatement cost. The key observations from this analysis are discussed as follows.

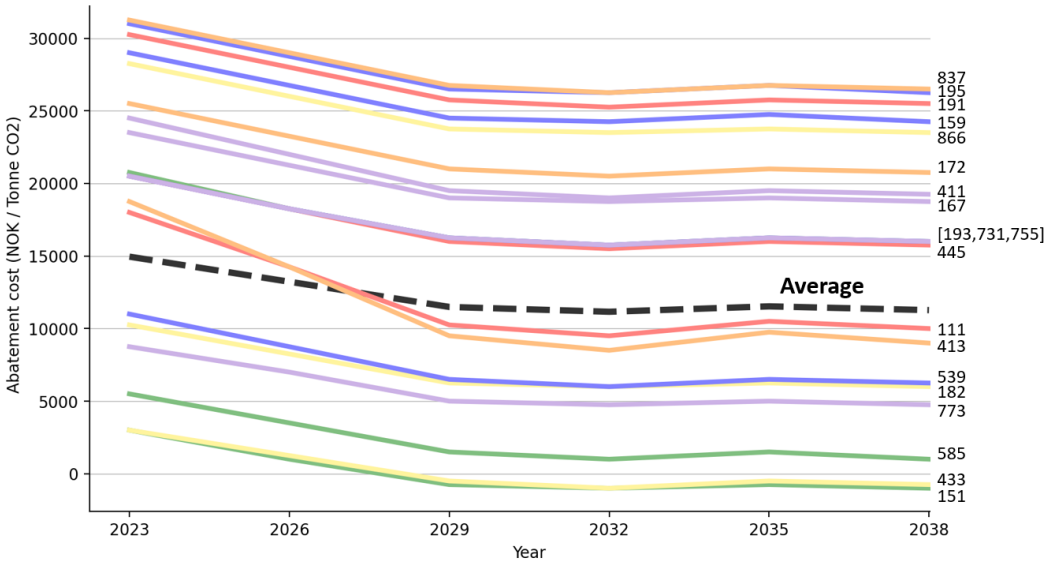

Figure 9.8: The abatement cost in NOK per tonne CO_2 for each route in each time step in the most likely scenario considered. The routes are listed next to the end of their graph. The dashed line represents the average abatement cost for a 100% ZE solution in each time step.

First, Figure 9.8 shows there are two routes, 151 and 433, that are profitable to transition to ZE from 2029 and onwards. Recall that route 151 was observed in Section 9.2.1 to transition to ZE in 2029. Surprisingly, route 433 did not do the same, despite being profitable. As described in the latter parts of Section 9.2.1, this is because the ideal bunkering alternative is to use battery-swapping in Halsa, but as Route 413 uses the electric charging infrastructure installed in Halsa in 2032, it is cheaper to wait and co-utilize its infrastructure with Route 413. This analysis suggests however that if no further demands are given, transitioning Route 151 and 433 to ZE in 2029 is the most profitable solution.

Second, the thresholds vary drastically among the routes. Routes 837, 195, and 191 demand a CO_2-tax of above 25 000 NOK, which substantially surpasses the taxation of 2 000 NOK suggested by the Norwegian government to implement by 2030 (Bjartnes et al., 2021). In practice, these results suggest that using governmental subsidies is the only viable solution in order to transition all routes. These results also show that even a CO_2-tax that accounts for the average abatement cost of the route network as a whole does not ensure a profitable ZE transition for 12 out of the 20 routes in the large instance. For comparison, Berg et al. (2022) presented a general taxation for the system as a whole and concluded that a CO_2-tax of 897 NOK would be sufficient to make the ZE transition profitable for every route, not accounting for different taxation thresholds. Nevertheless, the main driver of increased abatement costs compared to the analysis done by Berg et al. (2022) is a more realistic representation of hydrogen vessel operation. After receiving valuable input from some of the key partners in the (Enabling) Zero Emission (Passenger) Vessel Services (ZEVS) project, important additions, such as added security staff, longer bunkering overhead time, and added costs related to the hydrogen fueling process, have been made.

Third, there is a cluster of routes that have close to equal thresholds throughout the long-term planning horizon. This applies to routes 445, 193, 731, and 755. This can either happen because the routes' abatement costs are similar and the proportion of the total costs that the conventional energy costs constitute is similar. This results in both the same variation along the long-term planning horizon and the same initial level. It seems like this is the case for the relationship between routes 193 and the others. However, routes 445, 731, and 755 share a filling station in Bodø when all routes are operated with ZE. Whenever it is profitable for either one of these routes to invest in the filling station in Bodø, the same holds for the others as the investment cost can be considered sunk. This holds since they have similar initial abatement costs. The three other pairs of co-utilizing routes, 433 and 413, 159 and 172, and 191 and 193, have too different initial abatement costs to see this cascading effect.

Finally, the routes with the highest thresholds are consistently hydrogen routes. This has been a red thread throughout this chapter; electric (swappable) batteries are the preferred energy carriers. This is very noticeable in Figure 9.8 as the routes with the eight lowest thresholds throughout the long-term planning horizon either transition to electric batteries or electric swappable batteries.

9.2.4 Value of Stochastic Solution

In Section 9.2.1, the results indicated that the value of the stochastic solution was minimal or absent due to all scenarios being solved equally. This was not proved, however, in this sub-section, the exact value of the stochastic solution is presented. In order to evaluate this, an alternative deterministic method of solving the problem is outlined. First, the optimal investment plan is calculated using the expected value of each stochastic value. Then the first-stage decisions are fixed in the stochastic model, effectively calculating the expected value across scenarios given the predetermined first-stage decisions. The results showed that the exact same first-stage decisions were found in the proposed deterministic model, and thus, the value of the stochastic solution was zero.

9.3 Additional Analyses

This section provides additional analyses that accompany the strategic and tactical decision support provided in Section 9.2.1. First, Section 9.3.1 investigates the consequences of only accepting tenders from ZE operators in the future and discusses the results in the context of the trajectory currently laid out by the Norwegian government. Second, the model is run in Section 9.3.2 with the ability to optimize the sailing speed of each route. Lastly, Section 9.3.3 assesses the effect of removing safety personnel from hydrogen vessels, which could become a reality and drives the abatement costs for hydrogen-operated routes. Note that also in these analyses, the second-stage variables did not vary among the scenarios. Therefore, decisions for the entire long-term planning horizon are presented, while the energy prices from the base case are used to calculate the costs.

9.3.1 ZE Tenders

As mentioned in Chapter 2, the government has proposed that all new tenders for the current routes in Norway must be facilitated to be ZE. To find the costs of this decision, the model is solved with additional ZE constraints on each route from the expiry date of the current tenders retrieved from Statens Vegvesen and Kollektivtrafikkforeningen (2022).

This is implemented by imposing constraints (9.1) on the Master Problem, presented in Chapter 6. Here, T_r^{NEW} denotes the renewal date of route r, and whenever a tender expires, the new tender needs to be served by a ZE HSV.

$$\sum_{b \in \mathcal{B}_r} \sum_{v \in \mathcal{V}_{rb}^{ZE}} y_{rbvt}^s = 1, \qquad r \in \mathcal{R}, t \in \{T_r^{NEW}..|\mathcal{T}|\}, s \in \mathcal{S} \quad (9.1)$$

Table 9.4 summarizes the input data on the expiry dates of the tenders which are equally distributed between 2026 and 2029. One observation is that routes 191, 731, and 755, which were found to be the most expensive routes in the cost analysis in Section 9.2.2, all have tenders expiring in 2029. As input to the model, the original tenders are postponed by three years since many have expiry dates in 2023, and the investment latencies are usually three years. Also, the investment latency of the hub is reduced from six to three years in order to obtain a feasible solution.

The cell color shows the assigned energy carriers in 2038 in the optimal solution. Note that the solutions do not vary among scenarios, and assigned energy carriers for the routes are identical to the solution of the Large Instance (L) by the Main Model discussed in Section 9.2.

Year	Routes									
2026	167	182	193	411	413	433	445	539	773	837
2029	111	151	159	172	191	195	585	866	731	755

Table 9.4: Renewal dates of current tenders.

The total costs from these analyses are presented in Table 9.5 which shows the objective value of the main solution presented in Section 9.2, and the objective value of the solution obtained by imposing ZE constraints on new tenders. As the table shows, the total costs throughout the long-term planning horizon increase by 20%.

Model	**Total Costs**	**Key Differences**
Main Model (Large Instance)	7 492 $MNOK$	Hub in Bodø
ZE Tenders	9 010 $MNOK$	Hub in Mo i Rana

Table 9.5: Differences between the standard solution and the solution with ZE tenders

A visual map of the routes' expiry dates in 2026 and 2029 is shown in Figure 9.9a by the color orange and purple, respectively. Note that a cluster of orange routes with renewal dates in 2026 appears to be closer to Mo i Rana than Bodø, which helps explain the selected hub location in the two models.

A cost comparison in all time steps is presented in Figure 9.9b. The left bar in each time step represents the costs of the solution to the large instance (L) by the Main Model, and the right bars represent the costs of the solution when ZE tender constraints are included. Since the ZE tender constraints lead to an earlier transition to ZE HSV, the costs are higher in the time steps before 2038. However, in 2038, the costs with ZE tender constraints are slightly lower. Since the hub location is the only differing strategic decision, placing the hub in Mo i Rana must be slightly cheaper than placing it in Bodø when producing hydrogen for all routes in Nordland. While the solution without ZE constraints on new tenders reduces costs in 2032 and 2035 when only 50% is

transitioned, the solution with ZE constraints on new tenders finds a better solution for the final time step by placing the hub in Mo i Rana.

Finally, an interesting finding is the fact that the costs in 2038 are slightly lower with ZE tender constraints. Thus, this analysis shows that the costs during the transition period increase, but the yearly costs in the final time steps are not affected. This implies that in a case without technological development, the yearly costs in the final time step are not affected by making the transition to ZE straight away.

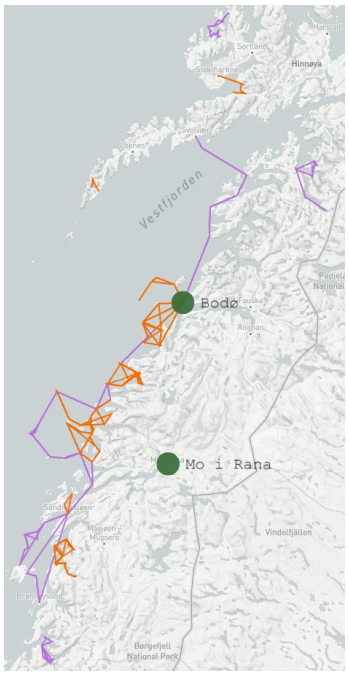

(a) Routes separated on tender renewal dates.
Orange - 2026,
Purple - 2029.

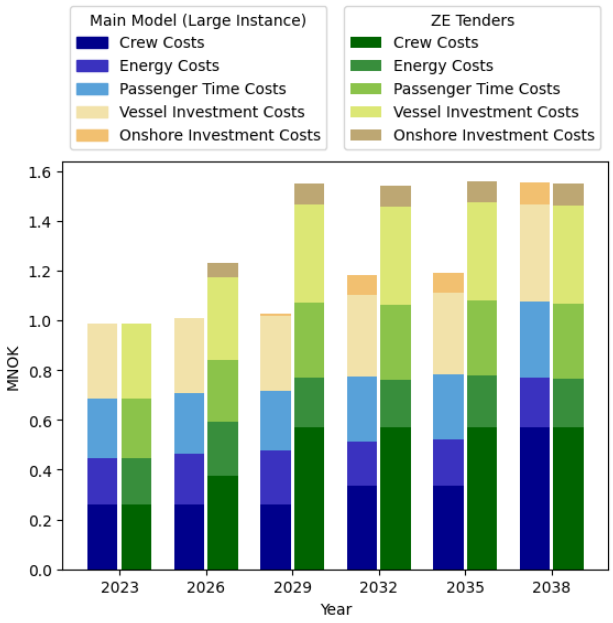

(b) A comparison of the cost composition for the solution of L by the Main Model, and the solution of L when imposing ZE constraints on all new tenders. The costs in each time step when solving the model with ZE tenders are on the right-hand side of each time step. The bars on the left-hand side are the costs in the solution of L by the Main Model, also found in Figure 9.6.

Figure 9.9: Visualizations of the routes by renewal dates and the cost composition in the optimal solution.

9.3.2 Varying Sailing Speeds

Sailing speed affects both the energy consumption per kilometer and of course the sailing time considerably. In turn, this affects the passenger, energy, and crew costs, and each route might save costs by sailing faster or slower than the current sailing speed of 25 *knots*. This sub-section presents the results from a model extension of the previously proposed ZEVIPP model. This extension is implemented by first solving each Sub-Problem with sailing speeds of 20, 25, and 30 *knots*, and then solving the Master Problem with the additional ability to select the speed with which each route is operated. The optimization model of the Master Problem is mainly unchanged, except for summing over the available sailing speeds in some restrictions. A route can be operated with different sailing speeds for different scenarios and time periods. However, the sailing speed of a route cannot vary within the same time step and scenario.

Table 9.6 presents the objective function of the Large instance L (fixed sailing speeds) and L-VS (Large instance with varying sailing speeds). These results show that for the duration of the long-term planning horizon, a reduction in total costs of 1.7% can be achieved. This is not very substantial, however, it does sum up to around 7.1 $MNOK$ each year and could be a good initiative

given that reducing the sailing speed to 20 *knots* for some routes is tolerated.

Instance	**Total Costs**
L (Fixed Sailing Speeds)	7 492 $MNOK$
L-VS (Varying Sailing Speeds)	7 364 $MNOK$

Table 9.6: Differences between the objective values of L and L-VS.

Figure 9.10 displays the sailing speeds selected in the optimal solution for each route in the initial time step in 2023, and in 2032 and 2038 when the carbon budget has decreased. The color of each bar specifies which energy carrier is selected for each route in the solution.

Figure 9.10a shows the sailing speeds selected in 2023 when the routes are operated with conventional energy. Comparing these results to Table 9.3, there can be drawn hard lines for the passenger demand on each route to determine the optimal sailing speeds. Every route with passenger demand below 11 per serving is operated at 20 *knots*, every route with passenger demand from 11 to 16 is operated at 25 *knots*, and more than 28 passengers entails an optimal sailing speed of 30 *knots*.

Figure 9.10b depicts the speeds selected in 2032 when the initial energy restriction on conventional energy takes effect. The sailing speeds selected by the ZE routes are the same as in 2038, which indicates that the optimal sailing speed is a highly independent choice for each route.

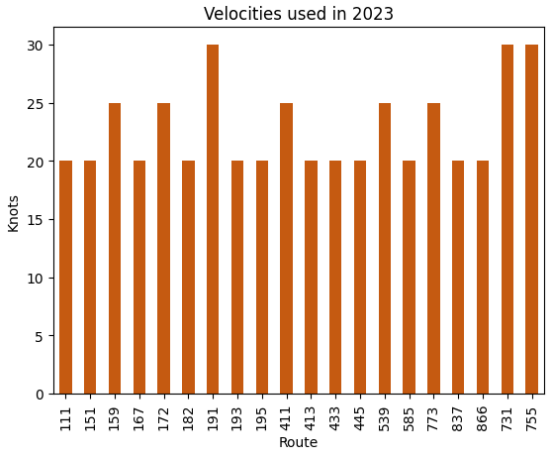

(a) Selected sailing speeds in 2023

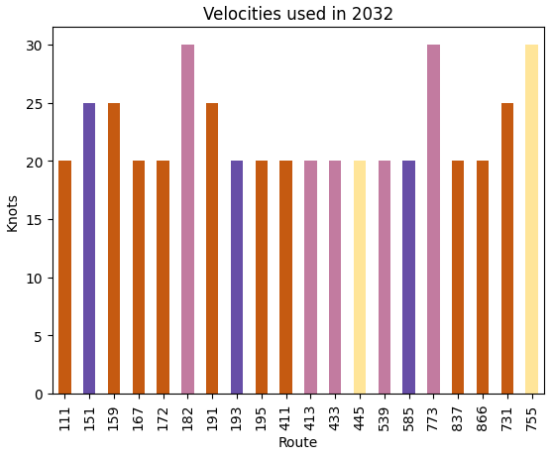

(b) Selected sailing speeds in 2032

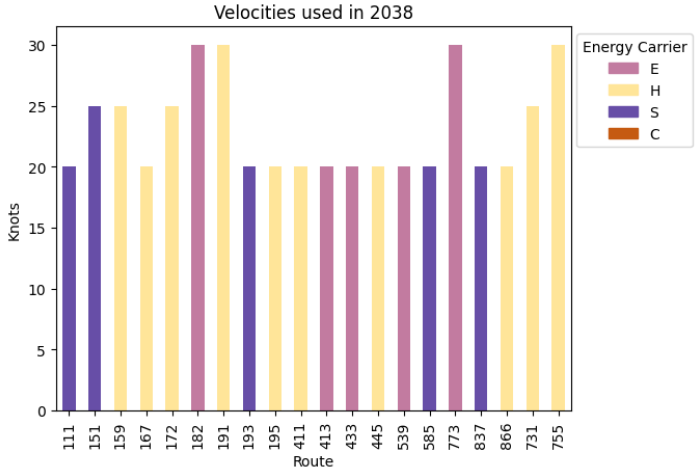

(c) Selected sailing speeds in 2038

Figure 9.10: Sailing speeds selected for each route in 2023, 2032, and 2038.

In contrast, some of the sailing speeds selected for routes operated by conventional vessels are reduced from 2023 to 2032. Routes 172, 191, 411, and 731, all reduce their sailing speed by 5 knots in order to comply with the conventional energy constraint of 50%. This alleviates the transition to ZE and, in specific, enables route 111 to postpone its ZE transition to 2038, in contrast to the solution with fixed sailing speeds.

Finally, Figure 9.10c shows the speeds selected in 2038 when all routes are forced to operate with ZE. The routes with fewer than five passengers each route-serving are also operated at 20 *knots*. However, the direct link between sailing speed and passenger demand is mostly not present for the remaining routes in 2038.

Figure 9.11 shows the relative effect of solving the routes with varying sailing speeds compared to the solutions found with fixed sailing speeds, presented in Section 9.2. Figure 9.11a and Figure 9.11b show each route's cost difference between both solutions in time steps 2023 and 2038, respectively. Similarly, Figure 9.11c and Figure 9.11d show each route's respective relative energy difference. Finally, the changes in investment and route-serving permutations for each route are presented in Table 9.7.

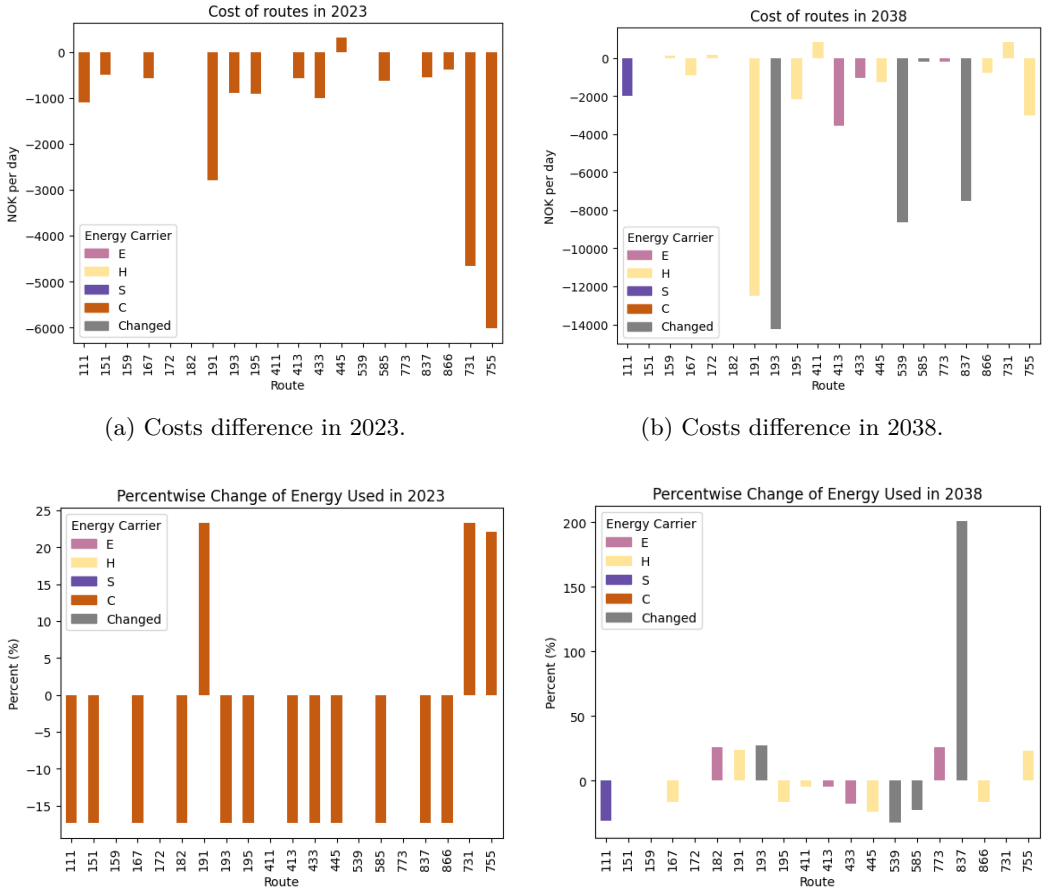

(a) Costs difference in 2023.

(b) Costs difference in 2038.

(c) Energy difference in 2023.

(d) Energy difference in 2038.

Figure 9.11: The relative difference in costs and energy usage between L and L-VS in 2023 and in 2038

The conventional routes are mostly solved independently of each other since they do not consider co-utilizing infrastructures. Thus, each route can select its sailing speed only considering the costs of energy compared to passenger costs as long as the total remains within the energy consumption boundaries. This leads to the results in Figure 9.11a and Figure 9.11b where almost all routes solved with 20 or 30 *knots* have reduced their costs compared to the solution with fixed sailing speeds. The only exception is route 411. This route has to reduce its sailing speed, which is locally

sub-optimal, but since it enables another route to increase its sailing speed, it is optimal for the system as a whole.

The main observations to draw from Figure 9.11b and Figure 9.11d are that four routes change energy carrier and that some routes incur higher costs than in the more restricted solution with fixed sailing speeds. Furthermore, routes 191, 193, 539, and 837, three of which change energy carriers, are the main drivers of cost reduction. Combining these plots with the selected operating speeds in Figure 9.10c, it can be shown that energy consumption increases with the operating speed for most routes. However, routes 193 and 837 do not follow this pattern. Finally, Table 9.7 shows that the four routes that changed their energy carrier are routes 151, 193, 539, and 837, two from hydrogen to electric swappable batteries, one from electric swappable batteries to electric batteries, and one from electric batteries to electric swappable batteries.

Route (Speed)	**Change of Bunkering Alternative**			
	L (Fixed Sailing Speeds)		**L-VS (Varying Sailing Speeds)**	
191 (30)	F-4	Stokkvågen	F-3	Stokkvågen
193 (20)	F-4	Stokkvågen	S-3	Langsetvågen
195 (20)	F-2	Selvær	F-1	Selvær
411 (20)	F-2	Kilboghamn	F-2	Halsa
539 (20)	S-3	Bodø	E-1	Bodø
585 (20)	E-1	Drag	S-1	Drag
837 (20)	F-2	Hanøy	S-3	Svolvær
866 (20)	F-2	Skjellfjord	F-1	Skjellfjord
755 (30)	F-1	Skutvik	F-2	Skutvik

Table 9.7: Changes in onshore investments when enabling varying sailing speeds.

Routes 193 and 837 change their energy carrier from hydrogen to electric swappable batteries. In the solution with fixed costs, these routes have to be supplied by hydrogen filling stations. However, reducing the sailing speeds increase the range of the vessels and enables the routes to bunker at a bunkering port with grid capacity. Energy costs are high for hydrogen vessels due to transportation costs, filling costs, and low energy conversion efficiency. Thus, there is a lot to save by bunkering remotely if this enables a route to be served with battery-electric and battery-swapping vessels.

Both routes 539 and 585 switch energy carriers, the former from electric swappable batteries to electric batteries and the latter from electric batteries to electric swappable batteries. By examining their operational details in the Sub-Problem solutions, it is evident that the energy bunkered each time a vessel bunkers is highly important for deciding which electric charging and battery-swapping infrastructure to choose. With high bunkering amounts, the expensive swap infrastructure S-3 is optimal. This applies to 539 being operated at 25 *knots*, bunkering close to 3 MWh every time it bunkers. With medium bunkering amounts, the cheaper option is the electric charger E-1, which is selected by route 539, operated at 20 *knots*, or the shorter route 585, operated at 25 *knots*. They bunker an amount of 1.9 and 1.5 MWh every time they bunker, respectively. Finally, with low bunkering amounts, the swap infrastructure S-1 is optimal. This is selected by route 585, sailing at 20 *knots*, which bunker 1.1 MWh for each bunkering activity. The optimal solutions for these types of routes are hard to determine since they are derived from intricate distinctions between the infrastructure investment costs, bunkering rates, and production rates among the infrastructures.

Routes 159, 172, and 731 have increased costs compared to the solution with fixed sailing speeds, even though they are operated at 25 *knots*. They bunker at filling stations and are responsible for a higher proportion of the investment costs of the hub since fewer routes bunker at filling stations. The same holds for route 411, which increases costs even though it optimizes its sailing speed to 20 *knots*.

From this sub-section, a few main insights can be drawn. It is shown that many routes can be solved more economically efficiently by reducing the sailing speed for low-demand routes and that high-demand routes may be improved by increasing the speed, given feasibility. Reducing the speed of the current conventional fleet is shown to alleviate the ZE transition as it can be cheaper per tonne abated CO_2 than transitioning a route to ZE. Finally, routes can reduce costs significantly

by avoiding using hydrogen, even though it has to bunker at a remote port.

9.3.3 Hydrogen Vessels Without Safety Personnel

As the previous analyses have shown, the presumed requirement for safety personnel on hydrogen vessels increases the total costs significantly. Due to uncertainty regarding hydrogen technology, the need for additional safety measures could be reduced in the future. Therefore, this subsection analyzes the abatement costs in a case where there are no additional requirements for safety on hydrogen vessels. This is implemented by removing the costs of the safety personnel on hydrogen vessels and performing a CO_2-tax sensitivity analysis on the large instance with varying sailing speeds (L-VS).

The main differences between the solution of the instance with varying sailing speeds and the instance with varying sailing speeds and without safety personnel are highlighted in Table 9.8. Firstly, it is observed that of all the electric charging and battery-swapping infrastructures, the most expensive battery swap system, S-3, is the only one converted to hydrogen. This shows that still, electric (swappable) batteries are often preferred as an energy carrier, if feasible.

Further on, lower operating costs of hydrogen vessels promote more co-utilization. A prerequisite for co-utilization is to use the same energy carrier, and in the solution of the instance without safety personnel, there are more hydrogen vessels. This is exemplified by three routes using the same filling station in Stokkvågen.

Route (Speeds)	**Change of Bunkering Alternative**			
	L-VS (Varying Sailing Speeds)		**L-VS without Safety Personnel**	
111 (30)	S-3	Sømna	F-2	Terråk
191 (30)	F-3	Stokkvågen	F-4	Stokkvågen
193 (20)	S-3	Langsetvågen	F-4	Stokkvågen
411 (20)	F-2	Halsa	F-4	Stokkvågen
837 (20)	S-3	Svolvær	F-1	Hanøy
	HUB	Bodø	HUB	Mo i Rana

Table 9.8: Changes in onshore investments when removing the costs of safety personnel.

Figure 9.12 illustrates the CO_2-taxation sensitivity for each route throughout the long-term planning horizon when the model is solved with varying sailing speeds and removed safety personnel. This solution shows very positive prospects compared to the results in Figure 9.8. The average abatement cost shows that already in 2029, one could transition the whole system of routes with an average abatement cost of 4500 $\frac{NOK}{tonne\ CO_2}$. This is still a lot higher than the suggested 2000 $\frac{NOK}{tonne\ CO_2}$, and as stated in Section 9.2.3, using a tax will only transition routes that have non-positive abatement costs. In this case, an additional tax of 12 500 NOK is needed to transition route 191 under the assumption that the operator maximizes social welfare. A contract can be proposed where all abatement costs are subsidized given that all routes are operated with ZE. This contract would be able to exploit the relatively attractive average abatement cost.

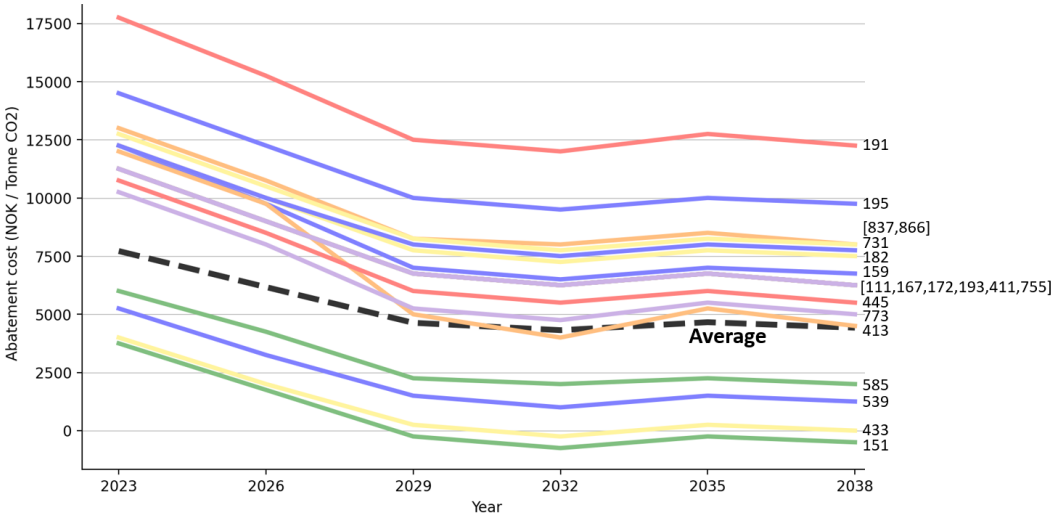

Figure 9.12: The abatement cost in NOK per tonne CO_2 for each route in each time step in the most likely scenario considered when security personnel is removed from hydrogen vessels. The routes are listed next to the end of their graph. The average abatement cost for the routes in total is marked by the dashed line.

Chapter 10

Concluding Remarks

Motivated by recent High-Speed Passenger Vessel (HSV) initiatives and proposed regulations to comply with climate obligations, this thesis has provided decision support for the transition towards Zero-Emission (ZE) HSV services. The focus has been on holistically approaching the transition, by considering several candidate ZE energy carriers and a set of routes simultaneously, to investigate whether related technical and economic challenges can be alleviated. First, the Zero-Emission (Passenger) Vessel & Infrastructure Planning Problem (ZEVIPP) was defined. The ZEVIPP spans a long-term planning horizon of several years and its main objective is to maintain the service level of a set of routes throughout the ZE transition while minimizing passenger and operator costs. It includes strategically deciding the optimal roadmap for infrastructure, grid, and vessel investments, tactically deciding the allocation of the vessel fleet and infrastructures to routes, and operationally managing energy production and consumption to ensure feasible services. Furthermore, the problem introduces uncertainty related to future bunkering prices to enhance the robustness of the proposed solutions.

The wide scope and many interdependencies in the ZEVIPP make it highly complex to solve accurately within a reasonable time. Hence, a solution approach was proposed to reduce the complexity while maintaining reliability in the emphasized strategic and tactical decisions. The long-term planning horizon was periodized into time steps for which decisions can be made. Further, the problem was decomposed into a strategic- and tactical-focused two-stage stochastic Master Problem and an operational-focused Sub-Problem, both formulated as Mixed Integer Linear Programming (MILP) models. The Sub-Problem pre-calculates the optimal operational decisions for all route-serving permutations and provides both the decisions and their associated costs as input to the Master Problem. The Master Problem then utilizes these inputs to make strategic and tactical decisions for each time step. This solution approach exploits redundancy in the operational decisions and enables the opportunity to computationally distribute the problem.

To assess the reliability of the models, they were implemented in and solved by the commercial MILP-solver *Gurobi* for several instances of data from HSV services in Nordland County. Nordland County contains a long coastal area in the north of Norway and is the county with the most HSV connections in the country. Hence, it served as a great reference to evaluate the scalability of the proposed models. The test instances used comprise in total seven variations of a small instance containing five routes and a large instance containing all 20 routes in the county. It was shown that the solution approach performed well in terms of running time for all of these instances but that the complexity increases rapidly with the number of routes and scenarios.

The conducted analyses showed quite consistently that battery-electric and battery-swapping vessels are preferred over hydrogen vessels whenever they are feasible. When the CO_2-emitting energy consumption is required to be halved, a large majority of the routes that are transitioned to ZE energy carriers become served by vessels with electric (swappable) batteries. Common for these routes is that they are within the range limitations of electric charging and battery-swapping vessels. Contrary, when the remaining conventional CO_2-emitting routes must be transitioned, most of the routes become served by the hydrogen vessels and infrastructure. However, these routes were

typically never feasible for electric (swappable) batteries. This reluctance to choose serving routes with hydrogen solutions is reflected in the cost decomposition. The main factors that contribute to hydrogen reluctance are an inefficient supply chain and safety regulations imposing relatively high operating costs compared to (swappable) battery-electric solutions. The safety regulations are particularly uncertain due to the immaturity of hydrogen in the maritime sector and might be pessimistically represented in the instances used. Therefore an analysis of the impact of removing the additional safety personnel for hydrogen vessels was conducted. The results showed that a considerably larger proportion of the routes transitioned to hydrogen solutions and, in particular, that hydrogen was preferred over the solutions using the most expensive battery-swapping infrastructure.

The analyses also showed that the abatement costs are higher than the CO_2-tax of 2 000 NOK per *tonne* CO_2 proposed by the Norwegian government. Per route, the abatement costs range from below zero (profitable to convert to ZE) to above 30 000 NOK per *tonne* CO_2, averaging to approximately 12 000 NOK per *tonne* CO_2. Another analysis combining the optimization of sailing speeds for each route and the removal of safety personnel on hydrogen vessels did, however, result in a far more optimistic average abatement cost of just below 5 000 NOK per *tonne* CO_2. On the other hand, the abatement costs still vary significantly across routes, and routes are typically operated by different operators. Thus, for the average route, a slight increase in the CO_2-tax would help incentivize the transition remarkably. However, for many routes, it still remains very expensive to transition to ZE solutions. Hence, *how* incentives should be provided is perhaps a just as interesting question to ask. For instance, an incentive scheme conditioned on transitioning a whole system of routes to ZE could possibly exploit the lower average abatement cost of 5 000 NOK per *tonne* CO_2.

The Norwegian government recently proposed a regulation for all HSV services to transition to ZE solutions in their next tenders, if possible. An extension of the models was created to analyze the impact of such a regulation. Since the next tenders for the routes generally occur earlier than the ZE requirements occur in the original model, the total costs for the planning horizon are, not surprisingly, much higher compared to the more gradual transition. The total costs increase by 20% over the entire planning horizon of 15 *years*, accounting for approximately 1 500 $MNOK$. However, an interesting observation is that the two solutions result in equally optimal terminal states. This means that the increase in costs virtually can be related to the acceleration of the transition and that it does not have implications beyond the planning horizon. Thus, it remains a question for the decision-makers to value this acceleration, accounting for possible technological improvements that can emerge throughout the period.

To conclude the thesis with its scope and analyses in consideration, some remarks about the future of HSV services can be offered. Although the suggested incentives to accelerate the ZE transition appear to be cost-inefficient under current circumstances, the thesis has shown that holistic planning indeed can alleviate the transition. Co-localization and co-utilization of infrastructure evidently exploit economies of scope, while the inclusion of centralized hydrogen production hubs has shown that also economies of scale can be exploited. Moreover, the considered ZE energy carriers have proved to complement each other well, albeit the results also suggest that it can be valuable to research the possibility and implications of increasing the feasibility of battery-electric and battery-swapping vessels. A positive remark is that the transition has received a considerable amount of attention from both the political atmosphere and the private sector in recent years. Thus, with properly designed incentives and regulations, and sound planning from the relevant decision-makers, the transition may very well be efficient.

Chapter 11

Future Research

This chapter presents suggestions for how this thesis can be extended in future research. Specifically, Section 11.1 presents different ways the Zero-Emission (Passenger) Vessel & Infrastructure Planning Problem (ZEVIPP) can incorporate more features to mimic the real-life problem at hand even more realistically, while Section 11.2 proposes an extension of the solution approach detailed in Chapter 5, Chapter 6, and Chapter 7.

11.1 Extensions of the ZEVIPP

In this section, three possible extensions to the ZEVIPP and its implementation are discussed. These extensions comprise implementing the problem with emerging technology for vessels and infrastructures, allowing vessels to optimize their sailing speeds for different activities, and including external hydrogen supply and demand to the problem.

11.1.1 Improved Technology

As highlighted in Chapter 2, better technology related to HSVs emerges rapidly. Some possible improvements can be higher energy efficiency at high speeds utilizing the new approaches from Fremtidens Hurtigbåt or developments in ZE energy storage capacity. Both of these could improve the range of HSVs and enable battery-electric and battery-swapping vessels to operate more routes. A general finding in Chapter 9 is that routes operated with these energy carriers have considerably lower costs. This model extension could reduce the dependence on hydrogen vessels, and thus, improve the solutions significantly.

This extension could possibly be implemented by enabling new technology whenever one expects it to be available. It could also account for technology development being associated with uncertainty, given that good data for this is obtainable. A proposed way to achieve this is to make the set of available vessel types dependent on the time step and scenario. This ensures that new technology can be available in the future with a certain probability, and strategic decisions are made accounting for the possibility of better technology being available later.

11.1.2 Varying Sailing Speed

Section 9.3.2 demonstrated that optimizing the service speed for each route can reduce costs significantly. In that analysis, the Sub-Problem was solved only using a single sailing speed of either 20, 25, or 30 *knots*. Thus, the Sub-Problem was not solved for varying speeds across sub-routes. Implementing optimization of sailing speed for each sub-route could enable a more granular balance between passenger time and energy costs. Furthermore, with passenger demand

information divided on each sub-route, the effect of varying the sailing speed between sub-routes could give even better results. This was an important part of the route optimization model by Havre, Lien and Ness (2022). Hence, a proposal is to add a version of each activity with each sailing speed to the Sub-Problem and run this with the same MILP-model defined in Chapter 7.

11.1.3 External Hydrogen Supply and Demand

Hydrogen solutions have throughout this thesis been shown to be more costly than for other energy carriers. This is somewhat due to the under-utilization of the hydrogen production infrastructures and the long transportation distances to the most distant filling stations. There are movements in the hydrogen market that are very uncertain and could affect routes forced to be served with hydrogen to a high degree. Using the scenarios, a proposal is to extend the model by incorporating a probability of a hydrogen market emerging outside the scope of this model. This would capture the fact that selling hydrogen to the outside market will reduce the total costs incurred within the system, and could encourage the installation of several hubs, possibly making hubs more locally present to northern filling stations and reducing the abatement costs of these routes substantially.

11.2 Extension of the Solution Approach: Sliding Window

The extensions described in the last section only imply minute modifications to the model and solution method. However, the considered extensions combined could increase the complexity in the model enough to require the Master Problem to be solved with a heuristic solution approach. In Section 9.2.1, a suitable matheuristic is proposed, which would exploit the trait that locally optimized route-serving decisions are often equal or similar on a global level. The algorithm would work as follows. Optimize smaller networks of routes with geographical proximity iteratively along the coastline, starting at one end. Similar to the common sliding-window matheuristic, some routes will have fixed operational decisions when moving to the next region, and the routes closest to the edge of the previous region will be variable when optimizing the next region. For instance, five smaller networks of routes at the size of the small test instance could be used to solve the whole system in $5 \cdot 10.2sec = 51sec$ instead of the $1010sec$ solution time of the large instance. Even though distant routes are faintly connected, the localization of hubs generates interdependencies across large distances. An exact solution to this would be to solve the problem for each permutation of hub installations, which would be viable in cases with few potential hub placements, like in the test instances used here. However, in cases where this is not tractable, an iterative optimization model could be formulated. First, the model is given a set of hub installations. Then, given the route-serving decisions, the hub placements are optimized and the model is run once more with the new set of hubs installed. The iteration terminates when the same set of hub installations is selected as in the previous iteration.

Bibliography

Aarskog, F., Danebergs, J., Strømgren, T., & Ullberg, Ø. (2020). Energy and cost analysis of a hydrogen driven high speed passenger ferry. *Transportation Research Part D: Transport and Environment, 99*.

Atchinson, J. (2021). Ammonia infrastructure: Panel wrap-up from the 2020 ammonia energy conference. Retrieved 14th December 2022, from https://www.ammoniaenergy.org/articles/ammonia-infrastructure/

Berg, V. M., Borgmo, A. K., & Opheim, S. S. (2022). *Infrastructure planning for zero-emission passenger vessel services* [Project thesis, Norwegian University of Science and Technology. Available upon request].

Bjartnes, A., Michelsen, L., & Øvrebø, O. (2021). *Statsbudsjettet: Her er de viktigste klima- og energisakene*. Retrieved 14th December 2022, from https://energiogklima.no/nyhet/statsbudsjettet-her-er-de-viktigste-klima-og-energisakene/

Brandt, T., Wagner, S., & Neumann, D. (2021). Prescriptive analytics in public-sector decision-making: A framework and insights from charging infrastructure planning. *European Journal of Operational Research, 291(1)*.

Brødrene Aa AS. (2017). *Brødrene aa wins contract for three high-speed catamarans*. Retrieved 24th November 2022, from https://www.braa.no/news/brdrene-aa-wins-contract-for-three-high-speed-catamarans

Bunker Oil. (2023). Bunker oil - anlegg kart of info. Retrieved 8th May 2023, from https://www.bunkeroil.no/no/anlegg-kart-og-info/

Cass, P. (1985). An economic analysis of high-speed ferry service. *Naval engineers journal, 97(2)*.

Cole, W., Frazier, A., & Augustine, C. (2021). Cost projections for utility-scale battery storage: 2021. Retrieved 14th December 2022, from https://www.nrel.gov/docs/fy21osti/79236.pdf

Danebergs, J., & Aarskog, F. G. (2020). Future compressed hydrogen infrastructure for the domestic maritime sector. *IFE/E*.

Danebergs, J., Buskop, A., & Fosen, Ø. S. (2023). Charging and bunkering infrastructure for zero emission high-speed vessels. *IFE/E*.

Danebergs, J., Rosenberg, E., Seljom, P. M. S., Kvalbein, L., & Haaskjold, K. (2021). Documentation of ife-times-norway. *2*. Retrieved 14th December 2022, from https://ife.brage.unit.no/ife-xmlui/bitstream/handle/11250/2977095/IFE-E-2021-005.pdf?sequence=1

Danielsen, D. J., Martinsen, M. W., & Kristoffersen, K. J. (2022). Først i verden: Milliardavtalen skal få lofoten-ferger over på hydrogen. Retrieved 15th December 2022, from https://www.nrk.no/nordland/hydrogenferge_-torghatten-og-vegvesenet-skriver-kontrakt-pa-5-milliarder-1.15826581

DNV GL AS Maritime. (2018). Utvikling i fartøystørrelser, motor- og drivstoffteknologi. Retrieved 6th May 2023, from https://www.kystverket.no/contentassets/16d5144075384953b5081095f7e6068c/utvikling-i-fartoystorrelser-motor--og-drivstoffteknologi.pdf/download

DNV GL AS Maritime. (2019). Comparison of alternative marine fuels. Retrieved 6th May 2023, from https://sea-lng.org/wp-content/uploads/2020/04/Alternative-Marine-Fuels-Study_final_report_25.09.19.pdf

Durán-Micco, J., & Vansteenwegen, P. (2022). A survey on the transit network design and frequency setting problem. *Public Transport, 14(1)*. Retrieved 5th June 2023, from https://www.scopus.com/inward/record.uri?eid=2-s2.0-85117257042&doi=10.1007%5C%2fs12469-021-00284-y%5C&partnerID=40%5C&md5=842eeaf77a8af1053b971ba60b102ae1

Elsevier. (2023). *About scopus - abstract and citation database*. Retrieved 20th May 2023, from https://www.elsevier.com/solutions/scopus

Farahani, R. Z., Fallah, S., Ruiz, R., Hosseini, S., & Asgari, N. (2019). Or models in urban service facility location: A critical review of applications and future developments. *European Journal of Operational Research*, *276(1)*.

Fjellstrand AS. (2023). Fjellstrand shipyard - all projects. Retrieved 12th May 2023, from https://fjellstrand.no/all-projects/

Flügel, S., Halse, A. H., Hulleberg, N., Jordbakke, G. N., Veisten, K., Sundfør, H. B., & Kouwenhoven, M. (2020). Verdsetting av reisetid og tidsavhengige faktorer. *TIØRapport*, *1762*.

FuelCellWorks. (2020). *Norse group announces launce of mf hydra, world's first lh2 driven ferry boat.* Retrieved 24th November 2022, from https://fuelcellsworks.com/news/norse-group-announces-launch-of-mf-hydra-worlds-first-lh2-driven-ferry-boat/

Godø, J., & Kramer, J. (2019). Batteridrift på alle hurtigbåtruter i trøndelag. rapport fra utviklingskontrakt for fremtidens hurtigbåt (in norwegian).

Google. (2023). *About google scholar*. Retrieved 19th May 2023, from https://scholar.google.com/intl/en/scholar/about.html

Greensight. (2021). Maritime energy density. https://www.greensight.no/insights/maritime-energy-density

Hancke, R., Danebergs, J., Kvalbein, L., & Aarskog, F. (2020). Efficient hydrogen infrastructure for bus fleets: Evaluation of slow refueling concept for bus depots and estimates of hydrogen supply cost. *IFE/E*.

Havre, H. F., Lien, U., & Ness, M. M. (2022). *Network design for zero emission passenger vessel services* (Master's thesis). Norwegian University of Science and Technology.

Havre, H. F., Lien, U., Ness, M. M., Fagerholt, K., & Rødseth, K. L. (2022). Cost-effective planning and abatement costs of battery electric passenger vessel services. *Transportation Research Part D: Transport and Environment*, *113*.

He, Y., Liu, Z., & Song, Z. (2022). Integrated charging infrastructure planning and charging scheduling for battery electric bus systems. *Transportation Research Part D: Transport and Environment*, *111*.

Hoff, A., Andersson, H., Christiansen, M., Hasle, G., & Løkketangen, A. (2010). Industrial aspects and literature survey: Fleet composition and routing. *Computers & Operations Research*, *37(12)*.

Ianssen, C., Sandblost, T., & Lanssen, E. (2017). Battery/fuel cell fast ferry. *Trondheim/Sandtorg*.

Iliopoulou, C., & Kepaptsoglou, K. (2019). Integrated transit route network design and infrastructure planning for on-line electric vehicles. *Transportation Research Part D: Transport and Environment*, *77*. Retrieved 5th June 2023, from https://www.scopus.com/inward/record.uri?eid=2-s2.0-85074570770&doi=10.1016%5C%2fj.trd.2019.10.016%5C&partnerID=40%5C&md5=c6c514f9e595a7f38232ad994879af1d

IMO. (2016). Sulphur oxides (sox) and particulate matter (pm)–regulation 14. *MARPOL Annex VI, MEPC*. Retrieved 6th May 2023, from https://www.imo.org/en/OurWork/Environment/Pages/Sulphur-oxides-(SOx)-%5C%E2%5C%80%5C%93-Regulation-14.aspx

IMO. (2020). Fourth imo ghg study 2020: Full report.

Jafarzadeh, S., Ladstein, J., Zenith, F., Ødegår, A., Sundseth, K., Ortiz, M., & Høyli, R. (2021). Elektrifisering av kystfiskeflåten ved bruk av batterier og brenselceller. *Sintef Ocean Rapport*, *2021:00632*.

Karimi, S., Zadeh, M., & Suul, J. A. (2020). Shore charging for plug-in battery-powered ships: Power system architecture, infrastructure, and control. *IEEE Electrification Magazine*, *8(3)*.

Klier, M., & Haase, K. (2015). Urban public transit network optimization with flexible demand. *OR Spectrum*, *37(1)*. Retrieved 5th June 2023, from https://www.scopus.com/inward/record.uri?eid=2-s2.0-84958754262&doi=10.1007%5C%2fs00291-014-0377-4%5C&partnerID=40%5C&md5=46d0574683f6b58f7bff4631c8910a3c

Lee, J., Shon, H., Papakonstantinou, I., & Son, S. (2021). Optimal fleet, battery, and charging infrastructure planning for reliable electric bus operations. *Transportation Research Part D: Transport and Environment*, *100*.

Londoño, A., & Granada-Echeverri, M. (2019). Optimal placement of freight electric vehicles charging stations and their impact on the power distribution network. *International Journal of Industrial Engineering Computations*, *10(4)*. Retrieved 5th June 2023, from https://www.

scopus.com/inward/record.uri?eid=2-s2.0-85067571982&doi=10.5267%5C%2fj.ijiec.2019.3.002%5C&partnerID=40%5C&md5=5d1e486d72af8827d75a0aa6564415d5

Miljødirektoratet. (2020). *Tabeller for omregning fra energivare til utslipp*. Retrieved 25th April 2023, from https://www.miljodirektoratet.no/ansvarsomrader/klima/for-myndigheter/kutte-utslipp-av-klimagasser/klima-og-energiplanlegging/tabeller-for-omregning-fra-energivarer-til-kwh/

NEL Hydrogen. (2022). Nel hydrogen. Retrieved 14th December 2022, from https://nelhydrogen.com/

Next Wave. (2021). *Hydrogen transport from large-scale production points to nordic consumers*. Retrieved 25th November 2022, from https://www.nordichydrogenpartnership.com/wp-content/uploads/2021/11/Next-Wave-D2_4-Large-scale-H-transport.pdf

Norwegian Ministry of Transport & Norwegian Ministry of Climate and Environment. (2019). Plan for fossilfri kollektivtrafikk i 2025. Retrieved 14th December 2022, from https://www.regjeringen.no/contentassets/383ec46d92b54c02af488558e2dbe0c1/handlingsplan-for-fossilfri-kollektivtransport.pdf

Norwegian Ministry of Transport, Norwegian Ministry of Climate and Environment, Norwegian Ministry of Finance, Norwegian Ministry of Local Government and Regional Development, Norwegian Ministry of Trade, Industry and Fisheries, Norwegian Ministry of Petroleum and Energy & Norwegian Ministry of Foreign Affairs. (2019). Regjeringens handlingsplan for grønn skipsfart. Retrieved 14th December 2022, from https://www.regjeringen.no/contentassets/2ccd2f4e14d44bc88c93ac4effe78b2f/handlingsplan-for-gronn-skipsfart.pdf

Pantuso, G., Fagerholt, K., & Hvattum, L. M. (2014). A survey on maritime fleet size and mix problems. *European Journal of Operational Research*, *235(2)*.

Patil, P., Kazemzadeh, K., & Bansal, P. (2023). Integration of charging behavior into infrastructure planning and management of electric vehicles: A systematic review and framework. *Sustainable Cities and Society*, *88*.

Regjeringen. (2022). *Karbonprisbaner for bruk i samfunnsøkonomiske analyser*. Retrieved 25th April 2023, from https://www.regjeringen.no/no/tema/okonomi-og-budsjett/statlig-okonomistyring/karbonprisbaner-for-bruk-i-samfunnsokonomiske-analyser/id2878113/

Regjeringen. (2023). Forsterket innsatsfordeling 2021-2030. Retrieved 18th April 2023, from https://www.regjeringen.no/no/sub/eos-notatbasen/notatene/2021/aug/forsterket-innsatsfordeling-2021-2030/id2878385/

Reis Nordland. (2022). *Her er en oversikt over alle rutetabeller for hurtigbåt i nordland*. Retrieved 4th December 2022, from https://www.reisnordland.no/rutetabeller-hurtigbt

Roni, M. S., Yi, Z., & Smart, J. G. (2019). Optimal charging management and infrastructure planning for free-floating shared electric vehicles. *Transportation Research Part D: Transport and Environment*, *76*.

SEAM. (2021). Norled partners up with seam for development of innovative battery system. Retrieved 15th December 2022, from https://seam.no/norled-partners-up-with-seam-for-development-of-innovative-battery-system/

Ship-Technology. (2015). *Ampere electric-powered ferry*. Retrieved 24th November 2022, from https://www.ship-technology.com/projects/norled-zerocat-electric-powered-ferry/

Skipsrevyen. (2021). Skal utvikle hydrogendrevet hurtigbåt. Retrieved 3rd December 2022, from https://www.skipsrevyen.no/hurtigbat-hydrogen/skal-utvikle-hydrogendrevet-hurtigbat/1117158

Skipsrevyen. (2022). Ms «medstraum» er ship of the year. Retrieved 3rd December 2022, from https://www.skipsrevyen.no/medstraum-ms-medstraum-ship-of-the-year/ms-medstraum-er-ship-of-the-year/1426888

Slette, H. T., Asbjørnslett, B. E., Fagerholt, K., Lianes, I. M., & Noreng, M. T. (2023). Effective utilization of service vessels in fish farming: Fleet design considering the characteristics of the locations. *Aquaculture International*, *31(1)*.

SSB. (2021). Økning i antall ladestasjoner for ferjer og anlegg for landstrøm. Retrieved 15th December 2022, from https://www.ssb.no/transport-og-reiseliv/sjotransport/artikler/okning-i-antall-ladestasjoner-for-ferjer-og-anlegg-for-landstrom

Štádlerová, Š., Aglen, T. M., Hofstad, A., & Schütz, P. (2022). Locating hydrogen production in norway under uncertainty. *Computational Logistics: 13th International Conference, ICCL 2022, Barcelona, Spain, September 21–23, 2022, Proceedings*.

Štádlerová, Š., Jena, S. D., & Schütz, P. (2023). Using lagrangian relaxation to locate hydrogen production facilities under uncertain demand: A case study from norway. *Computational Management Science*, *20(1)*.

Štádlerová, Š., & Schütz, P. (2021). Designing the hydrogen supply chain for maritime transportation in norway. *Computational Logistics: 12th International Conference, ICCL 2021, Enschede, The Netherlands, September 27–29, 2021, Proceedings 12*.

Stålhane, M., Halvorsen-Weare, E. E., Nonås, L. M., & Pantuso, G. (2019). Optimizing vessel fleet size and mix to support maintenance operations at offshore wind farms. *European Journal of Operational Research*, *276(2)*.

Statens Vegvesen. (2022). Markedsoversikt for ferje. Retrieved 15th December 2022, from https://www.vegvesen.no/globalassets/fag/trafikk/ferje/markedsoversikt-ferje-per-1-januar-2022.pdf

Statens Vegvesen and Kollektivtrafikkforeningen. (2022). *Markedsoversikt båt og ferje 2022*. Retrieved 25th May 2023, from https://kollektivtrafikk.no/innsikt/markedsoversikt-sjo/

Statnett. (2023). *Langsiktig markedsanalyse norge, norden og europa 2022-2050*. Retrieved 25th April 2023, from https://www.statnett.no/globalassets/for-aktorer-i-kraftsystemet/planer-og-analyser/lma/langsiktig-markedsanalyse-2022-2050.pdf

Sundvor, I., Thorne, R. J., Danebergs, J., Aarskog, F., & Weber, C. (2021). Estimating the replacement potential of norwegian high-speed passenger vessels with zero-emission solutions. *Transportation Research Part D: Transport and Environment*, *99*.

The Explorer. (2022). Hydrogen fast ferry for zero-emission passenger transport. Retrieved 15th December 2022, from https://www.theexplorer.no/solutions/hydrogen-fast-ferry-for-zero-emission-passenger-transport/

The Research Council of Norway. (2021). *Zevs: Enabling zero emission passenger vessel services*. Retrieved 25th November 2022, from https://prosjektbanken.forskningsradet.no/en/project/FORISS/320659

Trygstad, A. N. (2022). Offensive hydrogenplaner etter fergenyhet: – stort for norge. Retrieved 15th December 2022, from https://www.nrk.no/nordland/30_40-hydrogen-prosjekt-i-gang-_-sintef-mener-hydrogen-er-vesentlig-for-norge-etter-oljen-1.15242119

Turkoglu, D. C., & Genevois, M. E. (2020). A comparative study of service facility location problems. *Annals of Operations Research*, *292*.

Tveit, J. B. N., Fjørtof, M., Balgaard, T., & Haukenes, E. (2023). *Vil krevje nullutslepp for hurtigbåtar innan to år*. Retrieved 11th May 2023, from https://www.nrk.no/mr/regjeringa-foreslar-nullutsleppskrav-for-hurtigbatar-innan-2025-og-for-ferjer-so-raskt-som-rad-1.16403211

Tveter, E., Rødseth, K., Rødal, J., Hoff, K., & Thune-Larsen, H. (2020). Forslag til nye kriterier for båter i inntektssystemet for fylkeskommunene. *MFM Rapport*, *2003*.

Ulleberg, Ø., & Hancke, R. (2020). Techno-economic calculations of small-scale hydrogen supply systems for zero emission transport in norway. *International journal of hydrogen energy*, *45(2)*.

Villa, D., Montoya, A., & Herrera, A. M. (2020). The electric riverboat charging station location problem. *Journal of Advanced Transportation*, *2020*.

Wang, D. Z., & Lo, H. K. (2008). Multi-fleet ferry service network design with passenger preferences for differential services. *Transportation Research Part B: Methodological*, *42(9)*.

Yara International ASA. (2022). *Yara birkeland*. Retrieved 24th November 2022, from https://www.yara.com/news-and-media/media-library/press-kits/yara-birkeland-press-kit/

Zhang, L., Zeng, Z., & Qu, X. (2021). On the role of battery capacity fading mechanism in the lifecycle cost of electric bus fleet. *IEEE Transactions on Intelligent Transportation Systems*, *22(4)*.

Appendix A

Bunkering Price Derivations

It is assumed that the MGO price already factors in the complexity of production and inventory management. The bunkering price of MGO does however also include a CO_2 tax. For the "energy-producing" infrastructure archetypes energy is "produced" in terms of electricity being converted to usable energy for the respective compatible energy carriers. Hence, electricity price and energy conversion efficiency are components of the bunkering prices at these infrastructures. As hydrogen filling stations are supplied with hydrogen from the hubs by tube trailers, the energy price of these also includes an additional transportation cost per $kWh\ km$ delivered from the hubs.

Infrastructure Archetype	**Main Characteristics**	**Bunkering Price Components**
MGO Filling Station	Supports bunkering	MGO price CO_2 tax
Hydrogen Filling Station		Electricity price Energy conversion efficiency Distribution cost
Large-Scale Hydrogen Production Hub	Energy-producing	
Local Hydrogen Production Facility	Energy-producing Supports bunkering	Electricity price Energy conversion efficiency
Battery Bank Charger		
Battery Swap System		

Table A.1: Summary of infrastructure archetypes

Appendix B

Problem Example Solution

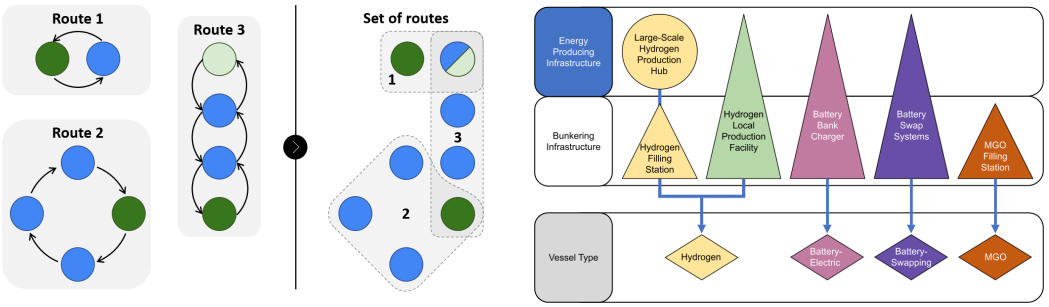

(a) Example set of routes

(b) Compatibility between infrastructures and vessel types

Figure B.1: Figure conventions used in Figure B.2

To start the walkthrough of the problem example solution provided in Figure B.2, some notation is explained. The set of routes to operate is the same as in Figure B.1a and the respective routes will be referred to accordingly, i.e., Route 1/2/3. Next, the colored diamonds and triangles represent vessels and infrastructures, respectively, and follow the same convention as in Figure B.1b. I.e., a brown diamond represents an MGO-driven vessel and a brown triangle represents an MGO filling station; a purple diamond represents a battery-electric vessel and a purple triangle represents a battery bank charger; a yellow diamond represents a hydrogen-driven vessel and a yellow triangle represents a hydrogen filling station. Top-most in the figure there is a time bar where the different ZE restrictions are represented by blue circles. E.g., one can see that between 2026 and 2030 the total ZE energy consumption has to account for at least 25% of the total energy consumption. The blue split arrow represents the scenario tree of the problem. I.e., when the arrow is split it means that new information about the problem is revealed, but this information may be represented by several scenarios. Prior to the split, it is uncertain what scenario will happen. The white arrows on top of the blue arrow represent the time steps of the long-term planning horizon. These time steps do in turn represent one short-term planning period (of one operating day) each. The strategic decisions, i.e., the investments, are illustrated above the time step arrows. The tactical decisions, i.e., the fleet and infrastructure allocation, are illustrated below and at the beginning/end of the time step arrows.

Now the notation is introduced, the step-by-step explanation of the problem solution can begin. In this example problem, the long-term planning horizon spans 9 years, beginning in 2023 and ending in 2032. This planning horizon is granulated into time steps of 3 years. Left-most in the figure, one can see that the problem is initialized with a vessel fleet solely consisting of MGO-driven vessels and consequently only MGO stations. Route 1 has a bunkering port in its main port and has one vessel operating it. Route 2 and Route 3 both have a bunkering port in their intersecting main

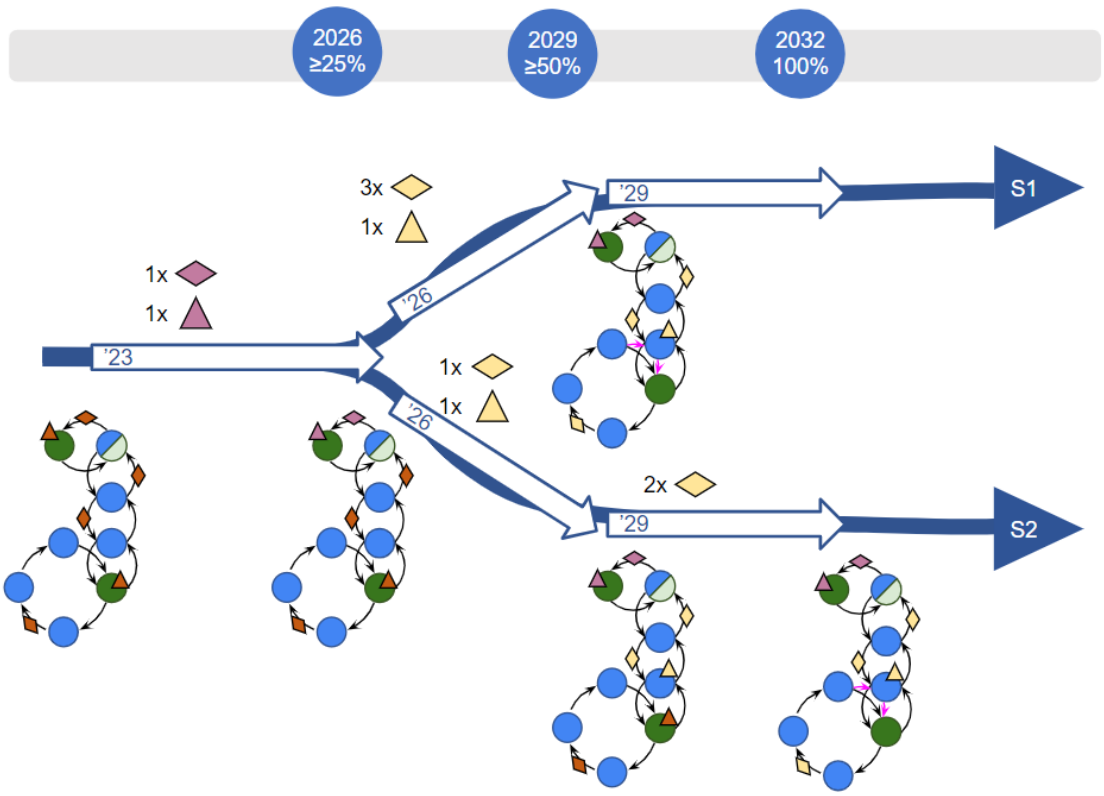

Figure B.2: Illustration of a solution of the ZEVIPP

port, while Route 2 is operated by one vessel and Route 3 is operated by two vessels.

Noting that from 2026 the total ZE energy consumption has to account for at least 25% of the total energy consumption, it is decided in the first time step (end of 2023 to the end of 2026) to invest in one battery-electric vessel and a battery bank charger. At the end of the time step (end of the white arrow), one can see that these investments replace the MGO-driven vessel and MGO station in Route 1 directly. For Route 2 and Route 3, there are no changes during the time step.

At the end of the first time step, new information about the problem is revealed and it is split into two possible scenarios denoted S1 and S2. In S1, it is invested in three hydrogen vessels and one hydrogen filling station in the second time step. At the end of the time step, one can see that these investments convert the entire fleet to being ZE, despite the ZE requirements only being 50%. The reason why can for instance be that the electricity price is sufficiently low and the CO_2 and/or MGO price is sufficiently high in the scenario, to make the conversion cost-efficient. After the investments, both Route 2 and Route 3 have also changed their bunkering port. However, they still share the bunkering port. Note that this bunkering port is no longer one of Route 2's original ports, so vessels operating Route 2 need to do a *detour* from the route whenever they bunker. This detour is denoted by pink arrows. Ultimately, in the third and last time step, no changes are made as the vessel fleet has already completed the ZE transition.

In S2, it is invested in one hydrogen vessel and a hydrogen filling station in the second time step. Comparing it to the decisions in the same time step in S1, it is a sign that the electricity price is not sufficiently low and the CO_2 and/or MGO price is not sufficiently high in the scenario to make ZE conversion cost-efficient. As a consequence, Route 3 changes its bunkering port, while the operation of Route 2 is not changed. In the third and last time step, there is invested in two more hydrogen vessels. Thus, the two scenarios end up in the same state.

Appendix C

Generation of Route-Serving Permutations

The potential route-serving permutations for each route are determined by pairing vessel types and potential bunkering alternatives for the given route. Only bunkering alternatives and vessel types operating with the same energy carrier are paired. If there are multiple vessels of an energy carrier and many bunkering alternatives, the number of sub-problem grows quickly. However, the set of potential permutations is filtered using heuristics that are detailed in Chapter 7.

How bunkering alternatives are generated is exemplified in Figure C.1. Here, there are two candidate bunkering ports, where port p_1 can have a hydrogen filling station, local hydrogen production, electric charging, and battery-swapping infrastructure, while the only feasible infrastructure at p_2 is a hydrogen filling station. When the bunkering alternatives are generated, only infrastructures of the same energy carrier may be combined in one bunkering alternative since only one vessel type is selected. Therefore, the hydrogen filling station at p_2 is only paired with hydrogen infrastructures at p_1.

Note that there may exist multiple candidate infrastructures of the same archetype which increases the number of bunkering alternatives quickly. Therefore, the problem is not suited for input with a large number of infrastructures of each archetype, but a few variations of each archetype is needed to provide some flexibility to the model.

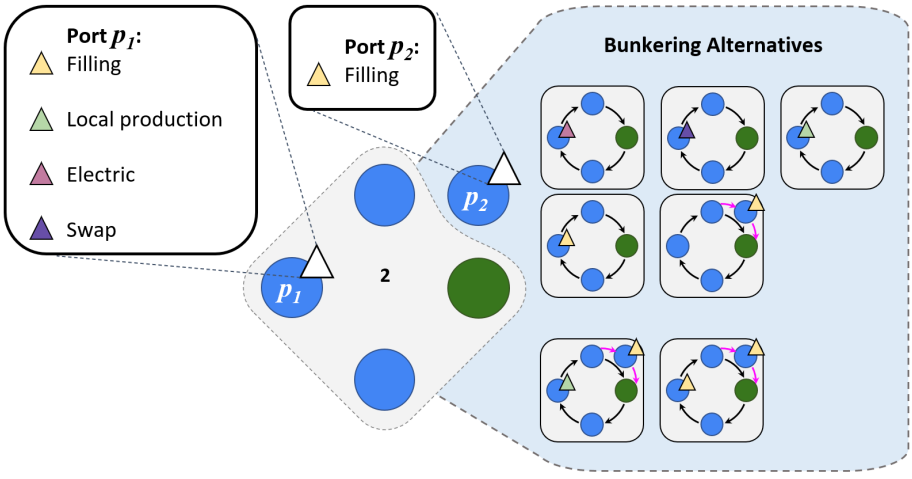

Figure C.1: The bunkering alternatives generated for a route that may bunker at two bunkering ports. Each port has a set of potential infrastructures.

Appendix D

Remaining Modeling Approaches in the Sub-Problem

D.1 Energy

The energy level on the vessels must always be within the vessel type's energy bounds. This restriction has to be maintained throughout each activity, even if an activity allows for bunkering several times. In practice, this means that the bunkering amount is restricted every time a vessel bunkers, given the difference between the energy level upon arrival at the bunkering port and the vessel's upper energy bound. Additionally, it has to bunker enough to reach the next bunkering port using only its *available energy*. Available energy denotes the current energy level less the lower bound of the vessel.

Three terms are introduced in the model; *energy usage*, *energy required* to initiate an activity, and *energy required to sail the last leg*. These terms are precalculated for each activity during the activity generation. The first term gives the energy used when sailing during the activity. The second gives the available energy required to either reach the first bunkering port in the activity or to conduct the activity and then sail to a bunkering port. Lastly, the latter denotes the amount of energy consumed from sailing the last *leg* before reaching a bunkering port. Here, a leg denotes traveling from one bunkering port or resting port to the next.

Activities that serve routes are sailing with passengers on board, and thus, incur passenger costs. This means that energy bunkered during a route-serving activity will incur passenger costs as well. Hence, the energy bunkered while passengers are on board is managed separately from the total energy bunkered.

Further on, energy can be bunkered at different bunkering rates. This could be due to differing infrastructures at different bunkering ports or due to the on-shore storage being emptied. The first is handled by separating the energy bunkered from each port. The second is handled by separating the energy bunkered before and after emptying the on-shore energy storage. The amount that a vessel could bunker before the on-shore storage is emptied is denoted the *bunkering threshold*. One might look at this as the perceived on-shore storage from the vessel's perspective. *The rest of this paragraph is quite technical and can be skipped without losing the thread.* First, a bunkering infrastructure is assumed to produce energy at the *effective production rate* and bunker energy at the *bunkering rate* simultaneously. The effective production rate denotes the rate of energy that is actually filling the infrastructure's storage, which is less than the energy consumption rate due to energy loss. The bunkering rate is the rate at which a vessel is filled from the infrastructure. If the effective production rate is higher than or equal to the bunkering rate, a vessel could bunker indefinitely. However, if it is lower, then the on-shore storage is emptied at a rate of the bunkering rate less the effective production rate. The bunkering threshold is equal to the time it takes to empty the on-shore storage multiplied by the bunkering rate. This holds under the assumption that the on-shore storage is at capacity whenever bunkering is initiated.

The decomposition of energy bunkered is illustrated in Figure D.1. Total energy bunkered is equal to both the energy bunkered before and after emptying the on-shore storage and the energy bunkered with and without passengers.

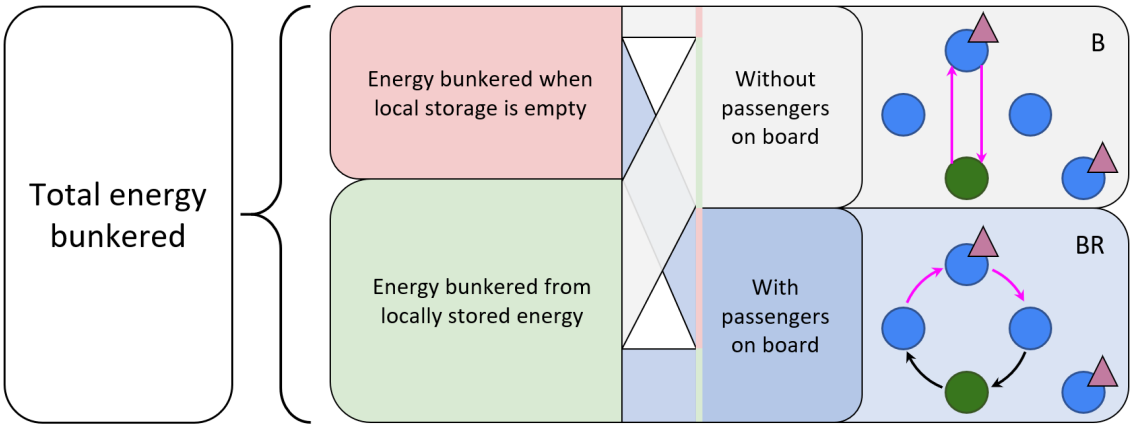

Figure D.1: Given a vessel, activity slot, and bunkering port, there are several ways to bunker energy. All of which influence either the costs or time spent bunkering.

D.2 Time

The short-term planning period of one day is divided into time periods. As given by the problem definition in Chapter 3, the time schedule should be maintained in the ZE solution. In order to reduce the granularity of the time schedule, however, the demanded sub-route servings are assigned a time period within which they should be served. This gives a demanded frequency of each sub-route for each time period. Figure D.2 illustrates how the demanded frequencies might be gathered in time period frequencies. It shows a route comprised of four sub-routes and how many times each sub-route should be served each time period.

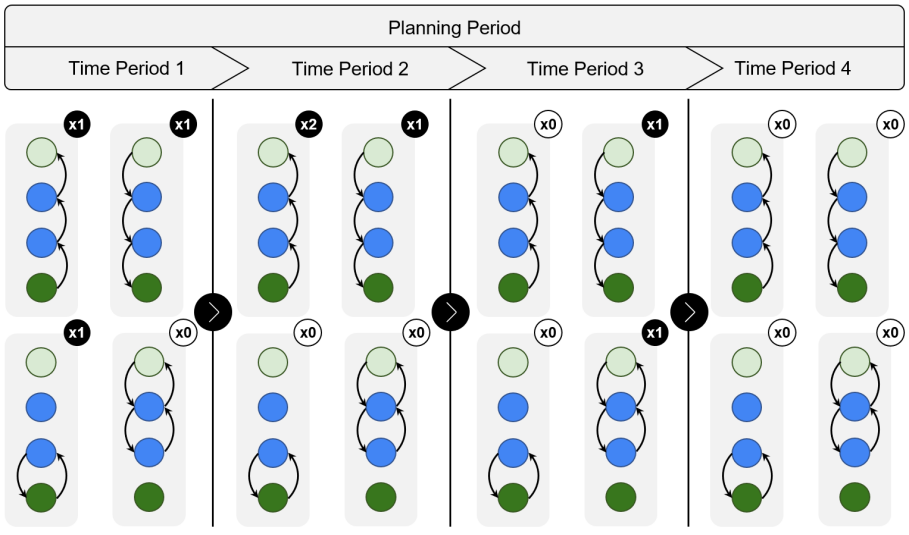

Figure D.2: Example of how the demanded sub-route servings are gathered in time period frequencies.

Each activity conducted in a time period has to start and end within the six-hour period of the time period. The start time of each activity slot is tracked and has to start later than the time the last activity slot ended its activity. The ending of an activity slot is given by its starting time

and the sum of time spent during its selected activity. The latter can be calculated by summing the sailing time of the activity and the time related to bunkering, as shown in Figure D.3. The bunkering time can be divided into *bunkering overhead time* and *variable bunkering time*. The former denotes the time spent initiating and ending the bunkering process and is only variable to the number of times an activity initiates bunkering. In contrast, the latter denotes the time spent bunkering which is variable to the amount of energy bunkered.

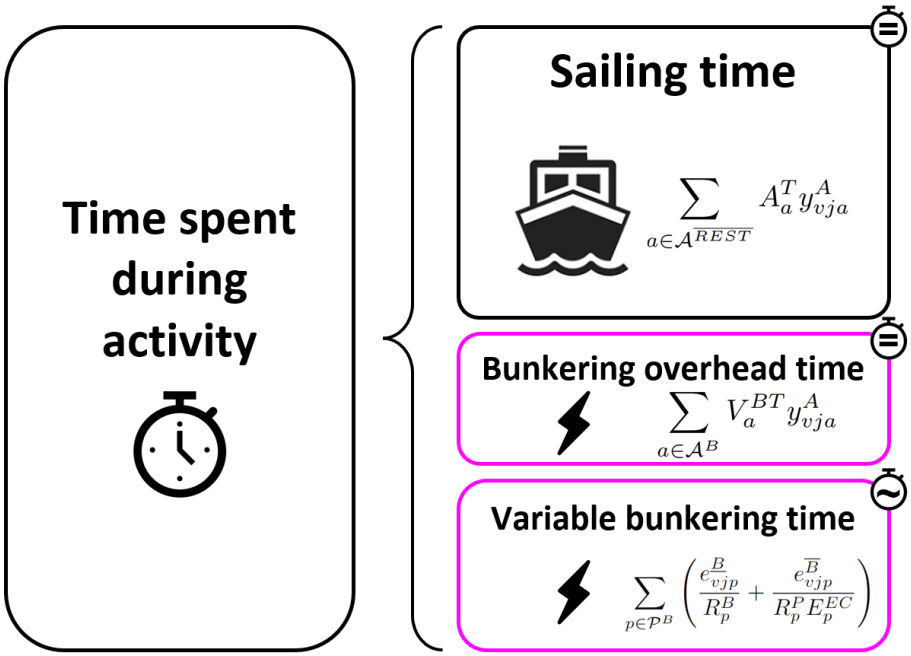

Figure D.3: Factors for calculating the time spent during an activity. For resting activities, the time spent is 0, and for route-serving activities that do not bunker, the time spent is equal to the sailing time.

D.3 Location

The vessels have to conduct an activity that starts in the same resting port as where the selected activity in the previous activity slot ended. Moreover, it is assumed that the vessels must start and end the short-term planning period in the same port, ensuring that a solution is feasible for the next day as well. Furthermore, it is assumed that at least one vessel starts at the main port. The other vessels, if any, may start in any resting port. This ensures that the model is flexible to route types where a route might be designed for a set of vessels starting in different ports.

Bunkering rates and energy costs may differ by location. For a given bunkering alternative, each bunkering port is assigned a single bunkering infrastructure, meaning that the model can uniquely define which infrastructure is installed at each bunkering port. Thus, the bunkering rate, production rate, energy conversion efficiency, and energy price can be determined by port. The former three may differ for different infrastructures. The latter, however, may differ based on both the selected infrastructure and the location of the bunkering port. This is due to energy conversion efficiency and energy usage during filling differing between infrastructures, and because of differing distances from a hub to a filling station.

D.4 Filtering Route-Serving Permutations

In order to minimize the running time of the model, measures are made to reduce the number of Sub-Problems solved. First, a Sub-Problem is solved only if the energy required to serve

each sub-route is less than the maximum available energy at the vessel. This is a simple check and ensures that little time is spent on infeasible Sub-Problems. Second, only vessel types that have a passenger capacity close to the passenger demand of the route are evaluated. Third, a route-serving permutation's infrastructure(s) and vessel type have to operate with the same energy carrier. Fourth, increasing the number of bunkering ports included in the same bunkering alternative increases the number of possible bunkering permutations considerably. Thus, bunkering alternatives that consider more than one bunkering port is manually selected and will only be available for longer routes, which are infeasible when solved for bunkering alternatives with a single bunkering port. Finally, it is assumed that it is optimal to use as few vessels as possible. This is motivated by the increased investment costs and crew shift costs dominating the reduction in passenger costs. Each Sub-Problem is therefore solved iteratively, incrementing the number of vessels until feasibility is reached.

D.5 Modeling Choice

Berg et al. (2022) solved the sub-problem by reducing it to a SPPRC and using a DP algorithm to find the shortest path giving the solution. This solution was viable for the problems solved in that paper, but it did have some drawbacks that a MILP would handle better. For instance, a MILP is able to decide how much is bunkered in every bunkering activity and may decide the optimal amount of energy to start and end the short-term planning period. This was not possible in the SPPRC and creating a MILP did initially show low running times, and was selected in the final modeling approach.

Appendix E

Compact Mathematical Formulation of the Master Problem

E.1 Notation

Sets

$\mathcal{R}$	Set of routes
$\mathcal{R}_b$	Set of routes with feasible Sub-Problems for bunkering alternative b, $\mathcal{R}_b \subseteq \mathcal{R}$
$\mathcal{P}$	Set of ports
$\mathcal{P}_b$	Set of ports which are considered in bunkering alternative b
$\mathcal{B}_r$	Set of candidate bunkering alternatives for route r.
$\mathcal{B}_{pi}$	Set of bunkering alternatives where infrastructure i is installed at port p
$\mathcal{I}_p$	Set of candidate infrastructures at port p
$\mathcal{I}_p^{ZE}$	Set of candidate ZE infrastructures at port p
$\mathcal{I}_p^{E}$	Set of candidate electric charging infrastructures at port p, $\mathcal{I}_p^E \subseteq \mathcal{I}_p$
$\mathcal{I}_p^{S}$	Set of candidate battery-swapping infrastructures at port p, $\mathcal{I}_p^S \subseteq \mathcal{I}_p$
$\mathcal{I}_p^{HUB}$	Set of candidate large-scale hydrogen production hubs at port p, $\mathcal{I}_p^{HUB} \subseteq \mathcal{I}_p$
$\mathcal{I}_p^{LP}$	Set of local hydrogen production infrastructures at port p, $\mathcal{I}_p^{LP} \subseteq \mathcal{I}_p$
$\mathcal{I}_p^{F}$	Set of hydrogen filling stations at port p, $\mathcal{I}_p^F \subseteq \mathcal{I}_p$
$\mathcal{I}_p^{B}$	Set of candidate bunkering infrastructures at port p, $\mathcal{I}_p^B = \mathcal{I}_p \backslash \mathcal{I}_p^{HUB}$
$\mathcal{I}_p^{GC}$	Set of candidate grid-consuming infrastructures at port p, $\mathcal{I}_p^{GC} = \mathcal{I}_p \backslash \mathcal{I}_p^F$
$\mathcal{I}_p^{SC}$	Set of candidate self-consuming bunkering infrastructures at port p, $\mathcal{I}_p^{SC} = \mathcal{I}_p^{GC} \cap \mathcal{I}_p^B$
$\mathcal{V}$	Set of vessel types
$\mathcal{V}^{ZE}$	Set of ZE vessel types

$\mathcal{V}^C$	Set of conventional vessel types
$\mathcal{V}_{rb}$	Set of feasible vessel types for a route r given a bunkering alternative b
$\mathcal{V}_{rb}^C$	Set of feasible conventional vessel types for a route r given a bunkering alternative b
$\mathcal{V}_{rb}^{ZE}$	Set of feasible ZE vessel types for a route r given a bunkering alternative b
$\mathcal{T}$	Set of time steps
$\mathcal{T}^{NS}$	Set of first-stage time steps
$\mathcal{S}$	Set of scenarios

Parameters

Parameters precalculated by solving the Sub-Problems

C_{rbvt}^{Os}	Running costs for operating route r with bunkering alternative b and vessel type v. Includes energy costs, passenger costs, and vessel Operational Expenditures (OPEX)
N_{rbvt}^{Vs}	Number of vessels used for serving route r with bunkering alternative b, and vessel type v
E_{rbvpt}^{Us}	Energy consumption at port p when operating route r with bunkering alternative b and vessel type v
T_{rbvpt}^{Us}	Time spent bunkering at port p when operating route r with bunkering alternative b and vessel type v

General

N^H	Number of hours in the short-term planning period
P^s	Likelihood of scenario s to occur
$\overline{E}_t^C$	Conventional energy budget in time step t
R^E	Ratio between peak weekly load and average daily energy consumption
N^D	Number of days in a time step

Vessels

X_v	The number of initially available vessels of type v
C_v^{VI}	Daily cost of investing in one vessel of type v for the duration of its lifetime
L_v^V	Investment latency for vessel of type v

Infrastructure

Y_{pi}^I	Binary parameter taking the value 1 if infrastructure i is available at port p, and 0 otherwise
Q_i^S	Energy storage capacity for infrastructure i
C_i^{II}	Daily costs of investing in infrastructure i for the duration of its lifetime

R_i^P	Maximum energy production rate for infrastructure i
E_i^{CE}	Energy conversion efficiency for infrastructure i
C^{HT}	Cost of transporting hydrogen (from hub to filling station) per km and kWh
$\Delta D_{p\hat{p}}^{F2H}$	Extra distance above minimum from port p to port $\hat{p}$
R_i^B	Bunkering rate for infrastructure i
U^F	Upper bound for the utilization of infrastructures
L_i^I	Investment latency for infrastructure i

Grid

Q_p^{GA}	Available grid capacity at port p without expanding the grid
$\overline{Q}_p^G$	The upper bound for grid capacity expansion at a port p
C_p^{IG}	Daily cost per MW for expanding the grid capacity at port p for the duration of its lifetime
L_p^G	Investment latency for grid capacity at port p

Variables

y_{rbvt}^s	Binary variable which takes the value 1 if route r is served by vessel type v using bunkering alternative b in time step t and scenario s, and 0 otherwise
y_{pit}^{Is}	Binary variable which takes the value 1 if the infrastructure i is installed at port p in time step t and scenario s, and 0 otherwise
$\tilde{y}_{pit}^{Is}$	Binary variable which takes the value 1 if it is determined in time step t to invest in infrastructure i at port p in scenario s, and 0 otherwise
q_{pt}^{GAs}	Amount of grid capacity available at port p at time step t and in scenario s. The available grid capacity in the initial time step is equal to Q_p^{GA}
$\tilde{q}_{pt}^{GAs}$	Determined amount of grid capacity invested at port p at time step t in scenario s
x_{vt}^s	Number of vessels of type v available in time step t and scenario s
$\tilde{x}_{vt}^s$	Determined number of ZE vessels of type v invested in time step t and scenario s
e_{pit}^{Ps}	Amount of energy produced at port p with the grid-consuming infrastructure i in time step t and scenario s
$e_{pi\hat{p}\hat{i}t}^{Hs}$	Amount of energy produced at the hub location $\hat{p}$ by the hub $\hat{i}$ which is allotted to port p where hydrogen filling station i is installed in time step t and scenario s

E.2 Objective Function

$$\min \quad z = \sum_{t\in\mathcal{T}}\sum_{s\in\mathcal{S}} P^s N^D z_t^s \tag{E.1}$$

$$\begin{aligned} z_t^s = &\sum_{p\in\mathcal{P}}\sum_{i\in\mathcal{I}_p^{ZE}} C_i^{II} y_{pit}^{Is} + \sum_{p\in\mathcal{P}} C_p^{IG}(q_{pt}^{GAs} - Q_p^{GA}) \\ &+ \sum_{v\in\mathcal{V}} C_v^{VI} x_{vt}^s + \sum_{r\in\mathcal{R}}\sum_{b\in\mathcal{B}_r}\sum_{v\in\mathcal{V}_{rb}} C_{rbvt}^{Os} R^E y_{rbvt}^s \\ &+ \sum_{p\in\mathcal{P}}\sum_{i\in\mathcal{I}_p^F}\sum_{\hat{p}\in\mathcal{P}}\sum_{\hat{i}\in\mathcal{I}_{\hat{p}}^{HUB}} C^{HT}\Delta D_{p\hat{p}}^{F2H} R^E e_{pi\hat{p}\hat{i}t}^{Hs} \end{aligned} \tag{E.2}$$

$$, t\in\mathcal{T}, s\in\mathcal{S}$$

E.3 Constraints

Logical investment constraints

$$\sum_{b\in\mathcal{B}_r}\sum_{v\in\mathcal{V}_{rb}} y_{rbvt}^s = 1, \qquad r\in\mathcal{R}, t\in\mathcal{T}, s\in\mathcal{S} \tag{E.3}$$

$$\sum_{i\in\mathcal{I}_p^{LP}\cup I_p^{HUB}} y_{pit}^{Is} \le 1, \qquad p\in\mathcal{P}, t\in\mathcal{T}, s\in\mathcal{S} \tag{E.4}$$

$$\sum_{i\in\mathcal{I}_p^{LP}\cup\mathcal{I}_p^{F}} y_{pit}^{Is} \le 1, \qquad p\in\mathcal{P}, t\in\mathcal{T}, s\in\mathcal{S} \tag{E.5}$$

$$\sum_{i\in\mathcal{I}_p^{E}} y_{pit}^{Is} \le 1, \qquad p\in\mathcal{P}, t\in\mathcal{T}, s\in\mathcal{S} \tag{E.6}$$

$$\sum_{i\in\mathcal{I}_p^{S}} y_{pit}^{Is} \le 1, \qquad p\in\mathcal{P}, t\in\mathcal{T}, s\in\mathcal{S} \tag{E.7}$$

$$\sum_{i\in\mathcal{I}_p\setminus\mathcal{I}_p^{ZE}} y_{pit}^{Is} \le 1, \qquad p\in\mathcal{P}, t\in\mathcal{T}, s\in\mathcal{S} \tag{E.8}$$

$$\sum_{r\in\mathcal{R}}\sum_{b\in\mathcal{B}_r} N_{rbvt}^{Vs} y_{rbvt}^s \le x_{vt}^s, \qquad v\in\mathcal{V}, t\in\mathcal{T}, s\in\mathcal{S} \tag{E.9}$$

Investment constraints across time steps and between scenarios

$$x_{vt}^s = X_v, \qquad v\in\mathcal{V}^{ZE}, t\in\{1..L_v^V\}, s\in\mathcal{S}, \tag{E.10}$$

$$y_{pit}^{Is} = Y_{pi}^I, \qquad p\in\mathcal{P}, i\in\mathcal{I}_p^{ZE}, t\in\{1..L_i^I\}, s\in\mathcal{S}, \tag{E.11}$$

$$q_{pt}^{GAs} = Q_p^{GA}, \qquad p\in\mathcal{P}, t\in\{1..L_p^G\}, s\in\mathcal{S}, \tag{E.12}$$

$$x_{vt}^s - x_{v(t-1)}^s = \tilde{x}_{v(t-L_v^V)}^s, \qquad v\in\mathcal{V}^{ZE}, t\in\mathcal{T}\setminus\{1..L_v^V\}, s\in\mathcal{S}, \tag{E.13}$$

$$y_{pit}^{Is} - y_{pi(t-1)}^{Is} = \tilde{y}_{pi(t-L_i^I)}^{Is}, \qquad p\in\mathcal{P}, i\in\mathcal{I}_p^{ZE}, t\in\mathcal{T}\setminus\{1..L_i^I\}, s\in\mathcal{S}, \tag{E.14}$$

$$q_{pt}^{GAs} - q_{p(t-1)}^{GAs} = \tilde{q}_{p(t-L_p^G)}^{GAs}, \qquad p\in\mathcal{P}, t\in\mathcal{T}\setminus\{1..L_p^G\}, s\in\mathcal{S}, \tag{E.15}$$

Non-anticipativity constraints

$$\tilde{x}^{s}_{vt} = \tilde{x}^{(s+1)}_{vt}, \qquad v \in \mathcal{V}^{ZE}, t \in \mathcal{T}^{NS}, s \in \mathcal{S}\backslash\{|\mathcal{S}|\} \quad \text{(E.16)}$$

$$\tilde{y}^{Is}_{pit} = \tilde{y}^{I(s+1)}_{pit}, \qquad p \in \mathcal{P}, i \in \mathcal{I}^{ZE}_{p}, t \in \mathcal{T}^{NS}, s \in \mathcal{S}\backslash\{|\mathcal{S}|\}, \quad \text{(E.17)}$$

$$\tilde{q}^{GAs}_{pt} = \tilde{q}^{GA(s+1)}_{pt}, \qquad p \in \mathcal{P}, t \in \mathcal{T}^{NS}, s \in \mathcal{S}\backslash\{|\mathcal{S}|\}, \quad \text{(E.18)}$$

Energy Production and Consumption Constraints

$$\sum_{r\in\mathcal{R}}\sum_{b\in\mathcal{B}_r}\sum_{v\in\mathcal{V}^{C}_{rb}}\sum_{p\in\mathcal{P}_b} E^{Us}_{rbvpt} y^{s}_{rbvt} \leq \overline{E}^{C}_{t}, \qquad t \in \mathcal{T}, s \in \mathcal{S} \quad \text{(E.19)}$$

$$\sum_{b\in\mathcal{B}_{pi}}\sum_{r\in\mathcal{R}_b}\sum_{v\in\mathcal{V}^{ZE}_{rb}} E^{Us}_{rbvpt} y^{s}_{rbvt} \leq e^{Ps}_{pit}, \qquad p \in \mathcal{P}, i \in \mathcal{I}^{SC}_{p}, t \in \mathcal{T}, s \in \mathcal{S} \quad \text{(E.20)}$$

$$\sum_{b\in\mathcal{B}_{pi}}\sum_{r\in\mathcal{R}_b}\sum_{v\in\mathcal{V}^{ZE}_{rb}} E^{Us}_{rbvpt} y^{s}_{rbvt} \leq \sum_{\hat{p}\in\mathcal{P}}\sum_{\hat{i}\in\mathcal{I}^{HUB}_{\hat{p}}} e^{Hs}_{pi\hat{p}\hat{i}t}, \qquad p \in \mathcal{P}, i \in \mathcal{I}^{F}_{p}, t \in \mathcal{T}, s \in \mathcal{S} \quad \text{(E.21)}$$

$$\sum_{p\in\mathcal{P}}\sum_{i\in\mathcal{I}^{F}_{p}} e^{Hs}_{pi\hat{p}\hat{i}t} \leq e^{Ps}_{\hat{p}\hat{i}t}, \qquad \hat{p} \in \mathcal{P}, \hat{i} \in \mathcal{I}^{HUB}_{\hat{p}}, t \in \mathcal{T}, s \in \mathcal{S} \quad \text{(E.22)}$$

$$\sum_{\hat{p}\in\mathcal{P}}\sum_{\hat{i}\in\mathcal{I}^{HUB}_{\hat{p}}} e^{Hs}_{pi\hat{p}\hat{i}t} \leq Q^{S}_{i} y^{Is}_{pit}, \qquad p \in \mathcal{P}, i \in \mathcal{I}^{F}_{p}, t \in \mathcal{T}, s \in \mathcal{S} \quad \text{(E.23)}$$

$$e^{Ps}_{pit} \leq M^{0}_{i} y^{Is}_{pit}, \qquad p \in \mathcal{P}, i \in \mathcal{I}^{GC}_{p}, t \in \mathcal{T}, s \in \mathcal{S} \quad \text{(E.24)}$$

$$\sum_{b\in\mathcal{B}_{pi}}\sum_{r\in\mathcal{R}_b}\sum_{v\in\mathcal{V}^{ZE}_{rb}} T^{Us}_{rbvpt} y^{s}_{rbvt} \leq N^{H} U^{F}, \qquad p \in \mathcal{P}, i \in \mathcal{I}^{B}_{p}, t \in \mathcal{T}, s \in \mathcal{S} \quad \text{(E.25)}$$

Grid Capacity Constraints

$$q^{GAs}_{pt} \leq \overline{Q}^{G}_{p} + Q^{GA}_{p}, \qquad p \in \mathcal{P}, t \in \mathcal{T}, s \in \mathcal{S} \quad \text{(E.26)}$$

$$\sum_{i\in\mathcal{I}^{GC}_{p}} \frac{e^{Ps}_{pit}}{E^{CE}_{i}} \leq N^{H} q^{GAs}_{pt}, \qquad p \in \mathcal{P}, t \in \mathcal{T}, s \in \mathcal{S} \quad \text{(E.27)}$$

$$\sum_{i\in\mathcal{I}^{E}_{p}} R^{P}_{i} y^{Is}_{pit} \leq q^{GAs}_{pt}, \qquad p \in \mathcal{P}, t \in \mathcal{T}, s \in \mathcal{S} \quad \text{(E.28)}$$

Non-Negativity, Binary and Integer Requirements

$$y^{s}_{rbvt} \in \{0,1\}, \qquad r \in \mathcal{R}, b \in \mathcal{B}_r, v \in \mathcal{V}_{rb}, t \in \mathcal{T}, s \in \mathcal{S} \quad \text{(E.29)}$$

$$y^{Is}_{pit} \in \{0,1\}, \qquad p \in \mathcal{P}, i \in \mathcal{I}_p, t \in \mathcal{T}, s \in \mathcal{S} \quad \text{(E.30)}$$

$$x^{s}_{vt} \in \mathbb{Z}^{+}, \qquad v \in \mathcal{V}, t \in \mathcal{T}, s \in \mathcal{S} \quad \text{(E.31)}$$

$$q^{GAs}_{pt} \in \mathbb{R}^{+}, \qquad p \in \mathcal{P}, t \in \mathcal{T}, s \in \mathcal{S} \quad \text{(E.32)}$$

$$\tilde{y}^{Is}_{pit} \in \{0,1\}, \qquad p \in \mathcal{P}, i \in \mathcal{I}^{ZE}_{p}, t \in \{1..|\mathcal{T}| - L^{I}_{i}\}, s \in \mathcal{S} \quad \text{(E.33)}$$

$$\tilde{x}^{s}_{vt} \in \mathbb{Z}^{+}, \qquad v \in \mathcal{V}^{ZE}, t \in \{1..|\mathcal{T}| - L^{V}_{v}\}, s \in \mathcal{S} \quad \text{(E.34)}$$

$$\tilde{q}^{GAs}_{pt} \in \mathbb{R}^{+}, \qquad p \in \mathcal{P}, t \in \{1..|\mathcal{T}| - L^{G}_{p}\}, s \in \mathcal{S} \quad \text{(E.35)}$$

$$e^{Hs}_{pi\hat{p}\hat{i}t} \in \mathbb{R}^{+}, \qquad p \in \mathcal{P}, i \in \mathcal{I}^{F}_{p}, \hat{p} \in \mathcal{P}, \hat{i} \in \mathcal{I}^{HUB}_{\hat{p}}, t \in \mathcal{T}, s \in \mathcal{S} \quad \text{(E.36)}$$

$$e^{Ps}_{pit} \in \mathbb{R}^{+}, \qquad p \in \mathcal{P}, i \in \mathcal{I}^{GC}_{p}, t \in \mathcal{T}, s \in \mathcal{S} \quad \text{(E.37)}$$

Appendix F

Compact Mathematical Formulation of the Sub-Problem

F.1 Notation

Sets

$\mathcal{V}^{VO}$	Set of vessel
$\mathcal{T}^{TP}$	Set of time periods
$\mathcal{R}^{SR}$	Set of sub-routes
$\mathcal{P}^{R}$	Set of resting- and main ports
$\mathcal{P}^{B}$	Set of bunkering ports
$\mathcal{P}^{B}_{ap}$	Set of bunkering ports which are bunkered at until bunkering at bunkering port p, including p, during activity a
$\mathcal{J}$	Set of activity slots
$\mathcal{J}_{\hat{t}}$	Set of activity slots in time period $\hat{t}$
$\mathcal{J}^{S}$	Set of activity slots initiating a time period
$\mathcal{J}^{\overline{S}}$	Set of activity slots not initiating a time period
$\mathcal{A}$	Set of activity types
$\mathcal{A}^{R}$	Set of activity types serving a sub-route
$\mathcal{A}^{R}_{\hat{r}}$	Set of activity types serving sub-route $\hat{r}$
$\mathcal{A}^{B}$	Set of bunkering activity types
$\mathcal{A}^{B}_{p}$	Set of activity types bunkering at bunkering port p
$\mathcal{A}^{BR}$	Set of bunkering activities, which also serve a sub-route
$\mathcal{A}^{REST}$	Set of resting activity types
$\mathcal{A}^{\overline{REST}}$	Set of non-resting activity types
$\mathcal{A}^{E}_{p}$	Set of activities that *end* in port p
$\mathcal{A}^{S}_{p}$	Set of activities that *start* in port p

Parameters

D^P	Passenger demand on all sub-routes
$F_{\hat{t}\hat{r}}$	The frequency demand of sub-route $\hat{r}$ in time period $\hat{t}$
T_j^{END}	The ending time of the time period containing activity slot j
C^{CREW}	Crew shift cost
C^{PT}	Passenger time cost
C^A	Passenger alternative cost
C_p^E	Unit cost of energy at bunkering port p
V^{PAX}	Passenger capacity of the selected vessel type
$\overline{Q}^{VS}$	Upper bound for energy level of the selected vessel type
$\underline{Q}^{VS}$	Lower bound for energy level of the selected vessel type
$\overline{\underline{Q}}^{VS}$	Maximum available energy for the selected vessel type
Q_p^{IS}	The energy storage capacity installed at bunkering port p
R_p^B	Rate of energy bunkering at bunkering port p
R_p^P	Rate of energy production at bunkering port p
E_p^{EC}	Energy conversion efficiency of the infrastructure installed at bunkering port p
A_a^{BT}	Bunkering overhead time associate with conducting activity a
A_a^T	Sailing time for activity a
A_a^{EU}	The total energy consumed when performing activity a
A_a^{ER}	The minimum energy required to initiate activity a
A_{ap}^{ELL}	The energy required to sail the last leg of activity a ending at bunkering port p

Variables

$y_{\hat{v}ja}^A$	1 if vessel $\hat{v}$ performs activity a in activity slot j, 0 otherwise
$y_{v\hat{t}}^T$	1 if vessel $\hat{v}$ is used in time period $\hat{t}$, 0 otherwise
$e_{\hat{v}j}^S$	Energy storage level at vessel $\hat{v}$ at the start of activity slot j
$h_{\hat{v}j}$	Time spent by vessel $\hat{v}$ by the start of activity slot j
$e_{\hat{v}jp}^B$	Amount of energy bunkered by vessel $\hat{v}$ in activity slot j at bunkering port p
$e_{\hat{v}jp}^{\underline{B}}$	Amount of energy bunkered from on-shore storage at bunkering port p by vessel $\hat{v}$ in activity slot j
$e_{\hat{v}jp}^{\overline{B}}$	Amount of energy bunkered with *empty* on-shore storage at bunkering port p by vessel $\hat{v}$ in activity slot j
$e_{\hat{v}jp}^{\underline{B}C}$	Amount of energy bunkered from on-shore storage at bunkering port p by vessel $\hat{v}$ in activity slot j while passengers are on board
$e_{\hat{v}jp}^{\overline{B}C}$	Amount of energy bunkered with *empty* on-shore storage at bunkering port p by vessel $\hat{v}$ in activity slot j while passengers are on board

F.2 Objective

$$\min \quad z = \sum_{\hat{v}\in\mathcal{V}^{VO}} \sum_{\hat{t}\in\mathcal{T}^{TP}} C^{CREW} y^T_{v\hat{t}} + \sum_{p\in\mathcal{P}^B} \sum_{\hat{v}\in\mathcal{V}^{VO}} \sum_{j\in\mathcal{J}} C^E_p e^B_{\hat{v}jp} + C^A M^{UD} \sum_{\hat{t}\in\mathcal{T}^{TP}} \sum_{\hat{r}\in\mathcal{R}^{SR}} F_{\hat{t}\hat{r}} \tag{F.1}$$

$$+ \sum_{\hat{v}\in\mathcal{V}^{VO}} \sum_{j\in\mathcal{J}} M^{PO} C^{PT} \left(\sum_{a\in\mathcal{A}^R} A^T_a y^A_{\hat{v}ja} + \sum_{a\in\mathcal{A}^{BR}} A^{BT}_a y^A_{\hat{v}ja} + \sum_{p\in\mathcal{P}^B} \left(\frac{e^{\underline{B}C}_{\hat{v}jp}}{R^B_p} + \frac{e^{\overline{B}C}_{\hat{v}jp}}{R^P_p E^{EC}_p} \right) \right)$$

F.3 Constraints

$$\sum_{a\in\mathcal{A}} y^A_{\hat{v}ja} = 1, \qquad j\in\mathcal{J}, \hat{v}\in\mathcal{V}^{VO} \tag{F.2}$$

$$\sum_{j\in\mathcal{J}_{\hat{t}}} \sum_{a\in\mathcal{A}^{\overline{REST}}} y^A_{\hat{v}ja} \le |\mathcal{J}_{\hat{t}}|\, y_{v\hat{t}}, \qquad \hat{v}\in\mathcal{V}^{VO}, \hat{t}\in\mathcal{T}^{TP} \tag{F.3}$$

Energy Constraints

$$e^B_{\hat{v}jp} \le \overline{Q}^{VS} \sum_{a\in\mathcal{A}^B_p} y^A_{\hat{v}ja}, \qquad \hat{v}\in\mathcal{V}^{VO}, j\in\mathcal{J}, p\in\mathcal{P}^B \tag{F.4}$$

$$e^B_{\hat{v}jp} = e^{\underline{B}}_{\hat{v}jp} + e^{\overline{B}}_{\hat{v}jp}, \qquad \hat{v}\in\mathcal{V}^{VO}, j\in\mathcal{J}, p\in\mathcal{P}^B \tag{F.5}$$

$$e^{\underline{B}}_{\hat{v}jp} \le M^0_p, \qquad \hat{v}\in\mathcal{V}^{VO}, j\in\mathcal{J}, p\in\mathcal{P}^B \tag{F.6}$$

$$e^{\underline{B}}_{\hat{v}jp} \le e^{\underline{B}C}_{\hat{v}jp} + M^0_p \left(1 - \sum_{a\in\mathcal{A}^R} y^A_{\hat{v}ja}\right), \qquad \hat{v}\in\mathcal{V}^{VO}, j\in\mathcal{J}, p\in\mathcal{P}^B \tag{F.7}$$

$$e^{\overline{B}}_{\hat{v}jp} \le e^{\overline{B}C}_{\hat{v}jp} + M^1_p \left(1 - \sum_{a\in\mathcal{A}^R} y^A_{\hat{v}ja}\right), \qquad \hat{v}\in\mathcal{V}^{VO}, j\in\mathcal{J}, p\in\mathcal{P}^B \tag{F.8}$$

$$e^S_{\hat{v}j} + \sum_{p\in\mathcal{P}^B} e^B_{\hat{v}jp} - \sum_{a\in\mathcal{A}^{\overline{REST}}} A^{EU}_a y_{\hat{v}ja} = e^S_{\hat{v}(j+1)}, \qquad \hat{v}\in\mathcal{V}^{VO}, j\in\mathcal{J}\backslash\{|\mathcal{J}|\} \tag{F.9}$$

$$e^S_{\hat{v}j} = e^S_{\hat{v}(j+|\mathcal{J}|-1)} + \sum_{p\in\mathcal{P}^B} e^B_{\hat{v}(j+|\mathcal{J}|-1)p} - \sum_{a\in\mathcal{A}^{\overline{REST}}} A^{EU}_a y_{\hat{v}(j+|\mathcal{J}|-1)a}, \qquad \hat{v}\in\mathcal{V}^{VO}, j\in\{1\} \tag{F.10}$$

$$e^B_{\hat{v}jp} \le \overline{Q}^{VS} - e^S_{\hat{v}j} + \sum_{\hat{p}\in\mathcal{P}^B_{ap}} A^{ELL}_{a\hat{p}} - \sum_{\hat{p}\in\mathcal{P}^B_{ap}\backslash\{p\}} e^B_{\hat{v}j\hat{p}} + \underline{\overline{Q}}^{VS} \left(1 - y^A_{\hat{v}ja}\right), \quad \hat{v}\in\mathcal{V}^{VO}, j\in\mathcal{J}, p\in\mathcal{P}^B, a\in\mathcal{A}^B_p \tag{F.11}$$

$$\sum_{\hat{p}\in\mathcal{P}^B_{ap}} A^{ELL}_{a\hat{p}} - \sum_{\hat{p}\in\mathcal{P}^B_{ap}\backslash\{p\}} e^B_{\hat{v}j\hat{p}} \le e^S_{\hat{v}j} - \underline{Q}^{VS} + \underline{\overline{Q}}^{VS} \left(1 - y^A_{\hat{v}ja}\right), \quad \hat{v}\in\mathcal{V}^{VO}, j\in\mathcal{J}, p\in\mathcal{P}^B, a\in\mathcal{A}^B_p \tag{F.12}$$

$$\sum_{a\in\mathcal{A}^{NR}\backslash\{\mathcal{A}^B\}} A^{ER}_a y^A_{\hat{v}ja} \le e^S_{\hat{v}j} - \underline{Q}^{VS}, \qquad \hat{v}\in\mathcal{V}^{VO}, j\in\mathcal{J} \tag{F.13}$$

Time Constraints

$$h_{\hat{v}j} = 0 \qquad \hat{v} \in \mathcal{V}^{VO}, j \in \{1\} \quad \text{(F.14)}$$

$$T^{END}_{(j-1)} = h_{\hat{v}j} \qquad \hat{v} \in \mathcal{V}^{VO}, j \in \mathcal{J}^{S} \backslash \{1\} \quad \text{(F.15)}$$

$$h_{\hat{v}j} + \sum_{a \in \mathcal{A}^{\overline{REST}}} A^{T}_{a} y^{A}_{\hat{v}ja} + \sum_{a \in \mathcal{A}^{B}} A^{BT}_{a} y^{A}_{\hat{v}ja} + \sum_{p \in \mathcal{P}^{B}} \left(\frac{e^{\underline{B}}_{\hat{v}jp}}{R^{B}_{p}} + \frac{e^{\overline{B}}_{\hat{v}jp}}{R^{P}_{p} E^{EC}_{p}} \right) \leq h_{\hat{v}(j+1)} \quad \hat{v} \in \mathcal{V}^{VO}, j \in \mathcal{J} \backslash \{|\mathcal{J}|\} \quad \text{(F.16)}$$

Frequency Constraints

$$F_{\hat{t}\hat{r}} = \sum_{v \in \mathcal{V}^{VO}} \sum_{j \in \mathcal{J}_{\hat{t}}} \sum_{a \in \mathcal{A}^{R}_{\hat{r}}} y^{A}_{\hat{v}ja}, \qquad \hat{t} \in \mathcal{T}^{TP}, \hat{r} \in \mathcal{R}^{SR} \quad \text{(F.17)}$$

Location Constraints

$$\sum_{a \in \mathcal{A}^{E}_{p}} y^{A}_{\hat{v}ja} = \sum_{a \in \mathcal{A}^{S}_{p}} y^{A}_{\hat{v}(j+1)a}, \qquad j \in \mathcal{J} \backslash \{|\mathcal{J}|\}, \hat{v} \in \mathcal{V}^{VO}, p \in \mathcal{P}^{R} \quad \text{(F.18)}$$

$$\sum_{a \in \mathcal{A}^{S}_{p}} y^{A}_{\hat{v}ja} = 1, \qquad j \in \{1\}, \hat{v} \in \{1\}, p \in \{1\} \quad \text{(F.19)}$$

$$\sum_{a \in \mathcal{A}^{E}_{p}} y^{A}_{\hat{v}ja} = 1, \qquad j \in \{|\mathcal{J}|\}, \hat{v} \in \{1\}, p \in \{1\} \quad \text{(F.20)}$$

$$\sum_{a \in \mathcal{A}^{E}_{p}} y^{A}_{\hat{v}ja} = \sum_{a \in \mathcal{A}^{S}_{p}} y^{A}_{\hat{v}(j+|\mathcal{J}|-1)a}, \qquad j \in \{1\}, \hat{v} \in \mathcal{V}^{VO} \backslash \{1\}, p \in \mathcal{P}^{R} \quad \text{(F.21)}$$

Symmetry Breaking Constraints

$$\sum_{a \in \mathcal{A}^{REST}} y^{A}_{\hat{v}(j-1)a} \leq \sum_{a \in \mathcal{A}^{REST}} y^{A}_{\hat{v}ja}, \qquad j \in \mathcal{J}^{\overline{S}}, \hat{v} \in \mathcal{V}^{VO} \quad \text{(F.22)}$$

Non-Negativity and Binary Requirements

$$y^{A}_{\hat{v}ja} \in \{0,1\}, \qquad v \in \mathcal{V}^{VO}, j \in \mathcal{J}, a \in \mathcal{A} \quad \text{(F.23)}$$

$$y^{T}_{v\hat{t}} \in \{0,1\}, \qquad v \in \mathcal{V}^{VO}, \hat{t} \in \mathcal{T}^{TP} \quad \text{(F.24)}$$

$$e^{B}_{\hat{v}jp} \in \mathbb{R}^{+}, \qquad v \in \mathcal{V}^{VO}, j \in \mathcal{J}, p \in \mathcal{P}^{B} \quad \text{(F.25)}$$

$$e^{\underline{B}}_{\hat{v}jp} \in \mathbb{R}^{+}, \qquad v \in \mathcal{V}^{VO}, j \in \mathcal{J}, p \in \mathcal{P}^{B} \quad \text{(F.26)}$$

$$e^{\overline{B}}_{\hat{v}jp} \in \mathbb{R}^+, \qquad v \in \mathcal{V}^{VO}, j \in \mathcal{J}, p \in \mathcal{P}^B \quad \text{(F.27)}$$

$$e^{\overline{BC}}_{\hat{v}jp} \in \mathbb{R}^+, \qquad v \in \mathcal{V}^{VO}, j \in \mathcal{J}, p \in \mathcal{P}^B \quad \text{(F.28)}$$

$$e^{\overline{BC}}_{\hat{v}jp} \in \mathbb{R}^+, \qquad v \in \mathcal{V}^{VO}, j \in \mathcal{J}, p \in \mathcal{P}^B \quad \text{(F.29)}$$

$$e^{S}_{\hat{v}j} \in \mathbb{R}^+, \qquad v \in \mathcal{V}^{VO}, j \in \mathcal{J} \quad \text{(F.30)}$$

$$h_{\hat{v}j} \in \mathbb{R}^+, \qquad v \in \mathcal{V}^{VO}, j \in \mathcal{J} \quad \text{(F.31)}$$

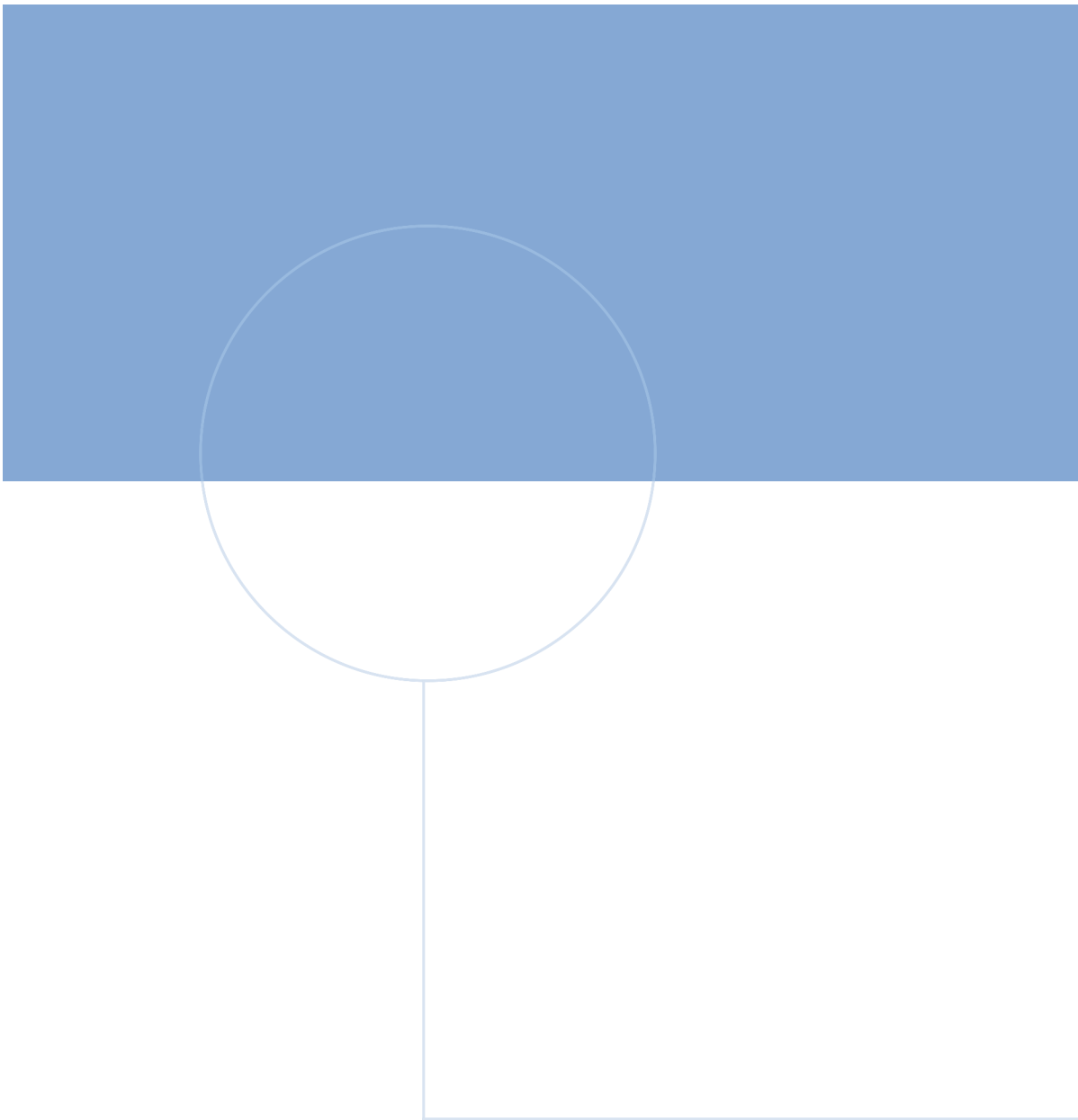

NTNU

Norwegian University of
Science and Technology